UNIVERSIDAD AUTÓNOMA DE MADRID

Programa de Doctorado de Biociencias Moleculares

The role of *Yme1l* in the progression of heart failure. Nutritional approaches for prevention

Rocío Villena Gutiérrez

Tesis Doctoral

PhD Thesis

Madrid, 2022

Departamento de Bioquímica
Facultad de Medicina
UNIVERSIDAD AUTÓNOMA DE MADRID

The role of *Yme1l* in the progression of heart failure. Nutritional approaches for prevention

Memoria que presenta para optar al título de Doctor
por la Universidad Autónoma de Madrid:

Rocío Villena Gutiérrez
Graduada en Biotecnología y Máster en Biociencias Moleculares

Director de la tesis: **Dr. Borja Ibáñez Cabeza**
Codirector de la tesis: **Dr. Eduardo Oliver Pérez**

Centro Nacional de Investigaciones Cardiovasculares Carlos III (CNIC)

Madrid, 2022

Department of Biochemistry
School of Medicine
UNIVERSIDAD AUTÓNOMA DE MADRID

The role of *Yme1l* in the progression of heart failure. Nutritional approaches for prevention

Doctoral Thesis presented to earn the Doctor of Philosophy degree
of the Universidad Autónoma de Madrid by:

Rocío Villena Gutiérrez
BSc. in Biotechnology and MSc. in Molecular Bioscience

Thesis director: **Dr. Borja Ibáñez Cabeza**
Thesis co-director: **Dr. Eduardo Oliver Pérez**

Spanish National Center for Cardiovascular Research (CNIC)

Madrid, 2022

Don **Borja Ibáñez Cabeza**, Doctor en Medicina y director del departamento de Investigación Clínica del Centro Nacional de Investigaciones Cardiovasculares Carlos III (CNIC) en Madrid, y

Don **Eduardo Oliver Pérez**, Doctor en Farmacología e Investigador Ramón y Cajal jefe de grupo del Centro de Investigaciones Biológicas Margarita Salas (CIB), CSIC en Madrid,

CERTIFICAN:

Que durante los últimos 5 años Doña Rocío Villena Gutiérrez ha realizado bajo su codirección el trabajo de investigación titulado: "*The role of Yme1l in the progression of heart failure. Nutritional approaches for prevention*" para alcanzar el Grado de Doctor. La presente memoria reúne los requisitos de originalidad y contenido exigidos y contribuye de manera significativa al ámbito de la investigación cardiovascular, por lo que autorizan su presentación para que pueda ser juzgada por el tribunal correspondiente.

Madrid, 11 de noviembre de 2022

Borja Ibáñez Cabeza
Director de Tesis

Eduardo Oliver Pérez
Co-director de Tesis

Acknowledgments

Nunca hubiera pensado que después de tanto tiempo estaría escribiendo estos agradecimientos. Son muchos los momentos que desde 2013 podría relatar. Me gustaría empezar dando las gracias al Dr. Jesús Borreguero, porque fue él quien me introdujo en CNIC cuando todavía no tenía ni la mayoría de edad. Desde entonces no he hecho más que conocer a personas que han marcado mi madurez profesional y también personal.

A Edu, mi codirector de tesis. Gracias por estar ahí en los momentos más difíciles, por no desesperar (o a veces sí) cuando lo único que quería era dejar la tesis, por nuestras discusiones por ver quién llevaba más razón, por tener una visión positiva siempre de los resultados, y por siempre estar dispuesto a tener 10 minutos para escucharme con lo que fuera. Admiro, de verdad, la dedicación que le pones a todo lo que haces. Sin ti esta tesis no hubiera sido posible.

A Borja, mi director de tesis. Me abriste las puertas de tu laboratorio con 18 añitos y casi 10 años después aquí estamos. Gracias por confiar en mí desde el principio. Por darle siempre el punto perfecto a todo, por buscar los puntos débiles y hacer que fueran los fuertes, por inculcarme ese trabajo constante. Siempre he pensado que entre la locura y la genialidad hay una fina línea que siempre has sabido transmitirnos y por eso todo nuestro grupo es así de brillante. Gracias por darme la libertad para innovar, proponer, cuestionar y ser tan crítica con todo lo que hago. Aunque tu agenda no lo ha permitido demasiado, siempre ha sido un placer un café, una comida o una charla sobre la vida contigo.

A Jaime García-Prieto, todavía recuerdo cuánto te mosqueabas porque no sabía hacer una dilución. Y, mírame ahora, sigo sin saber hacerlas del todo bien después de 9 años. Fuiste tú quién confió en mí para llevar parte de tu proyecto y puedo decir que gracias a ti tuve la oportunidad de seguir progresando dentro del grupo. Aunque ya no estés en CNIC, sigues teniendo la maravillosa habilidad de ponerme la cabeza como un bombo para intentar que haga lo que crees que es mejor para mí, aunque al final acabo haciéndolo como yo creo. Gracias por seguir siempre ahí, amigo.

A Andrés Pun, no puedo imaginar unos primeros años de prácticas sin ti en este grupo. Aunque tu mayor diversión era gastarme bromas, no he podido tener mejor compañero para ahora no fiarme de algo sospechoso. Siempre nos quedará París.

A Jorge Nuche, mi cardiólogo favorito, seguiremos yendo a comer y disfrutar de unas buenas copas de vino. A Javi Sánchez, la personificación de decir siempre las cosas claras. Aunque no estés de acuerdo con mi partida del mundo científico, sé que no me guardarás rencor. Volveré siempre y cuando me reserves más de 15 minutos para comer.

A mis incorporaciones estrella: Laura y Anabel. Luz del laboratorio estos dos últimos años para mí. Gracias por los experimentos a tres, por no estresaros demasiado cuando yo iba a toda velocidad y por echarme una mano siempre que lo he necesitado. Ojalá más personas como vosotras. Laura, aunque el ejercicio no es nuestro fuerte, sí que llegaste pisando fuerte al lab y es un placer trabajar y disfrutar todos los días contigo. Anabel, espero poder haberte enseñado de la mejor manera posible. Aunque ya lucieras por ti sola, me alegra saber que te he entrenado para ser mucho mejor que yo. Laura, cuídame a la polluela. Guíala por el “buen” camino de los sándwiches de pavo, las quejas, y los días de 14 horas.

A Miguelito, porque espero que algún día despuntes tanto como mereces. Sigue trabajando duro. Con esa constancia y delicadeza en todo lo que haces. Falla 100 veces y levántate otras 100, siempre. Y, por favor, deja de hacer Western Blots en un tiempo prudencial.

A Luci, nunca has puesto una mala cara y siempre te has ofrecido a ayudarme con todo. Personas como tú hacen los días mucho más fáciles. Nunca pierdas esa timidez que te caracteriza y que luego permite que conozcamos a una persona tan increíble. PS: acuérdate de regar las plantas cuando me vaya.

A Carlos, uno de los pilares de este grupo. Sólo Les Diablerets y París saben lo divertido que puede ser una noche de fiesta los dos + unos chupitos. Eres un excelente profesional y una persona mejor todavía. Nos quedan todavía muchas escaladas y viajes juntos. Por favor, deja de lavar la cafetera en la pila de acrilamida. Ah! Que viva el GraphPad.

A Moni, me has visto crecer desde los 18. Me lo advertiste entonces, pero lo hice igualmente. Me quedé en ciencia. Y mira, lo he conseguido. No sé cómo lo voy a hacer para llegar todas las mañanas al trabajo y no verte ahí sentada. No sé cómo le voy a explicar a alguien lo que son las *rociadas* y que me entienda. No sé quién me va a salvar de tantas como lo has hecho tú. Te debo mucho, Moni. Te llevo en mi vida como un ratón una ligadura permanente.

A Agus (pollito), my paired t-test. Me faltan varias tesis para poder describir todos los momentos que hemos vivido. Y cómo me conoces. Una mirada es suficiente para poder comunicarnos. Mi cómplice en todo. La parte profesional me la ahorro, prácticamente hemos crecido juntos y sabes lo orgullosa que estoy de ti, superestrella. Brillas en todo lo que haces y te espera un futuro increíble pollo y ahí estaré para verlo. Quiero darte las gracias por estar. Por estar en cada momento malo y bueno, por estar dispuesto a cualquier aventura, por saber mantener la calma cuando la situación lo requería, por tener las mismas inquietudes y ambiciones que yo, por confiarnos lo más íntimo y por saber que pase lo que pase, siempre vamos a estar ahí el uno para el otro. Hemos superado crisis, experimentos, ralladas, cabreos y mal humor, pero qué bien nos lo hemos pasado. Me encanta haberte conocido y saber que te tengo en mi vida. Has sido, eres, y serás uno de los mejores descubrimientos de mi tesis. Te quiero como un neutro a una plaqueta.

A todos en general que han pasado por el Lab. BI y me han aportado tanto: Valeria, Susana, David, Sergi, Monika, Alba…

Al Lab. VA, porque no podría haber un mejor grupo con quien compartir planta que vosotros. A María Jesús, por ser la jefa de la 1ª Sur, gracias por haber estado siempre pendiente de que estuviera bien. A Cris, gracias por acogerme desde aquel 2013. Nunca has desistido en intentar que bajara a desayunar. Gracias por cuidarme siempre. Rosita, sólo RRHH sabe la de horas acumuladas los findes en CNIC. Expertas en liarla y aplicar la ley de Murphy. Porque hubo una temporada que las jornadas laborales eran de 7 días y ni aun así salía nada. El récord de qPCRs es tuyo, pero el de WB me lo llevo yo. Lo hemos conseguido, amiga. Por el futuro que nos espera. A Álvaro Macías, si el Langendorff hablara, no sabría si escupir cardiomiocitos o conversaciones. Es un placer poder saber que, aunque ahora estés en otro grupo, siempre puedo contar contigo. Gracias por tu alegría y buen humor siempre que lo he necesitado.

Al Lab. DF, os lleváis el premio a horas nocturnas trabajadas. Sois un auténtico ejemplo de superación y trabajo constante. Jose, mi espejo en otro grupo. Sólo tú y yo sabemos lo que son los verdaderos sándwiches. Ha sido un placer compartir este fin de etapa contigo, pero nos queda mucho todavía. Por el futuro que nos merecemos. Alba1, nunca dejarás de sorprenderme con cada faceta tuya que descubro, ya sea llevando teles por la calle o hablando de la vida. Alba2, qué dura eres, jodía. Y luego, que corazoncito tienes tan blandito…Ana, nunca pierdas esa alegría que te caracteriza. Y, recuerda, sé lo que estás pensando mucho antes de que te acerques a contármelo. Jorge y Andrés, mis descubrimientos ingenieriles de este último año, fieles a cualquier plan. Qué bien haberos encontrado por el camino.

Al Lab. MCC, empezasteis pequeños y ahora no hacéis más que crecer. Al Lab. ELP, callados pero matones. El grupo que siempre lleva la bata puesta siempre dispuestos a ayudarte con todo.

¡La mejor planta de CNIC: la 1ª Sur!

A las *bases* de CNIC: Eeva, Irene, Cris Giménez, Edu Bieger, Yoli y Javi Mateos. Sabéis que en el Lab. BI la gestión de los *deadlines* no es nuestro fuerte. Gracias por ayudarme siempre a mandar todo en el último minuto antes de cierre de convocatorias, justificaciones y congresos. He aprendido a regular mis niveles de cortisol de una manera maravillosa.

Al equipo de animalario, desde la dirección hasta los técnicos. No sé la de pedidos de dieta que hemos hecho, ni la de cosas que os habré preguntado, pero sin vosotros no hubiera sido posible. Al equipo de microscopía, Elvira y Vero, no quiero pensar la de horas que hemos echado para poner a punto protocolos de cardiomiocitos. Lo mejor es poder hacerlo de la mano de profesionales como vosotras, que siempre me habéis ayudado con una sonrisa. A todo el servicio de cafetería, porque ya son tantos años con vosotros que me siento como en casa al bajar a comer. Os prometo que seguiré intentando comer más.

A Lorena y Ana, la pareja de ecógrafas a las que debo mucho. Me encanta saber que mantendré mi pódium en el número de ecos realizadas en CNIC. No sabría decir el número de horas que hemos echado juntas en esa sala, ni tampoco sabría decir si eran las 7 de la mañana o las 11 de la noche. Parte de este curro es todo vuestro.

A toda mi gente de CNIC, ha sido un placer levantarme todas las mañanas y saber que, aunque el proyecto me ha consumido, vosotros habéis estado al pie del cañón en todo momento. Ojalá en mi próxima etapa consiga gente tan buena como vosotros a mi lado todos los días.

Seguimos los agradecimientos:

A mis cojas tuertas del Valle. A las buenas y a las no tan buenas. Siempre ahí, porque sois parte de cada una de mis etapas durante la tesis. Por los comentarios de “Ro, qué haces leyendo un artículo” a las 4 am, por celebrar los experimentos exitosos con botella en mano. Y los no tan exitosos, para qué mentir. Porque hacéis de lo ordinario de ir a tomar un vino, algo extraordinario. Porque juntarme con vosotras siempre es garantía de felicidad constante, bailes, risas, armonía y cariño. Gracias por siempre sacar lo mejor de lo peor. Por quererme incluso con mis frikadas. Gracias por ser mis personas vitamina en todo momento. Intentaré no emocionarme mucho, lo prometo.

A mis amigos del cole, mis faisanes. Aunque lleguéis siempre tarde a todos lados y os odio por ello (hasta en mis cumpleaños), siempre estáis a tiempo cuando os necesito. A ti, Gonzalo Valle. Porque aparte de sacarte la residencia en neuro también te has sacado un grado en psicología del aguante. Eres de las personas con las que todo es más fácil (incluso los bolos). Mejor amigo y testigo de mi vida en cada paso que he dado. Porque siempre eres a quien llamo para darle la primera noticia de todo. Por muchos más años de cosas que contarnos, siempre. Por cierto, a partir de ahora te agradecería me llamaras Doctora Rocío Villena, porque yo SÍ soy doctora de verdad, no como tú. QTPCUPE. TQM.

A ti, Meri. Una de las personas más inteligentes y fuertes que conozco, pero, sobre todo, espontánea. Qué suerte tenerte conmigo. A Bea, por cuidar siempre que no se me fuera la cabeza demasiado e intentar mediar entre María y yo. A Anita, porque a pesar de que hayas intentado siempre huir de Madrid, somos familia. Y a Sonsi y Edu, no hace falta hablar para entendernos. Siempre fieles a cualquier plan sin postureo y sin cotilleos (jeje, no), gracias por cada momento juntos.

A Livier, fiel compañera, amiga, casi hermana de batallas y muchas historias. Gracias por enseñarme tanto. Dudo si tatuarme un Oroboros o un cardiomiocito. Dos años después te cojo el relevo. Qué bonito seguir teniéndote a mi lado.

A Alberto Hernández, te prometo que ya no voy a 1000 por hora, he decelerado. Seguiremos teniendo nuestras sesiones de terapia una vez cada X meses, pero esta vez, los dos como doctores en biomedicina.

A Clau, Anita y Ali. Sois eternamente especiales o especialmente eternas. Nuestras agendas hacen milagros para cuadrarnos, pero volver a casa después de veros es como recargar pilas para los siguientes meses. Guardamar nuestra segunda casa y paraíso personal. No concibo un verano sin vosotras a mi lado. A David, no he llegado tan cuerda como te prometí a la defensa de tesis, pero bueno, algo haremos. Gracias por acompañarme en cada paso que doy siempre. Y a ti Alberto Arroyo, sigo buscando la tranquilidad, pero confío en el destino.

Y, por último, mi soporte vital: mi familia:

Al tío JL y la tía Fiona, gracias por venir tantas veces desde Portugal. Estar con la familia es lo mejor. Lo hemos hecho fenomenal. A Mami, no quiero ni pensar las veces que has sufrido por mí y no entendías nada. Pero una palabra tuya siempre ha bastado y bastará para calmarme. Tienes ese poder inigualable de madre de conseguir que pueda ver todo bien y, sobre todo, fácil. Digna hija de mi madre el agobiarme por todo y acudir a ti en busca de paz. Aunque jugando al Continental no exista familia, siempre me gusta pensar que alguna vez me dejarás ganar. A José Luis, mi hermano. La positividad, el optimismo y la felicidad en persona. Siempre contagiando tu alegría y risa a todos los que te rodean. Cuidando de todos y a mí la que más. Eres el hermano que cualquier persona desearía tener, pero lo tengo yo. Gracias por ser luz siempre. A Barbu, mi padre, mi referente y guía en cada paso que doy. Tan difícil de igualar y mucho más de superar. Te quiero más que la trucha al trucho. Bossi, a ti también.

Esta tesis va por vosotros. We did it!

The faculty or phenomenon of finding valuable or agreeable things not sought for

Serendipity

Table of contents

List of Figures

List of Tables

Abbreviations

CVD: cardiovascular disease

DCM: dilated cardiomyopathy

HF: heart failure

LVEF: left ventricular ejection fraction

LVID: left ventricular internal diameter

ER: endoplasmic reticulum

SR: sarcoplasmic reticulum

ROS: reactive oxygen species

ATP: adenosine triphosphate

mtDNA: mitochondrial DNA

OxPHOS: oxidative phosphorylation

OMM: outer mitochondrial membrane

IMM: inner mitochondrial membrane

UPR: unfolded protein response

cYKO: cardiac yme1l knock-out

MAM: mitochondrial-associated membrane

CD: chow diet

LFD: low fat diet

HFD: high-fat diet

NFD: non-fat diet

CR: caloric restriction

IF: Intermittent fasting

AMI: acute myocardial infarction

TAC: transverse aortic constriction

I/R: ischemia/reperfusion

DRP1: dynamin-related protein

MFN2: mitofusin 2

OPA1: dynamin-like GTPase Optic Atrophy-1

YME1L: ATP-dependent metalloprotease

LC3: microtubule-associated protein 1 light chain

MCU: mitochondria calcium uniporter

CHOP: C/EBP homologous protein

Summary

Heart failure (HF) with reduced ejection fraction is prevalent in leading to reduced life expectancy, poor quality of life and is responsible for a large proportion of healthcare costs. Dilated cardiomyopathy (DCM) is one of the main etiologies responsible for HF, especially in young and middle-aged patients. DCM is defined by ventricular chamber enlargement and systolic impairment leading to progressive HF. Nowadays, there is a lack of specific therapies for DCM able to reverse this condition.

Our group has been a pioneer in demonstrating that imbalanced mitochondrial dynamics in cardiomyocytes results in an overt DCM phenotype. We generated a mouse with genetic ablation of the mitochondrial protease YME1L in cardiomyocytes (cYKO), which results in incorrect OPA1 processing and ultra-fragmented mitochondria in the heart in adulthood. These mice display normal cardiac function until week 30 of age, where a progressive DCM phenotype with reduced lifespan is shown. Moreover, cardiomyocytes display a metabolic switch characterized by preferential use of glucose as a metabolic substrate.

This thesis project focusses firstly on the causality of the protease YME1L during DCM development. Unexpectedly, we found mitochondrial abnormalities (larger size and increased respiration) in a subclinical stage of the disease, when no macroscopic cardiac phenotype is apparent. We demonstrate an autophagy impairment underlying *Yme1l* cardiac-genetic ablation. This is accompanied by increased ER stress, apparently mediated by dysregulation of Ca^{2+} handling. Interestingly, these defects are seen in animals before onset of the disease.

Secondly, our data show that a fat-restricted diet was able not only to prevent HF but also extends the lifespan of cYKO mice. We studied the molecular mechanisms underlying this cardioprotective effect. The mitochondrial ultrastructure indicates a restored mitochondrial number and enlarged size, which is not accompanied by enhanced mitochondrial respiration. Moreover, autophagy defects were still present. However, we speculate that better modulation of ER Ca^{2+} handling under this diet could be involved in enhanced cardiac performance.

These intriguing data call for a comprehensive evaluation of the mechanisms leading to HF prevention and to identifying a diet that could then be translated into clinics.

Resumen

La insuficiencia cardíaca (IC) con fracción de eyección reducida es una entidad prevalente que conduce a una esperanza de vida reducida, una calidad de vida deficiente y responsable de una gran proporción de los costes de atención médica. La miocardiopatía dilatada (MCD) es una de las principales etiologías responsables de la IC, especialmente en pacientes jóvenes y de mediana edad. La MCD se define por el agrandamiento de la cámara ventricular y el deterioro sistólico que conduce a una insuficiencia cardíaca progresiva. En la actualidad, existe una falta de terapias específicas para la MCD capaces de revertir esta condición.

Nuestro grupo ha sido pionero en demostrar que la dinámica mitocondrial desequilibrada en los cardiomiocitos da como resultado un fenotipo de MCD. Generamos un ratón con ablación genética de la proteasa mitocondrial YME1L en cardiomiocitos (cYKO), lo que dio como resultado un procesamiento incorrecto de OPA1 y mitocondrias ultra-fragmentadas en el corazón en estadios tardíos. Estos ratones muestran una función cardíaca normal hasta la semana 30 de edad, donde se muestra un fenotipo de MCD progresiva con una vida media reducida. Además, los cardiomiocitos muestran un cambio metabólico caracterizado por un uso preferencial de la glucosa como sustrato metabólico.

Este proyecto de tesis se centra en primer lugar en el papel de la proteasa YME1L durante el desarrollo de MCD. Casualmente, encontramos diferencias mitocondriales (mayor tamaño y mejor respiración) en etapas subclínicas de la enfermedad. Demostramos, por primera vez un deterioro de la autofagia subyacente a la ablación genética cardíaca de *Yme1l*. Esto se acompaña de un estrés del retículo endoplasmático (RE) elevado, presumiblemente mediado por una desregulación del manejo de Ca^{2+}. Curiosamente, estos defectos se observan en animales antes del inicio de la enfermedad, lo que señala estas vías como objetivo de estudio.

En segundo lugar, nuestros datos recientes no publicados muestran que una dieta restringida en grasas no sólo pudo prevenir la insuficiencia cardíaca sino también aumentar la vida media de los ratones cYKO. Estudiamos los mecanismos moleculares que subyacen a este efecto cardioprotector. Las ultraestructuras mitocondriales indican un número mitocondrial restablecido y un mayor tamaño, que no se corresponden con una mejor respiración mitocondrial. Además, la inhibición de la autofagia todavía estaba presente. Sin embargo, especulamos que una mejor modulación del manejo del Ca^{2+} del RE bajo esta dieta podría estar involucrada en un mejor rendimiento cardíaco.

Estos interesantes datos exigen una evaluación integral de los mecanismos que conducen a la prevención de la insuficiencia cardíaca mediante enfoques nutricionales y para identificar una dieta que luego podría traducirse en un escenario clínico.

Introduction

The topic of study covered in this doctoral thesis is the role of *Yme1l* in the progression of heart failure and the identification of new therapeutic targets amenable to nutritional interventions for its prevention. Specifically, this work explores the molecular mechanism underlying the onset of dilated cardiomyopathy (DCM) in the presence of cardiomyocyte-specific genetic ablation of *Yme1l*. The study then focuses on the use of nutritional approaches aimed at preventing onset of the disease and ameliorating the progression of heart failure through targeting pathways identified in the first part of the thesis.

Dilated cardiomyopathy

Heart failure (HF) is characterized by the inability of the heart to supply blood to meet the organism's demands. In many cases, the primary cause of HF is a disease of the actual heart, something known as cardiomyopathy. Dilated cardiomyopathy (DCM) refers to a myocardial disease characterized by chamber dilation and reduced contractile force. DCM is among the most frequent causes of HF in young and middle-aged individuals worldwide, being the leading cause of cardiac transplant in this population. This condition begins in the left ventricle, the heart´s main pumping chamber. Once the disease progresses, the left ventricle starts to dilate, stretching the heart muscle and becoming thinner. As the disease progresses, the contractile capacity of the heart is impaired (systolic dysfunction), progressively leading to congestive HF (Merlo et al., 2018, Schultheiss et al., 2019). Ventricular remodeling in DCM is driven by a complex cardiomyocyte pathophysiology which includes altered metabolism (Davila-Roman et al., 2002), fibrosis (Andersen et al., 2016), impaired calcium homeostasis (Luo and Anderson, 2013), and finally cell death (Sabbah, 2000). This condition can occur in the absence of any other abnormal condition that could explain the development of this cardiomyopathy, such as hypertension (Drazner, 2011), valvular disease, or metabolic disease (Nishida and Otsu, 2017).

The cause of DCM in 50% of cases remains unknown (idiopathic). However, research performed during the past two decades has identified a genetic basis in a significant number of DCM cases (30-50%), with several genes implicated in both familiar and sporadic cases (Hershberger and Siegfried, 2011, Rosenbaum et al., 2020), reducing the frequency of "idiopathic" DCM cases.

Understanding the complex genetic architecture of DCM is a significant challenge considering the variety of myocardial proteins involved in this disease, but it is likely that most of the gene mutations impair cardiomyocyte function by reducing the heart's ability to contract properly (McNally and Mestroni, 2017, Reichart et al., 2019). Beyond genetic factors, there is evidence indicating the contribution of non-genetic (acquired) factors in DCM risk such as alcohol, toxicity of chemotherapy agents, or diabetes (Bollen et al., 2014, Salvatore et al., 2021, Tayal et al., 2022). There is currently a lack of specific therapies with the ability to reverse this condition. Moreover, the heterogeneity of this disease challenges the search for new therapies to treat this devastating heart condition. Nowadays, treatment options for this condition are based on unspecific palliative care (pharmacological and implantable defibrillators) to slow progression of the disease and to avoid sudden cardiac death. Because the heart requires a constant energy supply for its pump function, it is not surprising that mitochondria, the *powerhouse* of the cell, plays a key role in regulating cardiac function and maintaining cell homeostasis (Brown et al., 2017, Ramaccini et al., 2020). Thus, the study of mitochondrial biology and its modulation could provide better understanding of the pathophysiological mechanism involved in the disease and thus help to identify cardioprotective targets for preventing DCM.

Mitochondrial dynamics and cardiac metabolism in heart failure

Mitochondria constitute essential complex organelles that vary widely across different cell types and tissues (Schaper et al., 1985, Fernandez-Vizarra et al., 2011). In the adult heart, mitochondria represent 30% of the myocardial mass, since the energy demands of the heart require a high production of energy in the form of adenosine triphosphate (ATP) (Piquereau et al., 2013). Mitochondria structure consist of four compartments: matrix, inner mitochondrial membrane (IMM), intermembrane space and outer mitochondrial membrane (OMM); each one providing mitochondria with specific functions. These functions include the production of ATP by the oxidative phosphorylation system (OxPHOS) and the regulation of cell homeostasis by maintaining physiological reactive oxygen species (ROS) and Ca^{2+} levels. Although most of cell DNA is stored in the nucleus of each cell; mitochondria have their own DNA (mtDNA), which is similar to bacterial DNA. The mtDNA contains 37 genes that encode for 13 proteins, including subunits of respiratory complexes I, III, IV and V and proteins essential for translation of mtDNA transcripts. Respiratory complex II is encoded by nuclear DNA. Despite having their own DNA, mitochondria cannot be generated *de novo*.

The mitochondrial biogenesis concept is based on one of the most distinct features of mitochondria: their potential role of dynamism. Thus, the population of mitochondria are always in constant flux between fusion and fission events (Friedman and Nunnari, 2014). Mitochondrial fusion involves the coordinated fusion of the outer and inner mitochondrial membranes but also the content of the mitochondrial matrix.

The opposite of mitochondrial fusion is fission, which depends on the dynamin-related protein DRP1. It is generally accepted that DRP1 exists on the cytosol of the cell and is recruited to promote a mitochondrial membrane constriction during fission (Frank et al., 2001, Fonseca et al., 2019). A coordinated (balanced) mitochondrial dynamic is critical for the bioenergetic function of mitochondria and therefore closely linked to metabolism. Fragmentation of the mitochondrial network (enhanced fission) is generally associated with metabolic dysfunction and is established in a wide variety of disease conditions such as HF, cancer, or obesity (Shirakabe et al., 2016, Dai and Jiang, 2019, Dai et al., 2020). On the other hand, fusion results in a hyperfused network that is normally accompanied by cellular integrity (Chen et al., 2011, Vidoni et al., 2013). However, although fusion is initiated to ameliorate cellular stress, recent studies show its negative impact on cellular health in disease conditions (Das and Chakrabarti, 2020). Recently, endoplasmic reticulum (ER) stress has been associated with stress-induced mitochondrial hyperfusion (SIMH) since its activation could protect mitochondria during ER stress by promoting their fusion (Tondera et al., 2009, Lebeau et al., 2018).

Pioneering studies on yeast over the last 15 years have identified part of the complex machinery of mitochondrial fusion and fission (Westermann, 2008). Among all this machinery, mitofusins 1 and 2 (MFN1 and 2, respectively) are responsible for outer membrane fusion and ER-mitochondria contact sites (Escobar-Henriques and Joaquim, 2019), while the manner in which dynamin-like GTPase Optic Atrophy-1 (OPA1) is processed emerges as the central step in coordinating fusion of the inner membrane (Baker et al., 2014). OPA1 cleavage is performed in the inner membrane by two key proteases: OMA1 and the i-AAA protease YME1L. These two proteases are pivotal in the development of this project since they regulate the balance between the two OPA forms: converting long OPA1 forms (L-OPA1) into proteolytically cleaved short forms (S-OPA1) (Del Dotto et al., 2018). This process is critically connected with metabolism and viability of the cell as the balanced accumulation of both forms maintains normal mitochondrial morphology (Wai and Langer, 2016): fusion depends solely on L-OPA1, while S-OPA1 is associated with mitochondrial fission.

Loss of *Yme1l* in cells induces an OMA1-dependent accumulation of different S-OPA1 forms that are associated with mitochondrial fragmentation, although fusion proceeds normally in these cells (Ruan et al., 2013). Furthermore, either an activation of *Oma1* due to cellular stress or a genetic ablation of *Yme1l* results in the increased conversion to S-OPA and associated mitochondrial fragmentation (Anand et al., 2014). However, the physiological relevance of stress-induced mitochondrial fragmentation remains unclear.

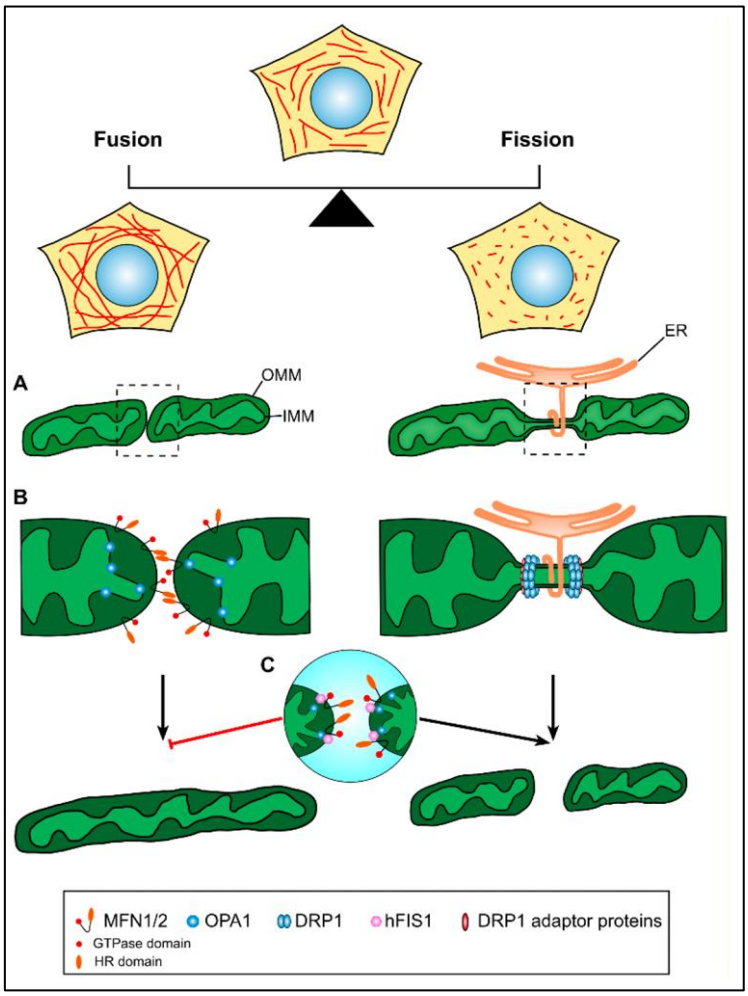

Figure 1. Schematic illustration of the balance between fusion and fission mitochondrial process (Kyriakoudi et al., 2021).

(A) Mitochondria fusion involves the merging of two outer mitochondrial membranes (left). On the right, mitochondrial fission requires a preconstruction of the mitochondrial membrane at the ER-mitochondria contact site.

(B) On the left, MFN1/MFN2 (red, orange) are responsible for the outer mitochondrial membrane fusion. OPA1 is responsible for the fusion of the inner mitochondrial membrane. On the right, mitochondrial division is mainly regulated by DRP1 protein.

(C) In some conditions, block of fusion shifts the balance towards mitochondrial fragmentation.

As previously mentioned, cardiomyocyte mitochondrial dysmorphology is associated with HF as mitochondria represent 30% of myocardial mass.

DCM associated with mitochondrial dynamics

In a clinical scenario, the most common genes involved in DCM are genes encoding for 1) sarcomeric proteins: titin (Tharp et al., 2019), myosin (Schmitt et al., 2006, Ujfalusi et al., 2018), or actin (Vang et al., 2005), 2) nuclear envelope defects (laminopathies): variants in the Lamin A/C gene (Hershberger and Jordan, 1993), 3) cytoskeleton cardiomyopathies: dystrophin, desmin (McNally et al., 2003) and 4) deficits of intercellular adhesion desmosomal cardiomyopathies (Delmar and McKenna, 2010). However, emerging evidence highlights the number of mitochondrial-related genes associated with cardiac dysfunction. In mice, ablation of *Mfn1* and *Mfn2* drastically decrease mtDNA, generating mitochondrial fragmentation and inducing HF (Papanicolaou et al., 2012). Interestingly, only the ablation of both mitofusins produces this phenotype. However, the impact of deletion of mitofusins in heart failure has been widely discussed. Also, *Drp1* deficient cardiomyocyte display enlarged mitochondria and suppressed mitophagy, a form of selective mitochondria elimination (Ikeda et al., 2015). This cardiac ablation leads to higher susceptibility to ischemia/reperfusion (IR) injury and cardiomyopathy. In fact, pharmacological treatment with mdivi-1, an inhibitor of *Dpr1*, increases the proportion of elongated mitochondria and protects them against IR, reducing infarct size (Ong et al., 2010). Moreover, *Oma1*-deficient mice have been shown to be protected against cardiomyocyte death in three different HF models (Acin-Perez et al., 2018).

YME1L mitoprotease also remains essential for preserving adult heart function. Data published by our group demonstrated that cardiomyocyte-specific genetic ablation of *Yme1l* (cYKO) activates OMA1, increasing OPA1 processing into S-OPA1 in cardiomyocytes and impairing mitochondrial morphology by inducing fission that develops into DCM. Interestingly, DCM phenotype is not apparent until later in lifetime (around 25-30 weeks old). Suppression of both proteases (YME1L/OMA1 double KO mice) restored mitochondrial morphology and normal heart function, suggesting that L-OPA isoforms remain essential for preserving heart function.

Mice with *defects in OxPHOS* system also manifest cardiomyopathy. Likewise, cardiolipin dysregulation, which constitutes up to 20% of IMM lipids and where OxPHOS occurs, has been demonstrated to accelerate HF development in spontaneously hypertensive rats and humans (Sparagna et al., 2007).

Lastly, *DCM associated with metabolism defects*. In physiological conditions, the transport of long-chain fatty acids requires the use of the carnitine palmitoyltransferase (CPT) system for its diffusion across the OMM and the IMM (McGarry and Brown, 1997). Energy *Cpt1* and *Cpt2 (*mitochondrial long-chain fatty acid oxidation enzymes) deficiency has been associated with cardiomyopathy. Heart specific CPT2-deficient mice inhibit fatty acid oxidation resulting in cardiac hypertrophy (Pereyra et al., 2017). Hence, targeting energy metabolism is a potential therapeutic target for HF.

The heart utilizes different substrates simultaneously to produce energy. The main source comes from mitochondrial fatty acid oxidation (FAO), which is responsible for 60-80 % of cardiac ATP production, followed by glucose, lactate and ketone bodies (Karwi et al., 2018). The metabolic flexibility of the healthy heart allows the contribution of these substrates to shift depending on variables such as energy demand, hormonal status, or substrate availability (Bertero and Maack, 2018b). In humans, blood ketone bodies and free fatty acid levels increase during fasting periods and remain high during HF (Selvaraj et al., 2020). Moreover, during a HF scenario where there is low oxygen concentration, the failing heart shows a preferential use of glucose as the main energy substrate (Lopaschuk et al., 2021). There is a consensus with regards to the glucose contribution during the heart failure stage. However, whether the fatty acid oxidation capacity of the mitochondria declines or is still maintained remains unclear in the literature. This shift in fuel to glycolytic pathways is energetically more efficient since more ATP is produced per mole of oxygen during carbohydrate oxidation. In the same study by *Wai et al* previously mentioned, we demonstrated a metabolic alteration led by a glucose uptake accumulation in cYKO mice with developed DCM when compared to WT animals (Wai et al., 2015). Whether this switch precedes HF or is a consequence of a decline in cardiac function remains controversial.

In the literature, targeting glucose utilization has shown promising results in mitigating cardiac remodeling and improving cardiac function (Tran and Wang, 2019). Enhancing glucose uptake by GLUT1 and GLUT4, cell membrane glucose transporters, was reported to improve heart function in mice (Liao et al., 2002, Faramoushi et al., 2016).

In humans, small clinical trials have reported the use of dichloroacetate (DCA), a pyruvate dehydrogenase kinase (PDK) inhibitor which increases glucose oxidation via enhancing PDH activity, as a promising treatment for improving cardiac contractility (Li et al., 2019). However, its use in congestive heart failure did not show beneficial effects. On the other hand, inhibiting fatty acid oxidation, for example inhibiting CPT2-dependent FAO proves detrimental for cardiac function (Makrecka-Kuka et al., 2020).

Interestingly, in the work published by our group, administration of a high-fat diet (HFD) was able to restore cardiac function, preventing the initial stage of DCM. In another study, hypertensive rats with different percentages of fat in their diet were seen to have better cardiac remodeling and less contractile dysfunction under the highest percentage of fat used (Okere et al., 2006), revealing the importance of dietary fatty intake. Nonetheless, the effects of fat in the heart remain controversial. Many studies report the use of HFD as a promoter of cardiac dysfunction (Kesherwani et al., 2015, Ternacle et al., 2017, Tong et al., 2019). Also, administration of a ketogenic diet (low carbohydrate) was shown to stimulate ketone oxidation and slightly improve cardiac outcome, probably as a stress defense (Horton et al., 2019). Overall, the use of dietary approaches may prove useful as a potential strategy to modulate metabolism and cardiac function in the failing heart, one of the main objectives of this thesis.

The role of autophagy in the heart

In general, the limited capacity of cardiomyocytes to regenerate is widely accepted, thus limiting cell renewal during a normal lifespan (Eschenhagen et al., 2017). This complication results in the accumulation of damaged cells and inevitably leads to cell death with no possibility of cell replacement. Hence, maintaining an intact *recycling* machinery in the cardiomyocyte is essential for the heart. It is therefore expected that aged cardiomyocytes present deficiencies in maintaining cell homeostasis due to cardiac aging (increased ROS, dysfunctional mitochondria, inflammation, impaired calcium homeostasis, apoptosis, telomere dysfunction, among others) (Bernhard and Laufer, 2008, Ruiz-Meana et al., 2020).

Depending on the physiological stress condition, the cell maintains homeostasis and quality control by two main *recycling* machineries that act in parallel: the ubiquitin (Ub)-proteosome system (UPS) and autophagy (Kocaturk and Gozuacik, 2018). While the UPS system is involved in the degradation of the major parts of cytosolic and nuclear proteins, autophagy is a degradation process that removes whole damaged organelles.

Defects in UPS can compromise degradation steps and contribute to cardiac disorders (Day, 2013). In desmin-related cardiomyopathy (DRC), mutations in the muscle-specific intermediate filament protein desmin promote protein aggregation, provoking an insufficient protein quality control (PQC) leading to cardiac disease (McLendon and Robbins, 2011).

In general, increased aggregates of ubiquitinated proteins are observed in hearts from animals suffering from a cardiac dysfunction (Hein et al., 2003, Depre et al., 2006, Birks et al., 2008), underscoring the importance of the UPS in cardiac pathogenesis and the need for research into new therapies targeting proteome deficiencies to treat heart disease.

Autophagy can be defined as a regulated process of degradation and recycling of long-lived, dysfunctional and/or damaged organelles. Under physiological conditions, autophagy remains at low levels to play a role in the normal clearance of aggregates that can cause cellular dysfunction. Autophagy is essential for maintaining mitochondrial function, as it prevents the accumulation of damaged mitochondria (mitophagy) (Chen et al., 2020). Disruption of the autophagy pathway in a cardiac context has been described in response to stresses, such as ischemia/reperfusion, exercise after fasting, and in HF (Kaludercic et al., 2020). The dual role of autophagy in the heart is yet to be clarified. However, it is generally accepted that autophagy in the heart under stress plays a role in the cell survival mechanism (although an excess of self-eating via this pathway may become part of the process of cell death). It is also known that intracellular Ca^{2+} regulates autophagy positively or negatively (Sun et al., 2016). Moreover, even though autophagy is maintained at very low levels, it can be rapidly induced within minutes upon starvation (Shang et al., 2011).

Based on the type of cargo delivery, there are three major types of autophagy in mammals (Feng et al., 2014): 1) Microautophagy, which consists of the direct uptake of cellular constituents by the invagination of the lysosomal limiting membrane, 2) Macroautophagy, in which whole regions of the cytosol are sequestered by a double membrane vesicle (autophagosome) and delivered for degradation and 3) Chaperone-mediated autophagy (CMA), in which only soluble proteins, and not whole organelles, are degraded. It differs from the other two with respect to the mechanism for cargo selection and delivery for lysosomal degradation.

Among the three of these, macroautophagy (herein referred to as autophagy) plays a major physiological role and it is better studied. Autophagy is a complex process consisting of sequential steps of formation of autophagosome, fusion between autophagosome and lysosome and efflux of degraded products to the cytoplasm. Autophagosome formation requires the expression of autophagy related genes (ATG-**Figure 2**). It is well established that autophagy in mammalian cells is initiated by a membrane nucleation step that requires the ubiquitin-like kinase (ULK1) complex with another regulatory complex that includes Beclin 1 (also known as Atg6) and a multimerization complex (Russell et al., 2013).

The next steps of vesicle nucleation and assembly are regulated by Beclin 1. Depending on the interaction's partners, Beclin 1 can activate or suppress autophagy (Kang et al., 2011). In the absence of a stress stimulus, anti-apoptotic Bcl2 protein physically interacts with Beclin 1 and inhibits its activity.

The conversion of microtubule-associated protein 1 light chain (LC3) from LC3B-I to LC3B-II by Atg4 is regarded as a crucial step in autophagosome formation (**Figure 2**). The LC3B-II form becomes conjugated to a lipid molecule, phosphatidylethanolamine (PE). This process will further continue until completion of the autophagosome. Then LC3B is released from the exterior surface of the membrane and becomes recycled. By this means, LC3B-II can serve as an analytical marker for monitoring autophagic flux (Loos et al., 2014). Another protein involved in the autophagy process is p62, also called sequestosome 1 (SQSTM1), a multifunctional ubiquitin receptor. Among its functions, p62 is a stress-responsive protein and its expression is tightly controlled at both the transcriptional and post-transcriptional levels (Liu et al., 2016). Emerging evidence places p62 as a critical sensor of proteotoxic stress in cardiomyocytes (Su and Wang, 2011). Consequently, p62 may also be used as a marker to study autophagic flux (Yoshii and Mizushima, 2017).

The newly formed autophagosome along with the cargo to be degraded finally fuses with lysosomes, formed by TFEB, a master gene of lysosome biogenesis (Di Malta et al., 2019), to form autolysosomes whose content is subsequently degraded by lysosomal enzymes. Cytoskeletal microtubules regulate and facilitate the fusion of lysosomes with autophagosomes by transferring the autophagosome to lysosomal proximity. Then, lysosomal membrane proteins LAMP1/2 and Rab7 and other endosomal sorting complexes mediate the process of fusion (Cui et al., 2020) (**Figure 2**).

Subsequently, the transient formation of autolysosome provides an acidic environment required for optimal activity of lysosomal hydrolases (referred to as cathepsins) and cargo degradation.

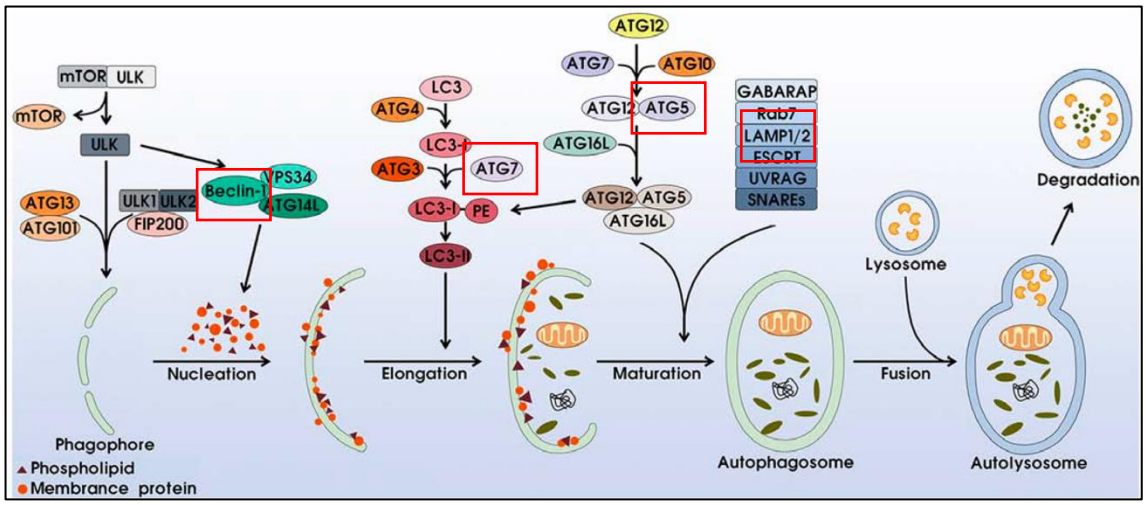

Figure 2. Schematic overview of the autophagy process: nucleation, elongation, maturation, and fusion with the lysosome. Outlined in red are examples of ATG genes whose dysregulation negatively affect heart function (Jin et al., 2017).

Autophagy is a master regulator of cellular wellness. Indeed, tinny deregulations can result in serious pathological conditions. In fact, it has been demonstrated that mutations of ATG genes or other autophagy main players result in cardiac dysfunction in animal models. Below we refer to some examples (Kaludercic et al., 2020):

Mutation	Animal model	Phenotype	Ref
Cardiac Atg5$^{-/-}$	Mice	• Autophagosome formation interrupted • Fibrosis • Mitochondrial structural abnormalities • DCM	(Taneike et al., 2010)
Cardiac overexpression Atg6 (Beclin1)	LPS-induced inflammation mice	• Promotes autophagy	(Sun et al., 2018)
Beclin1$^{+/-}$	TAC-induced pressure overload	• Diminishes cardiomyocyte remodelling • Decreases autophagy • Decreases cardiac dysfunction	(Zhu et al., 2007)
Lamp2$^{-/-}$	Mice	• Obstructed autophagosome-lysosome fusion • Hypertrophy • Premature mortality	(Nishino et al., 2000, Tanaka et al., 2000)

Parkin$^{-/-}$	AMI-mice	• Impaired mitophagy • Cardiac dysfunction	(Hoshino et al., 2013)
Cardiac Atg7$^{-/-}$	AMI-mice	• Aggravates autophagy • Severe contractile dysfunction • Myofibrillar disarray • Vacuolar cardiomyocytes	(Li et al., 2016b)

Table 1. Example of genetic mouse models for the study of macroautophagy in the cardiac system. LPS: lipopolysaccharide; TAC: transverse aortic constriction; AMI: acute myocardial infarction

The double-edged sword of autophagic flux in cardiovascular disease

As previously mentioned, immunoblotting of LC3 and p62 can be utilized to monitor autophagosome synthesis or degradation. However, these *steady-state* measurements only represent a single time frame. To better measure autophagic turnover, it is necessary to report the kinetics and flux of the autophagic system: autophagic flux. Autophagy flux is defined as the whole process of cargo moving through the autophagy system, from phagophore formation to autophagosome formation, autophagosome-lysosome fusion, and eventually cargo degradation plus recycling.

Overall, the existence of a causal relationship between impaired autophagy and cardiac disease is clear. Thus, modulation autophagy appears as an excellent therapeutic target to promote healthy cardiac aging. Among all the different options for modulating autophagy, there are life-style modifications (exercise, intermittent fasting, caloric restriction, fasting mimicking diets), pharmacological treatment (spermidine, resveratrol, metformin, NAD precursors, rapamycin) and genetic approaches (Galluzzi et al., 2017). The following figure shows an example of activators (blue) and inhibitors (red) of the different parts of the autophagic process.

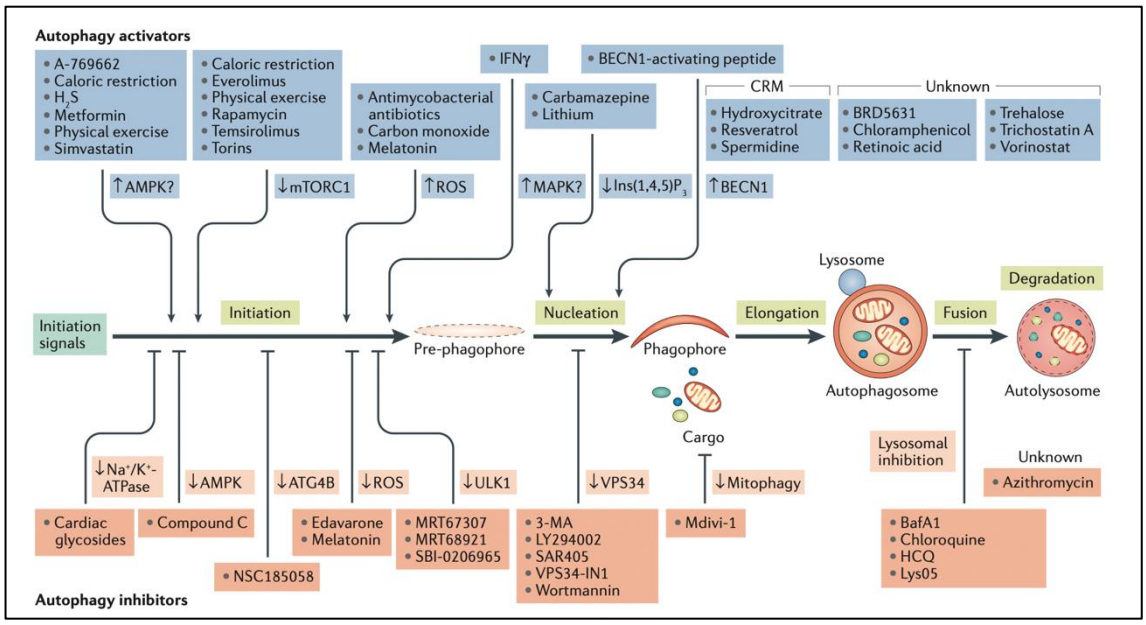

Figure 3. Pharmacological and nutritional interventions during autophagy process. Autophagy activators in blue and autophagy inhibitors in red (Galluzzi et al., 2017).

Different approaches have been described as capable of modulating (enhancing or inhibiting) the autophagic flux targeting different steps of the process: formation, fusion, or degradation. However, considerations should be taken as to how autophagy modulators (activators and inhibitors) can be beneficial according to the underlying defect in the flux:

1) *Scenario where excessive autophagy activation is involved in the development of the disease.* This can lead to excessive degradation of critical cellular organelles, and ultimately cell death. For example, during left ventricular (LV) pressure unloading (hypertrophy), there is a robust increase in autophagy, a decline in mitochondrial mass and function and early mortality (Cao et al., 2013, Hariharan et al., 2013). Inhibition of autophagic flux by targeting upstream steps by modulators of autophagosome formation could be a safe intervention. *Cao et al.,* demonstrated that suppression of autophagy by histone deacetylase inhibitors attenuates cardiac hypertrophy, improving cardiac function. Several studies suggest the dual role of autophagy during I/R, in which autophagy activation plays a protective role during ischemia but during reperfusion may not be protective. For instance, inhibition of autophagy during the reperfusion phase is accompanied by a significant reduction in infarct size and cardiomyocyte apoptosis in *Beclin* $1^{-/+}$ mice (Matsui et al., 2007).

2) *Scenario where autophagy inhibition is involved in the development of the disease*. In this scenario, any intervention activating autophagy could improve prognosis. Nutritional approaches such as caloric restriction or intermittent fasting have been shown to alleviate this defect. However, in this second scenario of autophagy inhibition participating in the pathophysiology of the disease, the step where the flux is inhibited has implications: 1) when autophagy is blocked upstream of autophagosome formation a limited number of autophagosomes are produced. Any intervention promoting the formation of autophagosomes should have a beneficial impact on the disease. Conversely, interventions targeting end-steps of the flux (i.e., lysosomal degradation) may have no impact on the disease progression. 2) when autophagy is blocked downstream of autophagosome formation because of a lysosomal defect, sufficient autophagosomes are produced thus further boosting autophagosome formation should not have any benefit or even a detrimental effect on the disease by aggravating the process through accumulation of excessive non-degrade autophagosomes. On the contrary, boosting lysosomal degradation may relieve the blockage and mediate beneficial effects. Paradoxically, in these cases of autophagy inhibition by a defect in final steps, inhibition of initial steps of autophagy (upstream formation) can partially alleviate the disease by precluding excessive accumulation of non-degraded autophagosomes. As a role model of the latter situation, in various models of doxorubicin-induced cardiotoxicity, autophagic flux has been shown to be inhibited in the late stages (Li et al., 2016a, Abdullah et al., 2019). The use of the autophagy inhibitor 3-methyladenine (3-MA) has been shown to prevent cell death in cardiomyocytes and improves cardiac function (Lu et al., 2009). Ideally, the combination of upstream autophagy activators and molecules that accelerate lysosomal degradation might overcome multiple forms of autophagic blockade.

3) *Scenario where autophagy activation compensates for disease*.

In some cases, autophagy activation may support compensatory mechanisms, including the degeneration of cells and tissues. For example, during reperfusion after I/R, the detrimental role of autophagy concurs with oxidative stress and the activation of endoplasmic reticulum stress, leading to apoptotic cell death (Sheng and Qin, 2015, Matsui et al., 2007). Although controversially, autophagy plays distinct roles during I/R: autophagy may be protective during ischemia, whereas it may be detrimental during reperfusion.

Endoplasmic reticulum (ER)-mitochondria interplay in heart failure

Mitochondrial Ca^{2+} handling in the heart

The ER is a complex reticular network of membranous organelles. It spans from the nuclear envelope to the plasma membrane. Its functions include the translation and folding of secretory and membrane proteins, lipids biogenesis and the sequestration of Ca^{2+}.

In the heart, Ca^{2+} plays a crucial role in cardiac contractile function (Eisner, 2014). The sarcoplasmic reticulum (SR) represents a specialized form of the ER in cardiomyocytes. In the ER/SR, several proteins are involved in Ca^{2+} uptake and release: Ca^{2+}-ATPases (SERCAs), transporting cytosolic Ca^{2+} into the ER lumen and the inositol triphosphate receptor (IP3R)/ ryanodine receptors (RyRs), in the ER and SR, respectively (Bers et al., 2003) (**Figure 4-orange**).

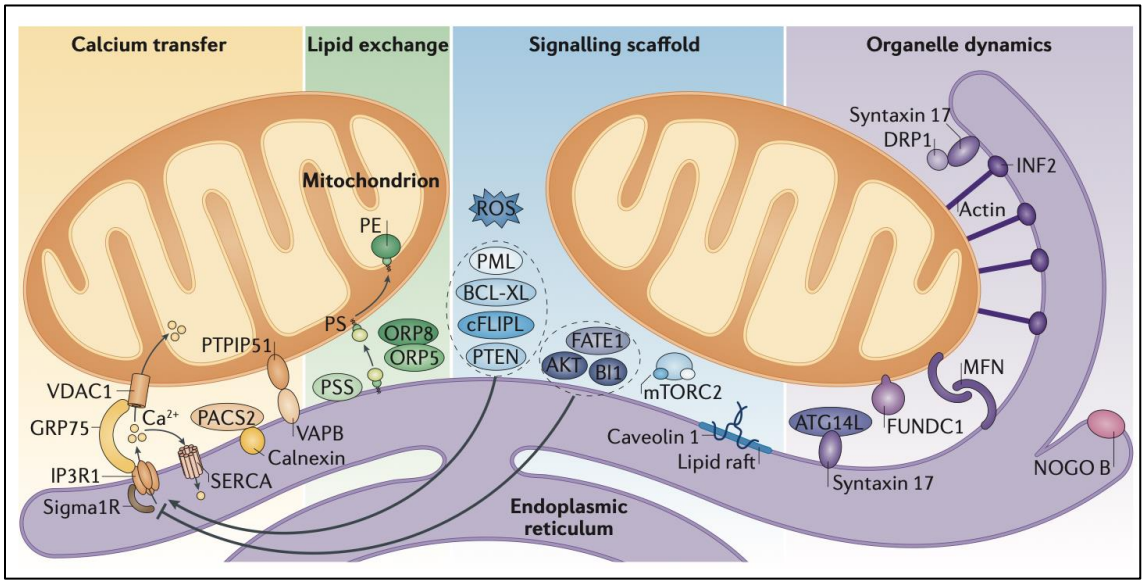

Figure 4. Schematic illustration showing the key components and players in mitochondria-associated membranes (MAMs) (Lopez-Crisosto et al., 2017).

The buffering capacity of the mitochondria converts the mitochondria into the most qualified organelle for its management. In the OMM, there are mitochondrial voltage-dependent anion channels (VDACs) that govern the transport of Ca^{2+} into the intermembrane space of the mitochondria. Among their isoforms, VDAC1 is the most abundant (**Figure 4-orange**). To move across the IMM, a calcium uniporter (MCU) complex is responsible for the passage of ions from the intermembrane space to the matrix.

Ca^{2+} levels in the cytosol remain very low when compared to mitochondrial levels (Xu et al., 2020). Defective Ca^{2+} handling is known to be the central cause of electrical dysfunctions observed during cardiac arrythmias and HF (Luo and Anderson, 2013). Upon I/R challenge, IP3R expression is upregulated, provoking Ca^{2+} overload in mitochondria, activating apoptotic signaling during reperfusion (Joiner et al., 2012). In diabetic cardiomyopathy, alterations between ER and mitochondria reduce the levels of RyR2, decreasing SR Ca^{2+} storage and promoting intracellular Ca^{2+} aberrant signaling contributing to cardiac dysfunction (Yaras et al., 2005).

In cardiomyocytes, Ca^{2+}ATPase 2a (SERCA2a) mediates Ca^{2+} reuptake into the SR. Expression levels of SERCA2a are reduced in failing hearts, inducing ER calcium depletion leading to ER stress (Mekahli et al., 2011, Liu et al., 2011).

Mitochondrial-associated membranes in the heart

Despite having their own functions, mitochondria and ER share the important role of Ca^{2+} homeostasis maintenance. This common feature enables their communication through mitochondrial-associated membranes (MAMs) (Gao et al., 2020).

ER-mitochondria tethering is formed by numerous proteins bridges. The IP3R/RyRs-GRP75-VDAC1 axis. As mentioned above, IP3R/RyRs are in the ER/SR membrane, respectively, and regulate Ca^{2+} release. VDAC1, linked by cytoplasmic GRP75 to ER, uptake Ca^{2+} on the OMM. Finally, calcium ions enter the mitochondrial matrix through MCU. The MFN1-MFN2 axis (**Figure 4-purple**). Interestingly, the fusion role of MFN2 is performed in the OMM (Papanicolaou et al., 2012). Here, it forms a dimmer with MFN1. MFN2-ablation has been shown to reduce SR-mitochondria connections in the heart, developing DCM (Tang et al., 2017, Sun et al., 2019). In MFN2-deficient cells, mitochondrial Ca^{2+} uptake is inhibited due to the disassociation of ER and mitochondria. However, the capacity of Ca^{2+} release from the ER was not affected (Eisner et al., 2017). Other axes conform the association between FUNDC1-IP3R2 and VAPB-PTPIP51 (Xu et al., 2020).

Significantly, upregulation of Ca^{2+} in physiological conditions activates mitochondrial enzymes, which facilitates the TCA cycle and oxidative phosphorylation (Balaban, 2009). The increase of ER-mitochondria proximity increases Ca^{2+} uptake, enhancing electron activity and resulting in elevated ATP synthesis (Rizzuto et al., 2009, Wang et al., 2021a).

In contrast, prolonged or excessive mitochondrial Ca^{2+} overload triggers the opening of the mitochondrial permeability transition pore (mPTP), resulting in mitochondrial swelling and activation of apoptotic pathways (Eisner et al., 2013). Increased Ca^{2+} levels initiate BCL2-associated X protein (BAX), which translocates to the mitochondrial membrane and increases permeability of the mitochondrial membrane (Fraysse et al., 2010). Therefore, MAM's formation, distance and function could be a potential target in the progression of cardiovascular diseases.

ER-mitochondria contact regulates ER stress

ER homeostasis is highly sensitive to perturbations in the cellular environment. In response to changes in the ER homeostasis, the cell activates an adaptive response known as the unfolded protein response (UPR). This UPR response is activated in conditions such as hypoxia, disturbed Ca^{2+} homeostasis, accumulation of misfolded proteins and oxidative stress (Wang et al., 2021a). There are three sensors located in the ER membrane which orchestrate ER stress: the protein kinase R (PKR)-like ER kinase (PERK), activating transcription factor-6 (ATF6), and inositol requiring eznyme-1 (IRE1). Under physiological conditions, these proteins are inactive because their luminal domains remain bound to GRP78. Upon the accumulation of unfolded proteins in the ER lumen, Grp78 dissociates from each of these, causing their activation. GRP78 was found to be increased in patients with heart failure (Okada et al., 2004).

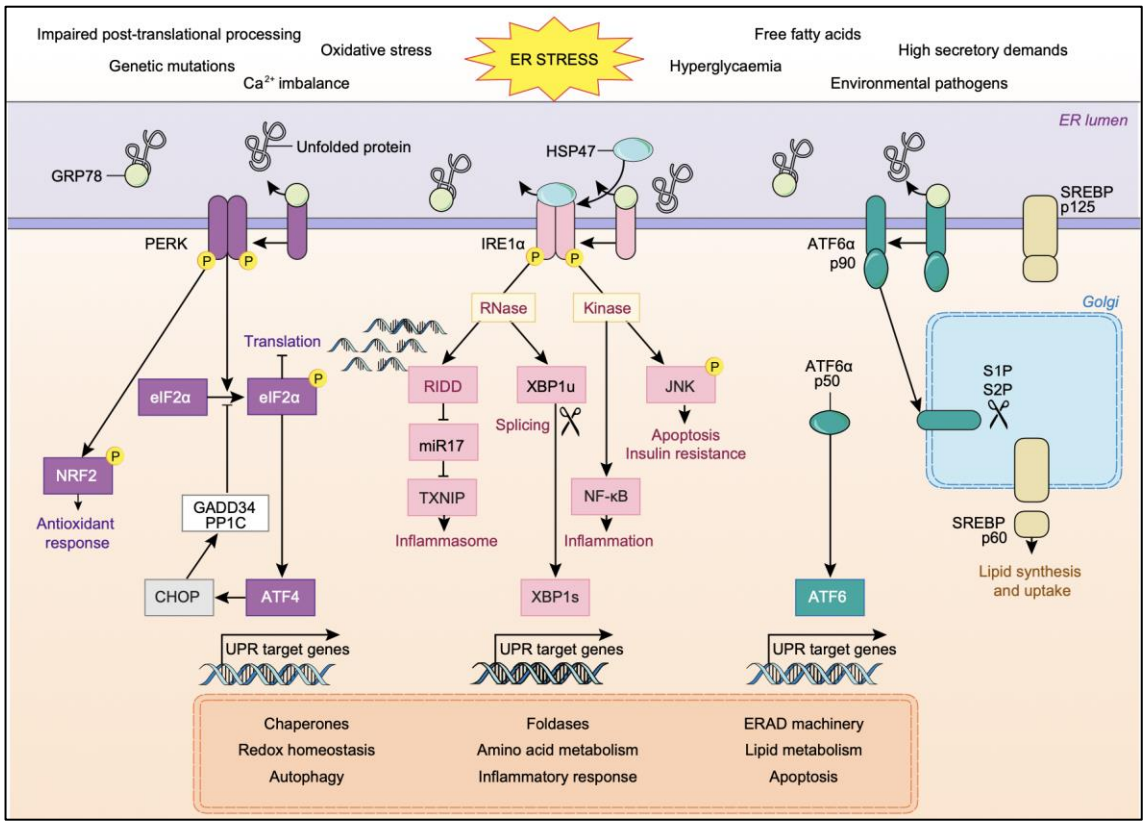

Figure 5. Overview of cascade of the three arms of UPR response (PERK, IRE1a and ATF6) and the biological process affected (Lebeaupin et al., 2018).

PERK dimerizes and becomes auto-phosphorylated, thus activating its cytosolic kinase domain, leading to phosphorylation of eIF2alpha (**Figure 5**). Specific cardiac genetic ablation of PERK showed enhanced cardiac dysfunction after TAC (Liu et al., 2014b, Liu et al., 2014a). Phosphorylation of eIF2 causes inhibition of the general protein synthesis and permits Cap-dependent translation of ATF4. Activation of ATF4 leads to the transcription of genes related to antioxidant response and amino acid synthesis and transports and promotes cell survival. However, ATF4 can also activate the expression of the pro-apoptotic transcription factor C/EBP homologous protein (CHOP) and mediate the ER stress apoptotic pathway (Hu et al., 2018). In fact, *Chop* knockout mice developed less cardiac hypertrophy after TAC (Fu et al., 2010). In the same study by *Liu et al.,* CHOP expression was induced in response to TAC in PERK knockout hearts, giving CHOP a role in apoptosis contributing to heart failure.

Dissociation of GRP78 from ATF6 stimulates translocation of ATF6 to the Golgi where it is processed by site 1 and site 2 protease (S1P and S2P) into an active transcription factor, which switches on transcription of XBP1 mRNA (**Figure 5**).

Dissociation of GRP78 from IRE1 results in dimerization and auto-phosphorylation of IRE1. Thus activated, the endoribonuclease activity of IRE1 leads to processing of unspliced XBP1 mRNA, while its kinase domain recruits TRAF2 and ASK1, leading to activation of JNK (**Figure 5**). *Duan et al.,* demonstrated two miRNas able to inhibit XBP1 in the progression of heart failure (Duan et al., 2015).

Interestingly, ER stress can promote ER-mitochondria contact, enhancing ATP production and Ca^{2+} uptake. This modest increase in stress contributes favourably to the cellular adaptation to ER stress (Bravo et al., 2011). However, when there is persistent ER stress, there is an induction of death mediated by mitochondria Ca^{2+} overload.

ER-mitochondria contacts and mitochondrial dynamics

As mentioned, MFN2, a fusion mitochondrial protein located on the surface of the OMM, also regulates ER morphology and MAMs. Intriguingly, mitochondrial fission at ER-mitochondria contact has been observed prior to DRP1 recruitment. Thus, in the ER-mitochondria contact sites there is a primary fission constriction that may allow DRP1 to induce fission (Friedman et al., 2011). In fact, previous studies show that DRP1 localizes at ER (Pitts et al., 1999). Furthermore, ER-mitochondria contact sites are the positions that mediate mtDNA synthesis and the distribution of the new mitochondria after fission (Lewis et al., 2016, Qin et al., 2020).

ER-mitochondria contacts and autophagy

Most of the lipids that conform organelle membranes are synthesized in association with the ER membrane (van Meer et al., 2008). Autophagy is also involved in the degradation of misfolded ER proteins. It has been established that autophagosome formation (the initial step of autophagy) occurs near the ER (Mizushima et al., 2011). Overexpression of VAPB, a protein involved in UPR response located at the ER membrane, reduces autophagosome formation by enhancing ER-mitochondria contact (Gomez-Suaga et al., 2017). Also, under starvation conditions, autophagy-related protein 14 (ATG14) is recruited to MAMs to stimulate autophagosome biogenesis (Hamasaki et al., 2013).

Autophagy is one of the responders to ER stress. Under these conditions, autophagy is activated via signaling that commonly involves activation of the nutrient energy sensor AMP kinase (AMPK) and inhibition of the mammalian target of rapamycin (mTOR). Generally, conditions that induce ER stress also activate autophagy. However, either ER stress itself can induce autophagy (Yorimitsu et al., 2006, Wiersma et al., 2017) or an impairment/increase of autophagy can promote/decrease ER stress, respectively (Gonzalez-Rodriguez et al., 2014).

Moreover, dysregulation of Ca^{2+} in MAMs leads to autophagy deficiency. This interruption of Ca^{2+} transport from ER to mitochondria causes AMPK translocation to MAMs and the activation of autophagy through BECLIN1. mTORC2, another inducer of autophagy, is in MAMs and regulates its integrity (Colombi et al., 2011). The mechanistic target of rapamycin (mTOR) is a widely studied sensor of nutrient sufficiency. Upon inhibition of mTOR autophagy is inducted, which related mTOR signaling as indispensable for cardiac function after pressure overload (Sciarretta et al., 2018).

ER-mitochondria contacts and apoptosis

An increase in UPR levels can promote cell survival. However, when ER stress is sustained (excessive), the ER apoptotic pathway is activated and promotes apoptosis. Members of the BCL2 family proteins are important during regulation of apoptotic cell death. During ER stress, BCL2 antiapoptotic protein has been shown to be translocated to MAMs, where an increasing Ca^{2+} influx from ER to mitochondria occurs as an adaptive response to further increase mitochondrial bioenergetics (Williams et al., 2016). Either an overexpression of BCL2 (Distelhorst and McCormick, 1996) or a deficiency of BAX and BAK proapoptotic proteins (Wei et al., 2001) confer protection against lethal ER stress. Activation of PERK leads to the induction of CHOP, which, as previously described, is an important element in pro-death signaling. However, the three arms of UPR can induce transcription of CHOP. GADD34, a protein involved in eIF2 dephosphorylation, has been shown to promote apoptosis (Adler et al., 1999).

Once the upstream activation of these proteins has occurred, the Caspase system executes the apoptosis. Among all, caspase 12 (in rodents) (Nakagawa et al., 2000, Szegezdi et al., 2003, Saleh et al., 2006) and caspase 4 in humans.

ER-mitochondria and lipid metabolism

Physical interactions linking ER and mitochondria play a role not only in Ca^{2+} transfer but also in lipid transferring between the two organelles (Rusinol et al., 1994).

MAMs are enriched in cholesterol and sphingolipids, related to the accumulation of caveolin-1 (Sala-Vila et al., 2016). MAMs promote the formation of the substrates of structural biological membranes: phosphatidylcholine, PE, and phosphatidylserine. In fact, cardiolipin, the most abundant IMM phospholipid, is firstly synthesized in the ER to further be modified in mitochondria to exert its cardioprotective effect (Osman et al., 2011). Cardiolipin strongly interacts with the membrane proteins of the IMM, including the MCU (Ghosh et al., 2020). Individual levels of cholesterol esters, PEs, and triacyclglycerols have been associated with cardiovascular diseases (Stegemann et al., 2014).

Nutritional strategies to shape cardiovascular system fitness

Non-pharmacological strategies for HF patients are a moving target. To date, studies underpinning nutritional recommendations for HF remain limited. Among all, the Mediterranean diet (PREDIMED study)- an intervention known to decrease the incidence of cardiovascular events with nuts and olive oil (Estruch et al., 2018) showed that major cardiovascular events were lower in patients assigned to a supplemented-Mediterranean diet than among those with a reduced-fat diet. Another intervention, the dietary approach to stop hypertension (DASH) diet (Guo et al., 2021), emphasizes the consumption of whole grains, fruit, vegetables and low-fat, among others. This antioxidant dietary approach was mainly addressing HF-induced inflammation and ROS generation (Aleksandrova et al., 2021).

Accumulated evidence links diets rich in carbohydrates with metabolic syndrome (Hyde et al., 2019, Liu et al., 2019). The restriction of sugar in the diet has been proposed as a therapy for metabolic disease, such as Non-Alcoholic Fatty Liver Disease (Cohen et al., 2021), insulin resistance or type 2 diabetes (Janket et al., 2003). Studies show that following a low-carbohydrate diet shares common weight loss benefits with low-fat diets (Hu et al., 2012, Bazzano et al., 2014). Special attention is made to the type of fat eaten under a low carbohydrate diet, in which fat is not restricted. Therefore, the use of this dietary restriction has emerged as a nutritional strategy for fighting cardiovascular diseases. During recent years, low-protein diets based on a reduction in sulfur-amino acids has been used for specific disease conditions, such as metabolic disorders or

kidney disease (Handoom et al., 2018, Watanabe, 2017). The use of this diet has also been linked to a reduction in the risk of cardiovascular events (Santesso et al., 2012, Moatt et al., 2020).

Low-protein intakes maximize lifespan and high protein intakes maximize reproduction (Han and Ren, 2010). The life-prolonging effects and the decrease in age-associated morbidity is a common pattern of calorie restriction practice (Han and Ren, 2010).

Dietary activation of autophagy

Caloric restriction (CR) is defined as a reduction in food intake without malnutrition. Many studies have related the importance of dietary patterns, specifically, calorie restriction with cardiac function prognosis (Weiss and Fontana, 2011, de Lucia et al., 2018). CR has been described as having cardioprotective effects and improving functional outcomes in animal models (Sandesara and Sperling, 2018) and in humans (Dolinsky and Dyck, 2011). The molecular mechanism responsible for this cardioprotection involves reduced inflammation (Ahmet et al., 2011), myocardial fibrosis (Escobar et al., 2019), or oxidative stress, among others. It is also known to reduce the nutrient sensing pathway mTOR, promoting the elimination of damaged organelles (autophagy) (Bagherniya et al., 2018). Modulation of autophagy is a primary mechanism underlying the lifespan and health promoting of CR.

It is yet to be clarified whether the energy restriction protocol benefit is also observed in a more time-restricted window, which could be linked to circadian rhythm leading it to be thought that it is not about not eating but about when. In this regard, a form of time-dependent CR is intermittent fasting (IF). IF involves significant energy restriction on alternate time frames with *ad libitum* consumption in non-fasting periods. Preclinical and clinical studies have confirmed the therapeutic effect of the IF diet on a wide range of chronic disease, including CVD: it reduces body weight (Grajower and Horne, 2019), type II diabetes (Grajower and Horne, 2019) or damage by myocardial infarction (Okoshi et al., 2019). Although the mechanisms are not fully understood, the beneficial influence of IF in the heart suggests that autophagy could also play a significant role in maintaining cardiac homeostasis in this scenario (Nishida et al., 2009). Under normal conditions of nutrients, low levels of autophagy help to maintain cellular homeostasis. However, during starvation or periods of energy deprivation, autophagy is induced in an attempt to supply cellular nutritional demands.

General summary of the state of the art

DCM represents an intervention-targetable disease in which mitochondria remains a critical organelle and its malfunction in any aspect (morphology, dynamism, or metabolism) negatively affects cardiac function. In general, cells are prepared to replace themselves when an error occurs, and apoptosis takes place. However, the poor heart regenerative capacity results in a total loss of cardiomyocytes. Thus, maintaining good cardiac fitness is essential. Autophagy is one of the mechanisms responsible for maintaining cell homeostasis, thus being vital in the heart. In fact, it is well known that deficiencies in autophagic flux impair cardiac function. Whether a dysregulated autophagic flux is the primary damage remains unknown. ER stress has been tightly associated with an impaired autophagy through its interaction with mitochondria. Any of these molecular pathways are plausible for being targeted with activators and/or inhibitors being also a useful tool for studying their impact in cardiac function. In fact, not only pharmacological interventions but also nutritional approaches have been used to tackle impaired autophagy and ER stress. In view of the current state of the art, the overall hypothesis of this work is that all the above-mentioned pathways play a relevant role in the development of DCM associated with *Yme1l* cardiac genetic ablation, and so different therapeutic strategies, such as nutritional interventions, to tackle these defects would be beneficial.

Main motivation of this study

DCM is the principal cause of clinical HF in young and middle-aged individuals worldwide. The lack of specific therapies has led us to investigate new strategies for its prevention. In addition, the molecular bases of the disease are yet to be fully understood. Previous studies have reported the role of mitochondria as one of the main disease contributors. For this purpose, our group established a mice model of DCM in which cardiac genetic deletion of the mitochondrial protease *Yme1l* progress to HF. However, the molecular mechanisms by which this genetic ablation develops to DCM have yet to be shown. In this thesis, we seek to uncover new potential roles of YME1L in development of the disease and the mechanism behind DCM. Moreover, due to our group's interest in translational medicine, we investigate in this mouse model the pre-clinical use of different nutritional approaches for targeting this untreatable disease.

Objectives

The **overarching goal** of this work is to characterize the mechanisms by which cardiomyocyte *Yme1l* ablation leads to DCM and the development of interventions to treat/prevent HF.

The overarching goal will be addressed through the following **specific aims**:

1. To delineate the molecular basis responsible for late-onset DCM upon genetic ablation of *Yme1l*. For this aim, we propose the following 3 specific objectives:

    a. To determine the impact of *Yme1l* ablation on cardiomyocyte metabolic pathways and their association with HF initiation and progression.

    b. To study the role of YME1L in cardiomyocyte quality control mechanisms (mitophagy and autophagy).

    c. To evaluate the role of YME1L in mitochondria-to-ER interplay and the impact of these on HF development.

2. To test nutritional interventions that could alleviate *Yme1l* ablation-associated HF. For this aim, we propose the following 2 specific objectives:

    a. To compare different dietary approaches based on variable fat concentrations (i.e., high fat, non-fat, low fat) as strategies able to ameliorate DCM and HF development in mice lacking YME1L in cardiomyocytes.

    b. To study the synergistic effect of the best dietary approach identified in (a) and intermittent fasting on their capacity to prevent development of DCM and HF in mice lacking YME1L in cardiomyocytes.

Materials and Methods

Mice handling

Yme1l cardiac specific knockout mice (cYKO) were generated as described in (Wai et al., 2015). Experimental procedures were approved by the CNIC animal Care and ethics committee and Madrid regional authorities (PROEX 099/16 and 176.3/20) and pursuant to EU Directive 2010/63EU and Recommendation 2007/526/EC, enforced in Spanish law under Real Decreto 53/2013. Mice were maintained under pathogen-free conditions in a temperature-controlled room and a 12-hour light-dark cycle at the CNIC animal facility. Water was available *ad libitum.* For the purpose of this thesis, different diets were administered *ad libitum* once the animals were adult onwards. The composition of each diet was as follows:

	Non Fat Diet E15100-147	**Chow CNIC Diet Lab5k54**	**Low Fat Diet** E15112-34	**High Fat Diet** E15742-347
Crude protein, %	20.8	19	20.7	24.1
Crude fat, %	0.2	4.6	10.2	34
Crude fibre, %	5	4.2	5	6
Crude ash, %	5.6	6.3	5.9	6
N free extracts, %	63.6	55.5	53.9	27.1
Starch, %	45	40.7	33.4	1.1
Sugar/dextrines %	16.8	~13	18.3	23.8

Table 2. Diet composition representing the percentage (%) of macronutrients and starch. N=nitrogen

The data from this table was extracted from the datasheet of each diet. The data regarding Sugar/dextrines from the chow CNIC diet was calculated considering that N free extracts should be the sum of starch + sugar + other components.

Intermittent fasting-feeding regimens

cYKO mice were subjected to different intermittent fasting protocols. The periodicity and feeding regimen after fasting was as described below.

	Energy restriction for two consecutive days and *ad libitium* intake of chow diet for other five days	Eating days-*ad libitum* chow diet intake Fasting days-energy restriction	Energy restriction for two consecutive days and *ad libitium* intake of NFD for other five days	preNFD for 10 weeks. Energy restriction for two consecutives days and *ad libitum* intake of NFD for other five days
Days of the week	**2Fast:5CD**	**2Fast:1CD:2Fast:2CD**	**2Fast:5NFD**	**NFD+2Fast:5NFD**
Monday	Fast	Fast	Fast	Fast
Tuesday	Fast	Fast	Fast	Fast
Wednesday	Eat-CD	Eat-CD	Eat-NFD	Eat-NFD
Thursday	Eat-CD	Fast	Eat-NFD	Eat-NFD
Friday	Eat-CD	Fast	Eat-NFD	Eat-NFD
Saturday	Eat-CD	Eat-CD	Eat-NFD	Eat-NFD
Sunday	Eat-CD	Eat-CD	Eat-NFD	Eat-NFD

Table 3. Overview of the feeding regimens used.
CD: Chow diet, NFD: non-fat diet

Echocardiographic analysis

Transthoracic echocardiography was blinded performed by an expert operator using a high-frequency ultrasound system (Vevo 2100, Visual Sonics Inc., Canada) with a 30-MHz linear probe. Two-dimensional (2D) and M-mode (MM) echography were performed at a frame rate above 230 frames/sec, and pulse wave Doppler (PW) was acquired with a pulse repetition frequency of 40 kHz. Mice were lightly anesthetized with 0.5-2% isoflurane in oxygen, adjusting the isoflurane delivery trying to maintain the heart rate at 450±50 bpm. Mice were placed in supine position using a heating platform and warmed ultrasound gel was used to maintain normothermia. A base apex electrocardiogram (ECG) was continuously monitored. Images were transferred to a computer and were analysed off-line using the Vevo 2100 Workstation software.

Systolic function analysis

For left ventricular (LV) systolic function assessment, parasternal standard 2D and MM, long and short axis views (LAX and SAX view, respectively) were acquired. LV ejection fraction, LV fractional shortening, and LV chamber dimensions were calculated from these views.

Positron Emission Tomography-Computed Tomography (PET/CT)

^{18}F-fluorodeoxiglucose (^{18}F-FDG) PET for imaging glucose uptake

PET-CT studies were performed with a small-animal PET/CT scanner (nanoScan, Mediso, Hungary). CT study was acquired 30 minutes after intravenous administration of 16,8 ± 0.6 MBq of 18F-FDG using an X-ray beam current of 178 μA and a tube voltage of 45 kVp and reconstructed using a Ramlack algorithm. After the CT scan, PET data were collected for 30 minutes and reconstructed using Teratomo 3D algorithm (Mediso, Hungary) with 6 subsets and 4 iterations, in an 85x65x236 matrix (voxel dimensions of 0.4mm).

For the PET-CT acquisition, mice were anesthetized using isoflurane 2% and 1.8 L/min oxygen flow. Ophthalmic gel was placed in the eyes to prevent drying. Glucose was measured before the 18F-FDG administration.

^{18}F-Fluoro-6-thia-heptadecanoic acid (^{18}F-FTHA) synthesis and PET for imaging fatty acid utilization

^{18}F-FTHA was synthetized as previously described (Degrado, 1991). Briefly, ^{18}F-FTHA is synthetized by nucleophilic radiofluorination of the precursor benzyl-14-(R,S)-tosyloxy-6-thiaheptadecanoate. Mixture of Kryptofix 222, K_2CO_3 (26.7 mg/mL) and commercial $^{18}F^-$ (ITP, K_2CO_3 as solvent) was dried at 100ºC under N_2 atmosphere. The precursor solution (1 mg in 0.5 ml acetonitrile) was added and allowed to react for 8 min at 90ºC under N_2 atmosphere. Hydrolysis of the benzyl protecting group was carried out by 0.2M KOH addition and heat. The solution was then neutralized with acetic acid and purified by C18 Sep-Pack. In order to make it injectable for mice, the purified product is reformulated by ethanol evaporation and PBS 1x addition, reaching a 20% ethanol solution in PBS 1x.

Purity was evaluated by high-performance liquid chromatography (HPLC) on a C18 column using methanol:water:acetic acid (88:12:0.4) as eluent at a flow rate of 0.8 ml/min.

In-vivo PET/CT imaging was performed in WT and cYKO mice. Before the imaging studies, mice had free access to food and water. After being anesthetized (2% isoflurane in 100% oxygen) each mouse received 8.2 ± 0.5 mBq of ^{18}F-FTHA intravenously.

PET/CT imaging (Mediso, Hungary) was carried out for 20 minutes immediately after the administration of the radiotracer. Four frames of 5 minutes were reconstructed to obtain the images. All data were corrected for dead time, decay, and photon attenuation.

PET imaging analysis

Images were analysed with AMIDE software. Quantitative analysis was performed by spherical regions of interest with voxel dimensions of 0.2 × 0.2 × 0.2 mm delineated on the coronal axis of the heart of each animal to capture the maximum ^{18}F-FDG uptake value. Standardized uptake value (SUVmax; proportional to the glucose metabolism) was calculated as the maximum ^{18}F-FDG or ^{18}F-FTHA uptake value normalized by the injected activity and the body weight of the animal.

Metabolic cages

Mice were handled under controlled temperature and lighting. Animals had free access to water and food. After an adaptation period of the animals, mice were monitored for 3 days in individual metabolic cages (Oxyletpro Physiocage) for food and water intake, energy expenditure, O_2/CO_2 respiration, respiratory exchange ratio and physical activity. Data was extracted and analysed with Metabolism 3.0 software. All data was normalized for body weight (kg.). For illustration, data is shown in day (white) and night (blue) cycles in a complete period of 44 hours.

Heart mitochondria isolation

Mice were sacrificed by cervical dislocation, animals were placed in a supine position, ventral thoracic regions were wiped with 70% ethanol. An incision was made on the descending aorta to exsanguinate and then two incisions were made in the heart to avoid blood accumulation inside the heart.

The heart was dissected and briefly washed with ice cold isolation buffer (IB) (Sucrose 275 mM, Tris base 20 mM, EGTA 1mM, pH 7.2) to remove excess blood. The heart was placed over a glass petri dish on ice and was immediately cut into small pieces with a #10 bistoury blade. The small pieces of tissue were placed inside a 2 ml glass tube on ice along with 2ml of IB plus Trypsin 100 µl/ml (Dutscher X0930), the tissue was gently homogenized with a PTFE grooved pestle for tissue grinder for 4 min in ice. The grinder was reshaped to avoid friction between the glass and the grinder allowing smooth homogenization and to avoid the generation of air bubbles.

Trypsin was inactivated with 8 ml of IB plus 0.025 % BSA fatty acid free (Sigma-Aldrich A6003). The suspension was transferred into a 15 ml centrifugation tube and centrifuged at 1000 x g at 4 C for 10 minutes. The supernatant containing mitochondria was collected and transferred into a 15 ml fresh tube for a second centrifugation at 32000 x g at 4 C for 15 minutes, the supernatant was discarded, and the crude mitochondrial pellet was gently resuspended in 100 µl of IB + BSA.

High-resolution respirometry

Oxygen consumption was measured by high-resolution respirometry (Oxygraph-2K, OROBOROS Instruments, Innsbruck, Austria). The oxygraph consists of a two-chamber respirometer with a peltier thermostat and electromagnetic stirrers. Fresh isolated mitochondria were incubated in a potassium medium containing 0.5 mM EGTA, 3 mM $MgCl_2$-$6H_2O$, 20 mM taurine, 10 mM KH_2PO_4, 20 mM HEPES, 200 mM sucrose, and 1g/l BSA, adjusted to pH 7.1 with KOH at 30°C. The medium had previously been equilibrated with air in each chamber completely open (set at 2 mL) at 37°C and stirred at 750 rpm until a stable signal was obtained for calibration at air saturation. A final concentration of 0.3 mg/mL of protein content in the respiratory buffer was used for the measurements. A protocol was developed for measurement of the different mitochondrial chain respiratory states, as follows. After closing the chamber, an initial state 2 or routine was measured in the presence of 5 mM malate and pyruvate, substrates for the complex I, which correspond to the basal respiration in absence of ADP. Active respiration (state 3) was then initiated by adding 2.5 mM ADP promoting a quick response of the ETC coupled to the oxidative phosphorylation translated into a rapid increase of oxygen consumption until all ADP was phosphorylated to ATP. Then oligomycin was added to inhibit ATP-synthase called mitochondrial respiratory state 4 or leak state, which corresponds to a non-phosphorylating resting state. After that, titrations of FCCP were added to measure uncoupled state.

Finally, complex III activity was inhibited by the addition of 2.5 µM antimycin A. The data was obtained at 0.2-s intervals using a computer-driven data acquisition system (Datlab, Innsbruck, Austria).

H_2O_2 flux, ATP production and extramitochondrial Ca^{2+} movement were simultaneously assessed with respirometry in the O2k-Fluorometer. H_2O_2 flux was measured using the H_2O_2-sensitive probe Amplex® UltraRed. 10 µM Amplex® UltraRed (AmR), 1 U/mL horse radish peroxidase (HRP) and 5 U/mL superoxide dismutase (SOD) were added to the chamber. Calibrations were performed with H_2O_2 repeatedly added at 0.1 µM steps.

Measurement of ATP production was performed using the fluorophore Magnesium Green™ as previously described in (Cardoso, 2021). CaGreen-5N, a single wavelength fluorescent dye, was used to measure extramitochondrial Ca^{2+} as performed by (Naszai et al., 2019).

Adult mice ventricular myocytes isolation

The protocol for adult mouse ventricular myocytes is described here (Garcia-Prieto et al., 2014). Briefly, Animals were euthanized with CO_2. Once pedal pinch reflexes were completely inhibited, animals were placed in a supine position and ventral thoracic regions were wiped with 70% of ethanol. The heart was quickly removed, cannulated through ascending aorta, and mounted on a modified Langendorff perfusion apparatus. The heart was retrogradely perfused for 5 min at room temperature with Perfusion Buffer [NaCl (113 mmol/L); KCl (4.7 mmol/L); KH_2PO_4 (0.6 mmol/L); Na_2HPO_4 (0.6 mmol/L); $MgSO_4$-$7H_2O$ (1.2 mmol/L); $NaHCO_3$ (12 mmol/L); $KHCO_3$ (10 mmol/L); Phenol Red (0.032 mmol/L); HEPES-Na Salt (0.922 mmol/L); taurine (30 mmol/L); glucose (5.5 mmol/L); 2,3-butanodione monoxime (10 mmol/L), pH 7.4]. Enzymatic digestion was performed with digestion-buffer [perfusion-buffer with Liberase™ (0.2 mg/mL); Trypsin 2.5% (5.5 mmol/L); DNase (5x10-3 U/mL) and $CaCl_2$ (12.5 µmol/L) for 20-25 min at 37ºC. At the end of the enzymatic digestion, both ventricles were isolated and gently disaggregated in 5 mL of digestion buffer. The resulting cell suspension was filtered through a 100µm sterile mesh (SEFAR-Nitex) and transferred for enzymatic inactivation to a tube with 10 mL of stopping-buffer-1 [perfusion-buffer supplemented with fetal bovine serum (FBS, 10% v/v) and $CaCl_2$ (12.5 µmol/L).

After gravity sedimentation for 20 min, cardiomyocytes were resuspended in a stopping buffer-2 containing lower FBS (5% v/v) for another 20 min. Cardiomyocytes Ca^{2+}-reintroduction was performed in a stopping buffer-2 with two progressively increased $CaCl_2$ concentrations (112 μmol/L and 1 mmol/L). Cells were resuspended and allowed to decant for 15 min in each step, contributing to the purification of the cardiomyocyte suspension.

For imaging studies, the homogenous suspension of rod-shaped cardiomyocytes was then resuspended in M199 supplemented with Earle´s salts and L-glutamine, penicillin-streptomycin (1%), 0.1x insulin-transferring-selenium-A, bovine serum albumin (BSA, 2g/L), blebbistatin (25μmol/L) and FBS (5%). Cells were plated in the corresponding plate precoated with 200ul of mouse laminin (10mg/mL) in phosphate-buffer saline (PBS) for at least 1 hour.

For transmission electron microscope studies, rod-shaped cardiomyocytes were resuspended in the corresponding fixation buffer.

Lysotracker staining

Isolated adult cardiomyocytes were plated for 1 hour in laminin-precoated p24 plates. After that time, the medium was removed and cardiomyocytes were stained with 100 nM of LysoTracker™ Red DND-99 (#L7528, Thermo Fisher) in M199 completed medium for 30 mins at 37ºC. After that time, the medium was removed and replaced with new M199 completed medium. Live cell imaging and fluorescent images were acquired with a Nikon Time-lapse microscope. Lysotracker was observed using a 577/590 excitation/emission filter.

Cathepsin function assay

WT and cYKO mice were euthanized, the heart was cut into three parts and collected in three cold PBS tubes for the study of different cathepsin activity. Protocols were followed as described in each datasheet: Cathepsin D activity (Abcam #65302), Cathepsin B activity (Abcam #65300) and Cathepsin L activity (Abcam #ab65306). Briefly, after collection in cold PBS, tissue was resuspended in a *cell lysis buffer* and homogenized using a PTFE grooved pestle for tissue grinder for 2 minutes on ice.

After 10-15minutes incubation on ice, samples were centrifuged for 5 minutes at 4ºC at maximum speed. The supernatant was transferred to a new tube and the assay procedure for measuring the activity was performed as indicated in each datasheet. For measuring the activity, fluorescence microplate available at CNIC with the following filters excitation was used: 355/460 for cathepsin D and 390/538 for cathepsin B and L. Fluorescence measurement in each sample was normalized to total protein content measured by BCA kit.

Transmission electron microscopy (TEM)

For adult isolated cardiomyocytes. Cells were fixed with a 3% glutaraldehyde in a 0.1M cacodylate buffer. After washing the fixative in a cacodylate buffer, post-fixation was carried out with 1% aqueous osmium tetroxide in 0.8% potassium ferricyanide for 1 hour. After washing, a block contrast was performed in 2% aqueous uranyl acetate for 30 minutes.

For heart tissue. Tissue was fixed with a mixture of 4% paraformaldehyde and 2% glutaraldehyde in 0.1 M a cacodylate buffer. After washing the fixative in a cacodylate buffer, the tissue was postfixed with 1% osmium tetroxide in 0.8% potassium ferricyanide for 1 hour.

After these steps, protocol continued as follows: the sample was dehydrated passing through ethanol in increasing concentration (30%-50%-70%-95%-absolute) and acetone to proceed to Durcu-pan epoxy resin infiltration. After polymerization of the resin, ultrathin sections (60 nm) were made with a Leica Reichert Ultracut S ultramicrotome and placed on grids. Finally, the sections were contrasted with 2% uranyl acetate and Reynolds lead. For the ultrastructural study, a Jeol Jem 1010 Transmission Electron Microscope was used, equipped with a Gatan Orius200 SC digital camera (Pleasanton-CA). Individual images were acquired at 10000X and 40000X magnification for: mitochondria quantification (10000X) in tissue samples and MAMs evaluation (40000X) in cardiomyocyte isolated samples using ImageJ software 1.52p Wayne Rasband from USA National Institute of health (NIH).

TEM analysis

Using ImageJ software, mitochondria was hand-delineated for measuring surface (μm2) and quantity in 10 images of 10000X magnification for each animal. For the study of the mitochondrial associated membranes (MAMS), we studied the following parameters in 40000X magnification images:

$$ER\ lenght\ (nm) = length\ of\ the\ ER\ and\ mito\ contact$$

$$MAMs\ coverage\ (\%) = \frac{ER\ lenght\ in\ contact\ with\ mitochondria}{Mitochondria\ perimeter}$$

$$ER\ to\ mito\ distance: physical\ distance\ (nm)\ between\ the\ two\ organelles$$

Leupeptin assay for measuring autophagic flux

Mice received an intraperitoneal injection (i.p.) of PBS or 40mg/kg Leupeptin (#109875-Merck Millipore). After 40 mins, the animals were euthanized, and heart tissue was frozen in liquid N_2 for further studies.

Tunicamycin assay for inducing ER stress

Mice received an intraperitoneal injection (i.p.) of DMSO or 2mg/kg Tunicamycin (#T7765-Sigma Aldrich). After 3 days, the mice were evaluated by echocardiography. The mice were then euthanized, and heart tissue was frozen in liquid N_2 for further studies.

Protein extraction

Tissue samples were lysed in a RIPA buffer containing protease inhibitors (complete-Roche) and phosphatase inhibitors (PhosphoSTOP-Roche) in a TissueLyser for 15 min at a frequency of 1/50 s. Samples were incubated in ice for 10 mins. The supernatant was separated by centrifugation at 12000 g for 20 min at 4ºC, and total protein concentration was detected using a BCA protein assay kit (ThermoFisher) using bovine serum albumin (BSA) as the standard. Protein was quantified with a *Thermo Scientific™ Pierce™ BCA Protein Assay Kit*.

Using a 96 well plate a standard curve of 10 µl of 0-2 concentrations mg/ml of BSA and 2/5 µl of sample were prepared. Reactives A and B from the kit were mixed in 1:50 proportion and 200 µl were added to each well. All samples were prepared in duplicate and incubated 30 min at 37 ºC. Absorbance was read at 562 nm using a *xMark™ Microplate Absorbance Spectrophotometer* (*BR*®).

Western blot

Equal amounts of protein (15-50ug, depending on the selected protein) were separated by SDS-PAGE and transferred to a 0.2 µm nitrocellulose membrane using transfer apparatus (*Trans-Blot®Turbo™ Transfer System)* according to the manufacturer´s protocol. Briefly, the transfer program was chosen according to the molecular weight of interest protein. Then, membranes were stained with ponceau S to check transfer efficiency and subsequently washed with 0.2% 1X TBST.

Blocking was performed in either 5% of non-fat milk or BSA (if phosphorylation) in 1X TBST for 1 hour at room temperature, membranes were washed 3 times 5 min each with TBST 1X and incubated overnight at 4ºC balancing with antibodies in 2.5% BSA / TBST solution.

Antibody	Dilution	Reference
LC3	1:1000	Abcam #51520
BECLIN1	1:1000	Cell Signaling #3738S
p62	1:1000	Cell Signaling #5114
p-AMPK	1:1000	Cell Signaling #2535
Total AMPK	1:1000	Cell Signaling #2532
PARKIN	1:1000	Abcam #77924
CHOP	1:1000	Cell Signaling #2895
MCU	1:1000	Cell Signaling #14997
ATF4	1:1000	Boster M00371
OxPHOs complex	1:5000-1:10000	Abcam #19615
OPA1	1:1000	Thermo Fisher #PA1-16991
p-DRP1	1:1000	Cell Signaling #3455S
Total DRP1	1:1000	Cell Signaling #8570S
MFN2	1:1000	Abcam #56889
VINCULIN	1:10000	Sigma Aldrich V4505
GAPDH	1:10000	Abcam #8245

VDAC1	1:10000	Abcam #14734

Table 4. Antibodies, dilution and reference used for immunoblotting experiments

The following day, membranes were washed 3 times 5 min each with TBST and incubated for 1 hour with HRP-conjugated anti-mouse or anti-rabbit (1:5000 or 1:10000). Bound antibody signals were developed with Immobilon® Western Chemiluminescent HRP Substrates (MERCK, MILLIPORE). Quantitative densitometry was performed using Fiji (ImageJ) software.

If phosphorylation was studied, the phosphorylated protein was revealed first. Then, stripping of the membrane was performed in a hood for 5 mins at 65ºC using stripping buffer (For 1L: 740 mL dH_2O, 200 mL SDS 10%, 125 mL HCL TRIS pH: 6.8, 8 mL β-mercaptoethanol).

After this, the membrane was incubated with the HRP-conjugated antibody to ensure band elimination. Incubation with the Total-antibody was done as normal.

RNA extraction and cDNA preparation

RNA extraction was performed using *RNeasy plus mini kit* (*# 74136, Qiagen*). Between 50-100 mg of tissue was digested using 300 µl of TRIzol reagent and homogenized using a TissueLyser LT-*QG*© 15 min 1/50 s frequency. Samples were incubated 5 min at RT. The sample volume did not surpass 10% of the TRIzol volume used. 0.1 ml of chloroform per 300 µl of TRIzol were added and samples were energetically vortexed 15 s and incubated at RT 3 min. Centrifugation at 12000xg at 4ºC 15 min was carried out. RNA remained in the upper aqueous phase after centrifugation, which was transferred into a fresh tube. Following kit protocol, RNA was eluted in 40ul of mqH2O and quantified as described with DNA.

Isolated RNA was reverse-transcribed into cDNA using *Applied Biosystems™ High-Capacity cDNA Reverse Transcription Kit*. For the reaction, between 200-1000 ng of RNA were added to 2 µl of RT buffer, 0.8 µl of DNTPs, 2 µl of random primers and 1 µl of reverse transcriptase to each well. Reaction was incubated in a *C1000 Touch Thermal Cycler* (*BR*®) instrument using this protocol:

Priming (25ºC, 10 min), Reverse Transcription (37ºC, 120 min), RT inactivation (85ºC, 5 min), Optional Step (4ºC, hold). qPCR was conducted as explained, with ***Hprt*** as loading control. Primers were designed with **PrimerBlast.**

Gene	Reference	Primer forward (FW) Primer reverse (RV)
ATPaseVI	NM_027439.4	FW: TGGGGAAAGCAAACTCGGTG RV: AGAAAGAGCAGGTCAACCTCATTA
CtsB	NM_007798.3	FW: ATTCACACCAATGGCCGAGT RV: CCACCATTACAGCCGTCCC
CtsD	NM_009983.3	FW: GGCAGTGCCTCTTATCCAGG RV: CACCCTGCGATACCTTGAGT
CtsL	NM_009984.4	FW: GTGGACTGTTCTCACGCTCA RV: ACAAGATCCGTCCTTCGCTT
Lamp1	NM_001317353.1	FW: GGTAACAACGGAACCTGCCT RV: TCTGGTCACCGTCTTGTTGT
Lamp2	NM_001017959.2	FW: TGGCTAATGGCTCAGCTTTCA RV: GAACTTCCCAGAGGGGCATC
Tfeb	NM_001161722.1	FW: AGATGCCTAACACGCTGCC RV: CTCGCTTCTGAGTCAGGTCG
Perk	NM_001313918.1	FW: CCGAAGTGACCGTGGAGGAC RV: TGATTACCAAGGACCTGCCG
Chop	NM_001290183.1	FW: ACCTGAGGAGAGAGAACCTGG RV: CGTCTCCAAGGTGAAAGGCA
Grp78	NM_001163434.1	FW: TCTCAGATCTTCTCCACGGC RV: AGGGGTCGTTCACCTTCATAG
Atf6	NM_001081304.1	FW: TGTATTACGCCTCCCCTGGA RV: TGGTAATAGCAGATGATCCCTTCG
Ire1a	NM_023913.2	FW: AGCTGTGGTCAAGATGGACTG RV: TCCCGGTAGTGGTGTTTCTTGT
Atf4	NM_001287180.1	FW: ACCATGGCGTATTAGAGGCAG RV: GATTTCGTGAAGAGCGCCAT
Hprt	NM_013556.2	FW: AGGGATTTGAATCACGTTTGTGTC RV: TTTGCAGATTCAACTTGCGCT

Table 5. Genes, reference and primers used for real-time quantitative PCR experiments

DNA extraction

Total heart DNA was extracted using DNeasy® Blood and Tissue kit (#69504 Qiagen). Briefly, a small heart tissue piece was incubated with an ATL buffer + proteinase K at 56ºC until completely lysed (minimum 3 hours to overnight). After this, an AL buffer was added and mixed thoroughly by vortexing. 100% ethanol was added and mixed thoroughly. The sample was added to a DNeasy spin column placed in 2 ml collecting tubes. Following Qiagen protocol steps, DNA was eluted in 40 μl of mqH2O. Concentrations were determined using *ND-1000 UV-Vis Spectrophotometer-NanoDrop™*. 1 μl of sample was placed onto a reader, absorbance was read at 260 and 280 nm. A ratio of 1.8-2 was considered as adequately pure for studies. After this, all samples were normalized to 3 ng/μl.

Mitochondrial DNA quantification

For preparing the Master Mix: 5.4 μl from SYBR green PCR master mix (# 4368702, Applied Biosystem) + 0.3 μl of forward primer (10 μM) + 0.3 μl of reverse primer (10 μM). To each well, 4 μl of the sample (3 ng/μl) + 6 μl of the Master Mix were added. Running was performed in a *CFX384Touch RT-PCR Detection System-Bio-Rad® (BR®)* instrument with the following protocol: step1 (50ºC, 2 min), step2, (95ºC, 10 min), step3 (95ºC, 15 s and 60ºC, 1 min; x39 cycles), step4 (65 to 95ºC with 0,5ºC increment each 5 s).

For mitochondrial DNA (mtDNA) quantification, the ratio between a ND2 mitochondrial gene and HPRT nuclear reference gene was calculated. Primers were designed with Primerblast. Template, reference sequence, orientation, sequence, annealing Tº and product length respectively showed for each gene:

Hprt (NC_000086.7): FW: GCTTGCTGGTGAAAAGGACC-59.7ºC, RV: TGATTGGCCAAAGGGCATCT-59.9ºC. 74 pb

Nd2 (NC_005089.1): FW: TCAGCCTACTAGCAATTATCCCC-59.4ºC, RV: CTGTTGCTTGTGTGACGAAGT-59.3ºC. 93 pb

Statistics

Experimental data are represented as mean ± standard error of the mean (SEM) or standard deviation (SD), as indicated in each figure. Data were analyzed with Prism Software (Graph Pad, Inc.). For normally distributed variables, comparison between two groups were made by unpaired two-tailed Student t-test. For non-normally distributed variables, the nonparametric Wilcoxon-Mann-Whitney test was used. Comparison between more than two groups was made by One-way ANOVA with Dunnett´s or Šidák´s multiple comparison test, depending on the experimental setting addressed. The Two-way ANOVA t-test with Tukey´s post-hoc test was used for two-group comparisons considering tunicamycin treatment and genotype. Power calculations were used to obtain statistical significance at p-values below 0.05; *$p<0.05$, **$p<0.01$, ***$p<0.001$, ****$p<0.0001$

Results

Cardiac-specific *Yme1l* ablation causes a late-onset dilated cardiomyopathy

We previously showed that mice lacking YME1L in cardiomyocytes (cYKO) display a DCM phenotype in adulthood (Wai et al., 2015). To better characterize the cardiac function trajectories in mice lacking cardiomyocyte´s YME1L, we performed a serial longitudinal echocardiographic study (i.e., every 10 weeks from birth). As shown in **Figure 6A**, LV size (LV internal diameter, LVID) and LV systolic function (LV ejection fraction, LVEF) were unaffected during the first 20 weeks of life, showing a progressive deterioration with pathognomonic features of DCM (LVID enlargement along with LVEF decline) which becomes apparent at 30 weeks of age (**Figure 6A**). In **Figure 6B, 6C**, an echo representative image showing the ventricular chamber dilation, clearly evidencing an enlargement of the heart of a 40-week-old cYKO mice when compared with a wild-type animal.

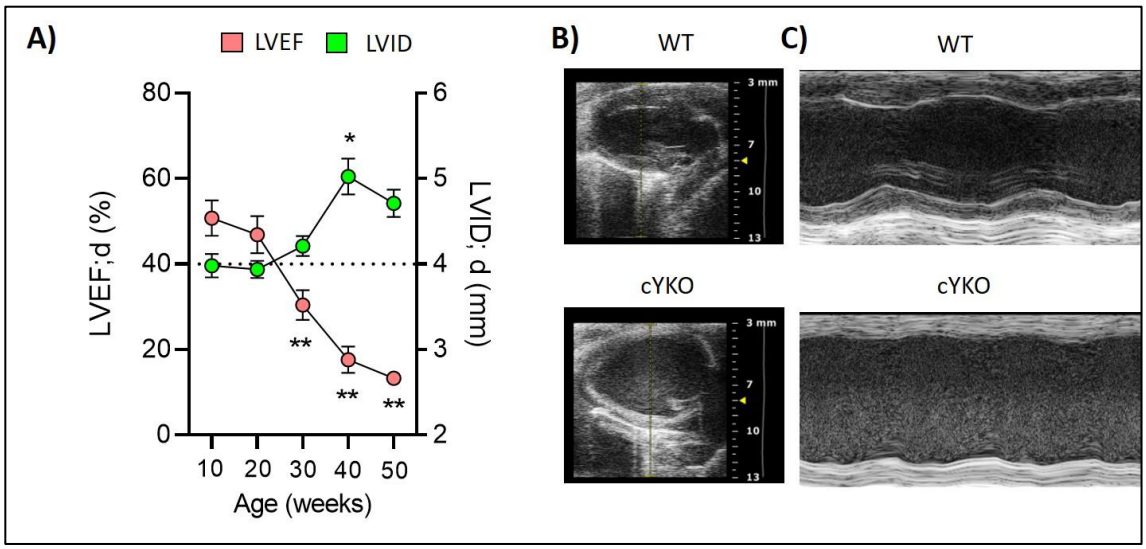

Figure 6. Cardiac function progression in cYKO mice

(A) Echocardiographic evaluation of cardiac function of cYKO male mice in weeks. Left Y axis: Left ventricular ejection fraction (LVEF-red), right Y axis: Left ventricular internal diameter (LVID-green). X axis: age (weeks). Black dotted line represents selected LVEF (<40%) and LVID (>4mm) values for cardiac dysfunction. Data represent means ± SEM, *P<0.05, ** P<0.01 after Dunnett multiple comparison paired t-test (N=11).

(B) Representative 2D echocardiography images of a WT animal (upper panel) and cYKO animal (lower panel) from 40-week-old.

(C) Representative M-mode echocardiography images of a WT animal (upper panel) and cYKO animal (lower panel) from 40-week-old.

The slow progression and the late onset of the disease allowed us to establish two differentiated timepoints to study the molecular correlates of the functional status: (1) 10 weeks of age represents a subclinical stage of the disease, where LV size and function are unaffected. (2) 35 weeks of age represents a timepoint of overt DCM with end-stage HF phenotype (**Figure 6A**).

Before the onset of dilated cardiomyopathy, mitochondria from cardiomyocytes lacking YME1L are large and display an enhanced respiration capacity

We previously showed that *Yme1l* ablation in cardiomyocytes is associated with fragmented mitochondria, which are smaller and more numerous, and a DCM phenotype in adult mice (Wai et al., 2015). This mitochondrial phenotype was identified at late stages of DCM, when HF was already present. Whether the mitochondria phenotype preceded the onset of the DCM and HF phenotype remained unexplored. To this aim, we studied the cardiomyocyte mitochondrial ultrastructure in cYKO mice (and WT littermates) at the early timepoint chosen (10 weeks of age), where hearts were anatomically and functionally normal.

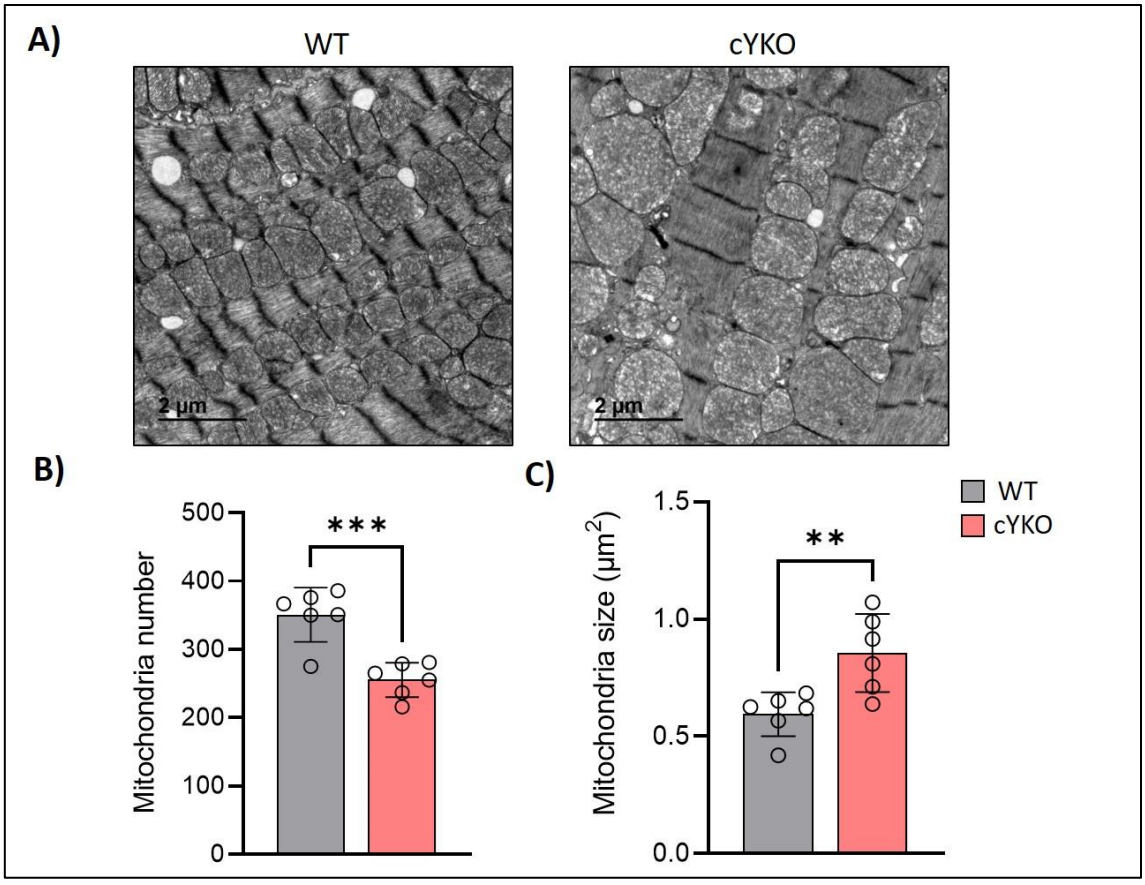

Figure 7. Mitochondrial ultrastructure before DCM

(A) Representative transmission electron microscopy (TEM) images of heart tissue from 10-week-old WT and cYKO mice. Scale bar corresponds to 2um.

(B) Mitochondrial number. Data represent means ± SD. ***P<0.001 after parametric unpaired t-test (N=6)

(C) Mitochondrial size (μm^2). Data represent means ± SD. **P<0.01 after parametric unpaired t-test

Strikingly, transmission electron microscope (TEM) images (**Figure 7A**) revealed a reduction in the number of mitochondria in cYKO mice (**Figure 7B**). Furthermore, mitochondria were not only not smaller than those of WT, but they displayed an increase in their size (surface) (**Figure 7C**).

These results suggest that lack of YME1L (and OPA1 processing) is not *per se* enough to induce mitochondrial fragmentation.

The number of mitochondria DNA copies (surrogate for biogenesis) was significantly reduced in cYKO mice (**Figure 8**). The latter suggests that the increase in organelle size observed before cardiac function does not result from fusion or pre-existing mitochondria. This is in line with the inability of YME1KO mice to undergo mitochondrial fusion.

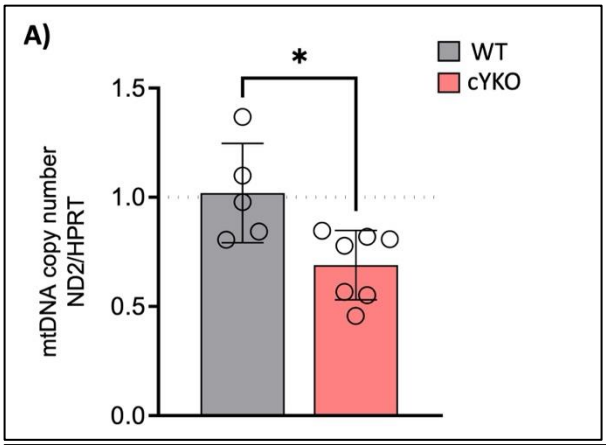

Figure 8. Mitochondrial DNA content before DCM

(A) Mitochondrial DNA (mtDNA) copy number measured by the ratio between ND2 (mitochondria) and HPRT (nucleus) in heart tissue from 10-week-old WT and cYKO mice. Data represent means ± SD. *P<0.05 after parametric unpaired t-test (N=5-7)

Mitochondrial DNA density is often correlated with the respiratory capacity of this organelle (i.e., a reduction in mtDNA is linked with reduced ATP production and less respiration). In order to study whether the reduction in mtDNA copies observed at the tissue level was due to a reduction of mtDNA per mitochondria on the contrary to a reduction of the number of mitochondria that are otherwise normofunctional, we decided to evaluate mitochondrial bioenergetics using a High-Resolution Respirometer (HRR) with the O2k in isolated mitochondria at the early stage where cardiac function is still unaltered.

Briefly, the principle of the HRR-O2k is based on the monitorization of oxygen concentration over time while performing various titrations of substrates and inhibitors of the OXPHOS complexes to define the bioenergetic contribution and the effects of the OXPHOS complexes.

Mitochondria from cYKO cardiomyocytes displayed a significant increase in OxPHOS respiration and ETS capacity when compared to their control littermates (**Figure 9B, 9C**). Moreover, ATP production in isolated mitochondria from cYKO mice was also higher (**Figure 9C**). Finally, ROS production was significantly reduced in mitochondria isolated from cYKO mice (**Figure 9D**).

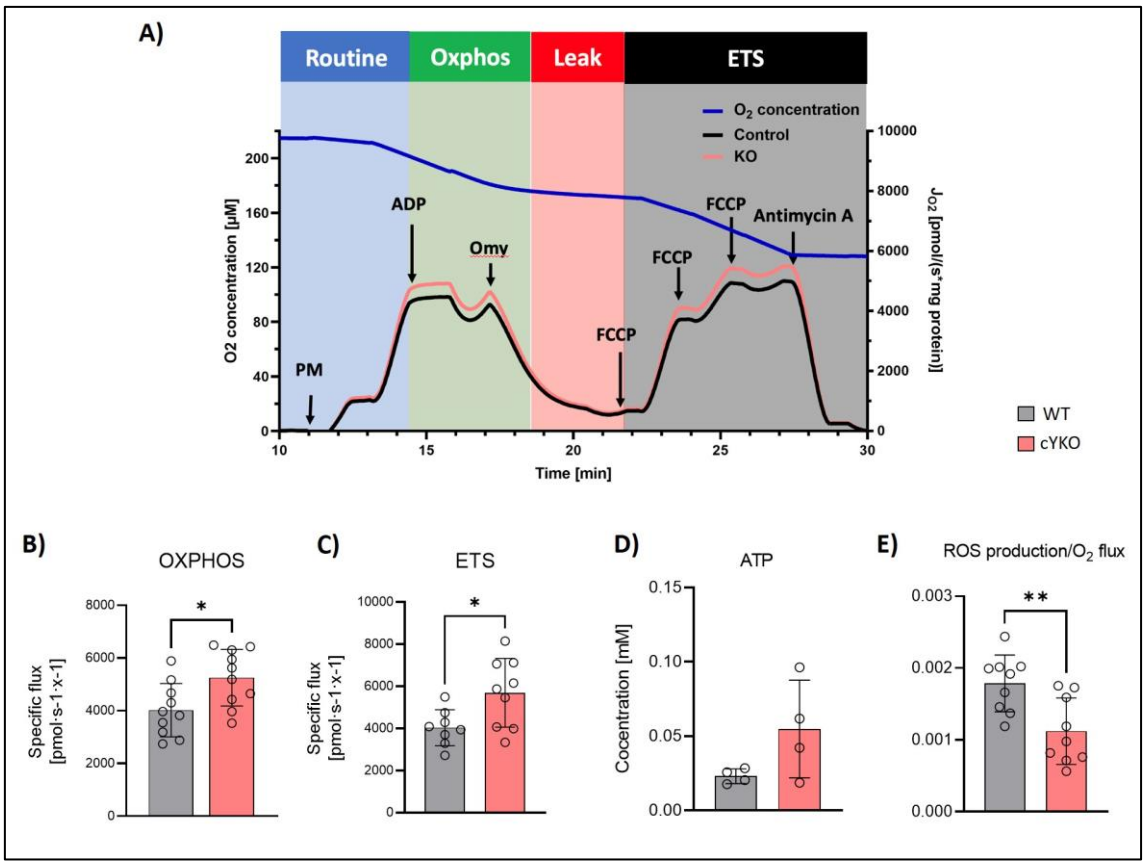

Figure 9. Respiration of isolated heart mitochondria before DCM

(A) Representative trace of High Resolution Respirometry taken from the DatLab software. Left axis refers to O_2 concentration [µM], right axis refers to O2 flux per Volume [pmol/(s*ml)], X axis represents time in hours and minutes [h:m]. Blue line along the trace indicates oxygen concentration, black and red line indicate oxygen consumption or (JO2) by the biological sample, WT and cYKO, respectively.

(B) Oxidative phosphorylation (OxPHOS) from isolated heart mitochondria from WT and cYKO. Oxygen consumption of mitochondria was measured in the presence of Pyruvate + Malate (PM), adenosine diphosphate (ADP) and oligomycin (Omy). Data represent means ± SD. *P<0.05 after parametric unpaired t-test (N=10)

(C) Maximal respiration of the electron transport system (ETS) from isolated heart mitochondria from WT and cYKO mice. ETS was measured in the presence of uncoupler FCCP + Antimycin A. Data represent means ± SD (N=10). *P<0.05 after parametric unpaired t-test (N=10)

(D) ATP production (mM) in isolated heart mitochondria from WT and cYKO mice. Data represent means ± SD (N=4).

(E) ROS production from isolated heart mitochondria from WT and cYKO mice. ROS was measured in the presence of H2O2 and normalized against oxygen consumption. Data represent means ± SD. **P<0.01 after parametric unpaired t-test (N=9-10)

When individual complexes were analyzed by immunoblot (**Figure 10A**) an increase in Complex II expression was observed (**Figure 5B**).

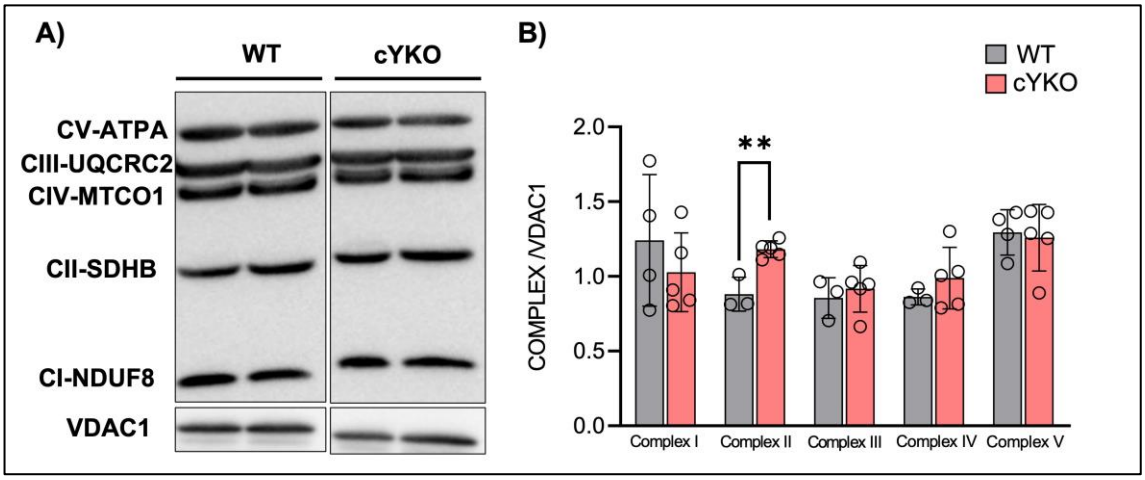

Figure 10. OxPHOS complexes expression in isolated heart mitochondria before DCM

(A) Immunoblot analysis of individual expression of OxPHOS complexes in isolated heart mitochondria from WT and cYKO 12-week-old mice. VDAC1 was used as a loading control.

(B) Quantification of individual OxPHOS complexes in isolated heart mitochondria from WT and cYKO 12-week-old mice. Data represent means ± SD. **P<0.01 after parametric unpaired t-test (N=3-5)

Collectively, these data indicate that cardiomyocyte mitochondria from young cYKO mice (i.e., when there is no cardiac dysfunction) are larger (due to the inability to fuse with one another) and display higher (compensatory) respiratory capacity. These data suggest that the lack of YME1L is not directly associated with disbalanced mitochondrial dynamics in early timepoints of cYKO mice development.

Ruling out that primary dysfunction of mitochondria is present in a subclinical stage of the disease, we explored organelle quality control processes.

Loss of cardiomyocyte´s YME1L results in impaired autophagy

In order to identify altered molecular pathways associated with future development of DCM, we studied quality control machinery in 10-week-old cYKO mice (a time when no phenotype is yet apparent). We speculate that maintenance of an efficient removal of injured organelles (mitochondria and others) should be vital for the conservation of cardiomyocyte homeostasis before the onset of cardiac dysfunction.

We explored LC3, a key marker recruited into autophagosomes during induction of autophagy. We found an accumulation of LC3-II in cardiomyocytes of cYKO animals (**Figure 11B**). BECLIN1, implicated in early steps of autophagy initiation, was also significantly upregulated in cYKO animals (**Figure 11B**).

To determine whether the observed accumulation of LC3-II was due to enhanced induction of autophagy or by contrast is resulting from defective autophagic degradation (last steps of the process), we checked the density of p62/SQSTM1, a protein that is a specific target of autophagy degradation.

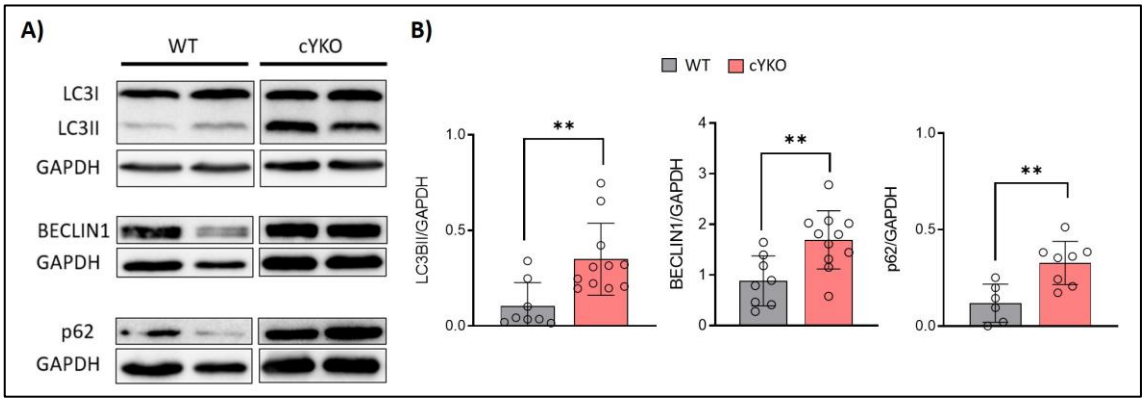

Figure 11. Autophagy markers expression in heart tissue before DCM.
(A) Immunoblot analysis of LC3, BECLIN1 and p62 expression in heart tissue from WT and cYKO 12-week-old mice. GAPDH was used as a loading control.
(B) Quantification of LC3II, BECLIN1 and p62 expression in heart tissue from WT (grey) and cYKO (red) 12-week-old mice. Data represent means ± SD. **P<0.01 after parametric unpaired t-test (N=8-11)

The intracellular accumulation of p62 in cYKO mice confirmed the overt insufficient autophagy in cardiomyocytes of these animals (**Figure 11B**).

Altogether, these data indicate that the autophagic flux in cardiomyocytes from cYKO mice is impaired by a defect in the final steps of the process.

Autophagosome-to-lysosome processing is altered in cardiomyocytes lacking YME1L

Autophagosome-to-lysosome fusion is a critical step in the final execution of autophagy. We evaluated whether a defect in this last step was responsible for the impaired autophagy flux in cYKO cardiomyocytes.

Firstly, we evaluated the presence of acidic organelles (lysosome-associated organelles) in isolated cardiomyocytes from cYKO and WT mice by using LysoTracker Red (**Figure 12A**). As shown in **Figure 12B**, cardiomyocytes from cYKO displayed a significantly higher density of Lysotracker Red puncta.

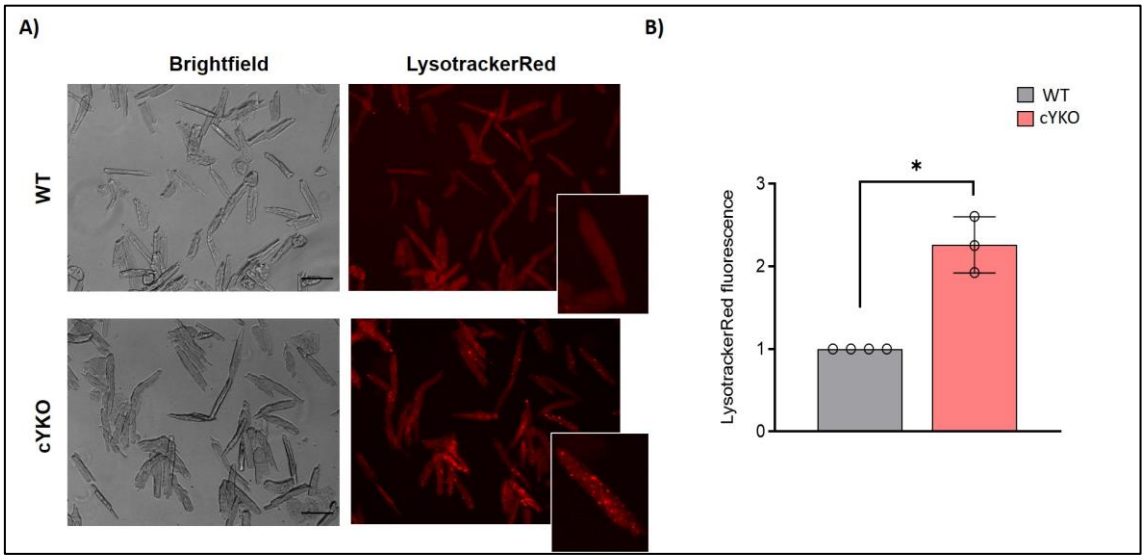

Figure 12. Lysosome staining in isolated adult cardiomyocytes before DCM

(A) Representative fluorescence pictures of Lysotracker Red staining of isolated adult cardiomyocytes from WT and cYKO 12-week-old. Brightfield pictures on the left.

(B) Quantification of Lysotracker Red staining signal of isolated adult cardiomyocytes from WT (grey) and cYKO (red) 12-week-old mice. Data was normalized to WT fluorescence. Data represent means ± SD. *P<0.05 after non-parametric Mann-Whitney test (N=3-4)

To confirm the status of the lysosome formation process, we measured the expression of some lysosome-related genes by qPCR.

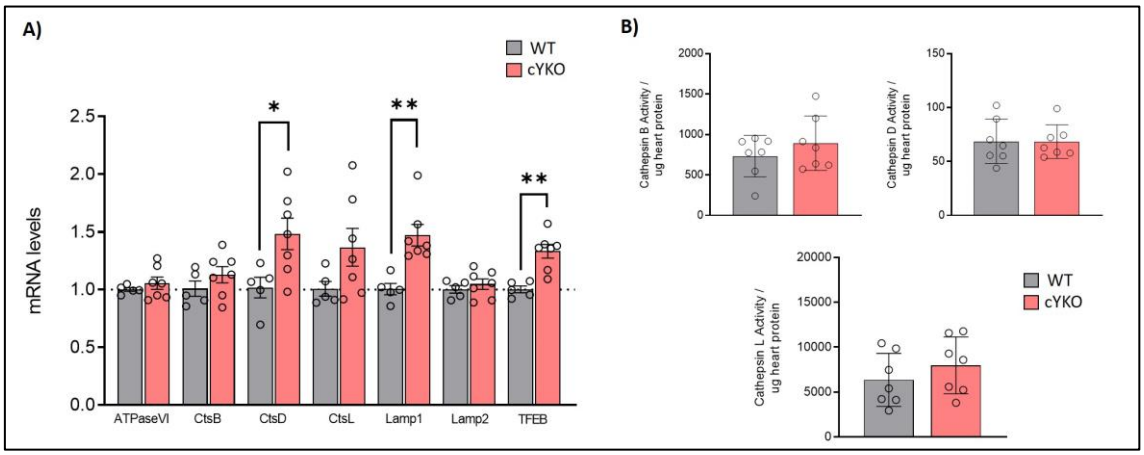

Figure 13. mRNA expression of lysosomal markers and function before DCM

(A) mRNA expression of *ATPaseVI*, *CtsB, CtsD, CtsL, Lamp1, Lamp2, TFEB* in heart tissue from WT (grey) and cYKO (red) 12-week-old mice. Data represent means ± SD. *P<0.05, **P<0.01 after parametric unpaired t-test (N=5-7).

(B) Cathepsin B, D and L activity in heart tissue from WT (grey) and cYKO (red) 10-week-old mice. Activity was normalized to μg of heart tissue protein. Data represent means ± SD (N=7).

We found a pattern of gene expression suggestive of enhanced lysosomal formation, as shown by the overexpression of *Tfeb*, *Lamp1*, and *CtsD,* (**Figure 13A**). These data are in line with the higher abundance of lysosomes observed by LysoTracker (**Figure 12B**).

We then wanted to explore whether a defective lysosome function was responsible for the impaired autophagic flux. For this purpose, we measured the lysosome functional capacity to fuse with autophagosome by measuring the activity of cathepsins B, D, L. As shown in **Figure 14B**, we did not find any abnormality in cathepsin function, suggesting that lysosome capacity to fuse with autophagosome is intact in cYKO cardiomyocytes.

To confirm that the apparent defect in autophagosome-to-lysosome fusion was responsible for the impaired flux, we performed a functional analysis by intraperitoneal (i.p.) injection of 40mg/kg of the lysosomal inhibitor leupeptin (or vehicle) in cYKO mice at the early timepoint (i.e., 10 weeks of age) and WT littermates. 40 min after leupeptin injection, the mice were sacrificed and the heart levels of LC3-II in the presence and absence of leupeptin were analyzed (**Figure 14A**). As expected, in WT mice, LC3-II levels significantly increased after leupeptin injection.

However, LC3-II levels (which are significantly higher in cYKO mice as shown previously in **Figure 11B**) variably increase further upon leupeptin challenge (**Figure 14B**).

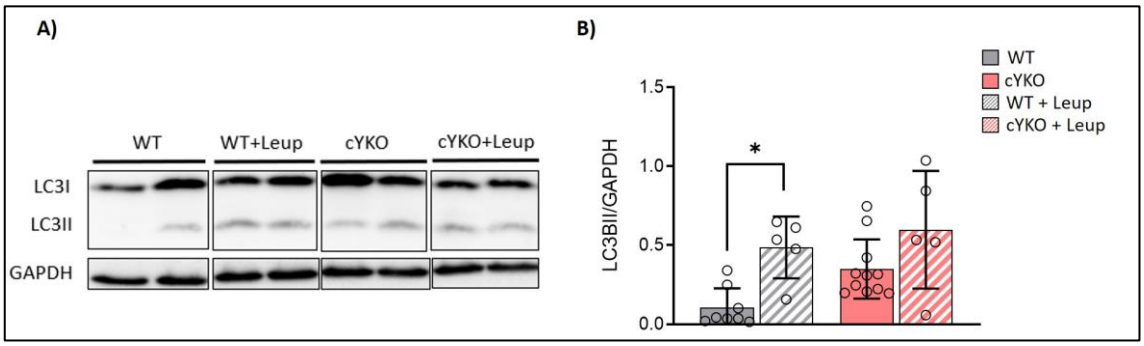

Figure 14. Autophagic flux measurement with leupeptin before DCM

(A) Immunoblot analysis of LC3 expression in heart tissue from WT and cYKO 12-week-old mice under 40mins of 40mg/kg of the lysosomal inhibitor leupeptin. GAPDH was used as a loading control.

(B) Quantification of LC3-II in heart tissue from WT mice with (grey) and without (striped grey) leupeptin and cYKO 12-week-old mice with (red) and without (striped red) leupeptin. Data represent means ± SD. *P<0.05 after parametric One-Way ANOVA test (N=5-11).

Altogether, these data confirm that lysosomes are normally generated in cardiomyocytes lacking YME1L and suggest that the impairment of autophagy is not due to a lysosomal defect. Therefore, these data identify a defective autophagosome-lysosome fusion and/or degradation as a key feature of *Yme1l* ablation in cardiomyocytes.

Lack of YME1L disrupts ER-mitochondria tethering increasing Ca^{2+} overload to mitochondria

We speculated that the dysregulation of autophagy may be governed through the interplay between mitochondria and another organelle. Since we observed an overt structural change (enlargement) in mitochondria, we hypothesized that the interaction with endoplasmic reticulum (ER) might be affected. In addition, ER is involved in mitochondrial dynamics, which is disbalanced in cYKO mice.

To address this, we evaluated by TEM the ER-mitochondria spatial interactions (**Figure 15A**) by determining the distance, length and proportion of the mitochondrial surface that was closely opposed to ER with a distance of less than 30 nm. A reduction in MAMs coverage (**Figure 15B**), along with a reduction in ER length (**Figure 15C**) was observed in isolated cardiomyocytes from cYKO mice, together with a decrease in ER-mitochondria distance observed in isolated cardiomyocytes from cYKO mice (**Figure 15D**).

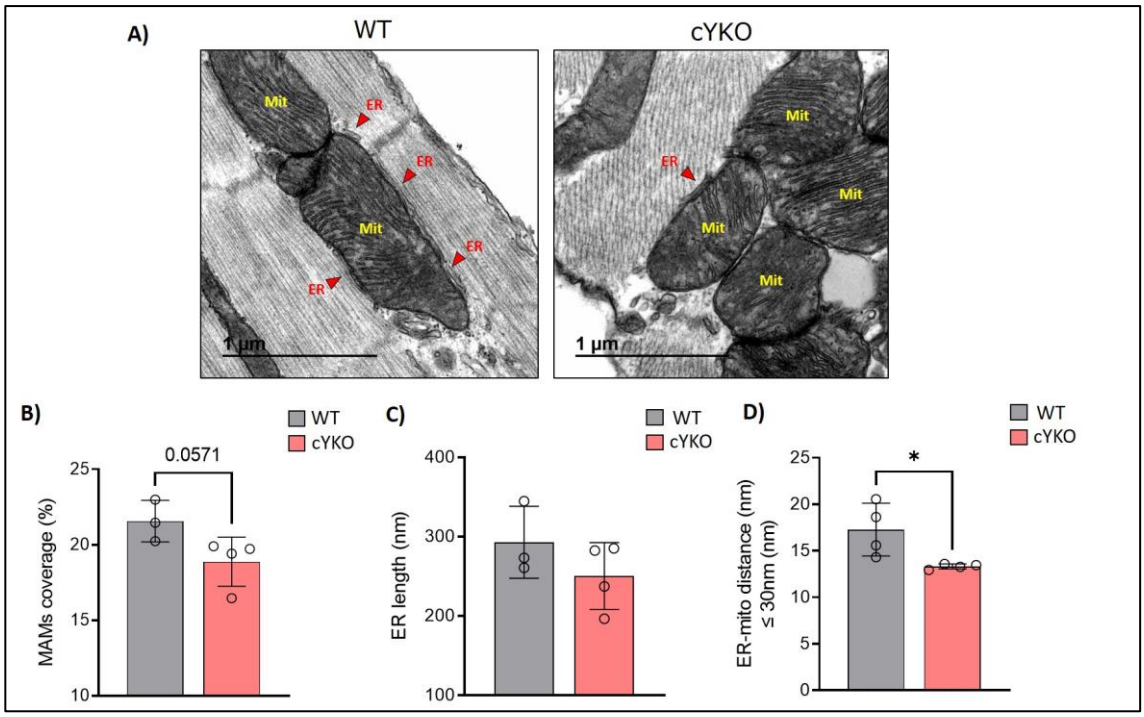

Figure 15. Impact of *Yme1l* ablation on MAMs association before DCM

(A) Representative transmission electron microscopy (TEM) images of isolated adult cardiomyocytes from 10-week-old WT and cYKO mice. Mit (yellow)=mitochondria, ER (red)=Endoplasmic Reticulum. Scale bar corresponds to 1um.

(B) Mitochondrial associated membrane (MAM) coverage (%), represented as the ratio between the ER length in touch with mitochondria and mitochondrial perimeter. Data represent individual animals ± SD (N=3-4).

(C) Endoplasmic reticulum (ER) length (nm), represented as the length of ER in touch with mitochondria. Data represent individual animals ± SD (N=3-4).

(D) ER to mitochondria distance (nm). Data represent individual animals ± SD. *P<0.05, after parametric unpaired t-test (N=4)

To evaluate whether the altered ER-mitochondria spatial interaction had any functional impact, we examined calcium content in mitochondria isolated from cYKO mice (and their control littermates). As expected, cYKO cardiomyocytes´ mitochondrial had a significant increase in Ca^{2+} concentration (**Figure 16A**). In line with this, we found a significant upregulation in MCU (**Figure 16B**), the mitochondrial uniporter responsible for Ca^{2+} transfer from the inner mitochondrial membrane to the matrix (**Figure 16C**).

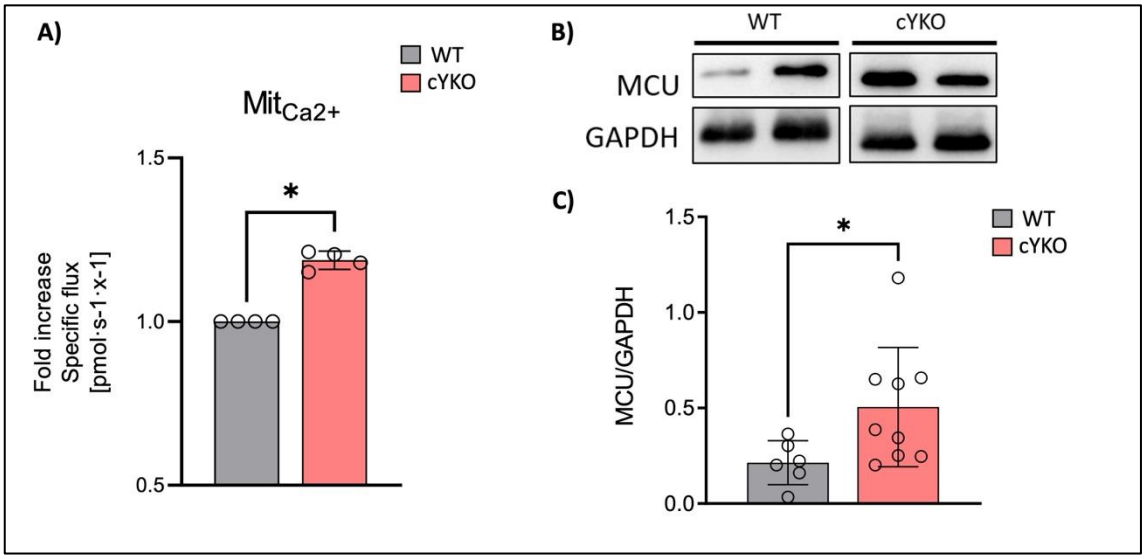

Figure 16. Mitochondrial Ca^{2+} flux before DCM

(A) Mitochondrial Ca^{2+} flux in isolated heart mitochondria from WT and cYKO 10-week-old mice. Data represent means ± SD. Data represent fold increase means ± SD. *P<0.05, after non-parametric unpaired t-test (N=4).

(B) Immunoblot analysis of MCU expression in heart tissue from WT and cYKO 10-weel-old mice. GAPDH was used as a loading control.

(C) Quantification of MCU expression in hearts from WT and cYKO 10-week-old mice. Data represent means ± SD. *P<0.05, after unpaired t-test (N=4-5)

Cardiac ablation of *Yme1l* predispose to ER stress aggravating cardiac dysfunction

After documenting the altered spatial interactions between mitochondria and ER, we explored whether this was associated with ER stress. This was plausible since ER stress regulates autophagy through mediating Ca^{2+} handling.

Firstly, we examined whether cardiomyocytes from cYKO mice displayed activation of ER stress signaling. We observed an mRNA overexpression in *Chop (***Figure 17A***)* (the downstream target of the most well-known UPR branches), and *Atf4 (***Figure 17A***)*, associated with a modest increase at the protein level (**Figure 17C**). No significant changes were observed at the protein level of CHOP (**Figure 17E**).

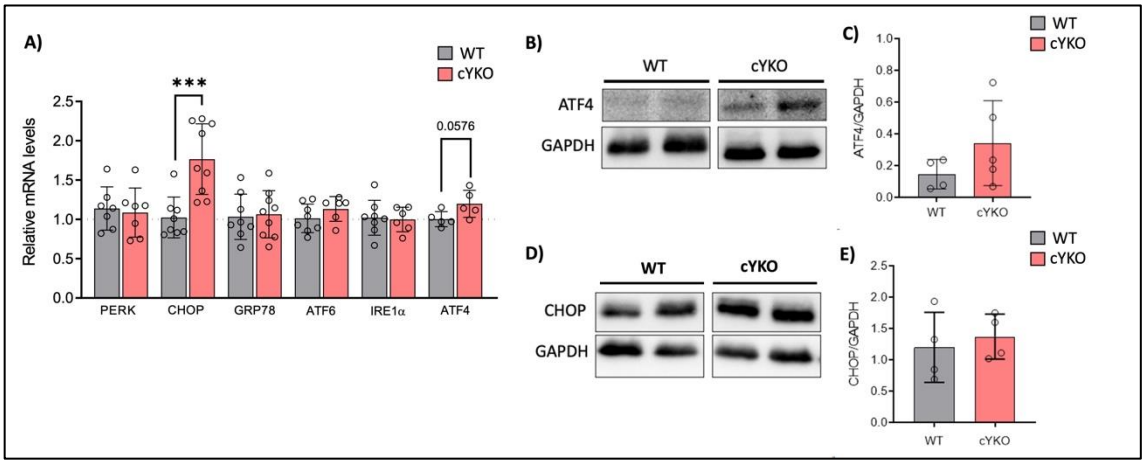

Figure 17. mRNA expression and immunoblot of ER stress markers before DCM

(A) mRNA expression of *Atf4, Atf6, Chop, Grp78, Ire1a, Perk* in heart tissue from WT and cYKO 10-week-old mice. Data represent means ± SD. ***P<0.001 after parametric unpaired t-test

(B) Inmunoblot analysis of ATF4 expression in heart tissue from WT and cYKO 10-week-old mice. GAPDH was used as a loading control.

(C) Quantification of ATF4 expression in heart tissue from WT and cYKO 10-week-old mice. Data represent means ± SD (N=4-5)

(D) Inmunoblot analysis of CHOP expression in heart tissue from WT and cYKO 10-week-old mice. GAPDH was used as a loading control.

(E) Quantification of CHOP expression in heart tissue from WT and cYKO 10-week-old mice. Data represent means ± SD (N=4).

These data suggest that a mild ER stress might take place in cardiomyocytes from cYKO mice. To evaluate the functional impact of the mild ER stress observed at the early stages where no DCM and HF are evident, cYKO mice (and their control littermates) were challenged with intraperitoneal injection of DMSO or tunicamycin (TN) 2mg/kg for 72 hours. TN injection is a classical experiment used to elicit activation of the UPR and unmask organ dysfunction related to ER stress.

Before TN, cardiac function in young mice was normal on echocardiographic evaluation. However, 72h after TN injection, an overt systolic dysfunction (significant deterioration in LVEF) was observed only in cYKO mice (**Figure 18**).

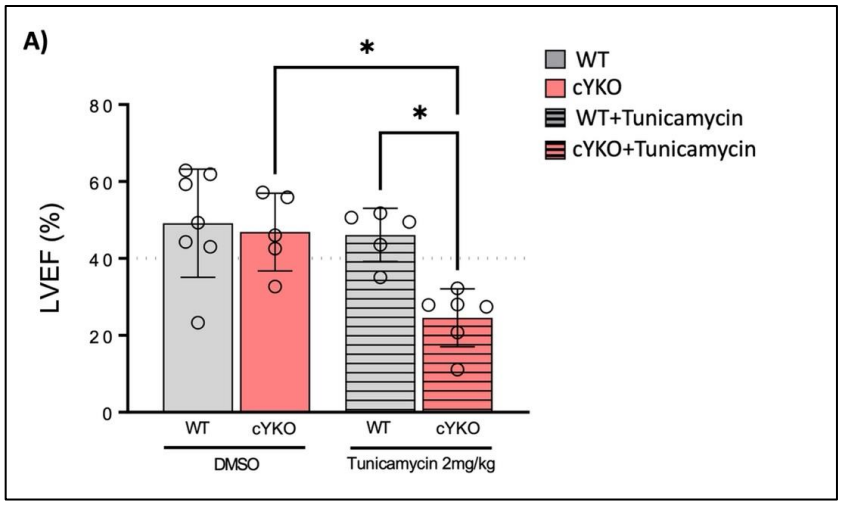

Figure 18. Cardiac function under ER stress induction with Tunicamycin

(A) Echocardiographic evaluation of cardiac function (%LVEF) of mice under 2mg/kg of i.p. DMSO/Tunicamycin for 3 days. WT+DMSO (grey), cYKO+DMSO (red), WT+Tunicamycin (striped grey), cYKO+Tunicamycin (stripped red). Data represent means ± SD. *P<0.05 after Two-Way ANOVA test (N=5-7) with Tukey´s multiple comparisons test.

Altogether, these data show that cardiomyocyte ablation of *Yme1l* predispose to ER stress, which can lead to overt cardiac dysfunction when the system is challenged.

Collectively, this first part of the study demonstrates that: Lack of YME1L in cardiomyocytes results in an OMA1-mediated OPA1 processing, which impairs mitochondrial fusion. As an early mechanism to compensate the inability to fuse, mitochondria enlarge and display an increased respiration capacity along with enhancement of ETS and reduced ROS. The structurally altered mitochondria results in a remodeling of MAMs, evidenced by altered spatial interaction between mitochondria and ER and by increased Ca^{2+} flux into mitochondria. These changes result in a subtle ER stress, which upon tunicamycin challenge unmask a rapid cardiac systolic dysfunction. ER stress results in an impaired autophagy. Impaired autophagy results in progressive accumulation of waste material that would finally result in cardiomyocyte dysfunction upon age, resulting in an overt DCM phenotype with associated HF and early death of mice.

In order to demonstrate that impaired autophagy was the ultimate cause of late-onset DCM and HF development, we tested interventions known to impact the autophagic flux: dietary approaches.

Since there are several diets known to modulate autophagy, firstly we evaluated the impact of different diets on survival and cardiac function to then perform a mechanistic evaluation on the selected diet(s) on autophagy, ER-to-mitochondria interaction, and cardiac function.

A fat-restricted diet prevents the onset of dilated cardiomyopathy and expands lifespan in cardiac-specific YME1L KO mice

To identify the best nutritional approach to alleviate the DCM and HF phenotype, 10-week-old cYKO mice were randomly assigned to chow diet (≃5% crude fat), non-fat (NFD, <0.2% fat crude fat), low fat diet (10.2% crude fat) and high fat diet (HFD, 34% crude fat) (see material and methods for more details regarding diet composition). Cardiac function was serially monitored by echocardiography every 10 weeks. Confirming our previous studies (Wai et al., 2015), HFD was associated with a delay in the onset of DCM (LV volumes were more preserved, and LVEF was significantly better than that in control-diet-treated mice at 40 weeks of age) (**Figure 19A, 19B**). However, mice receiving NFD displayed even more preserved LV volumes and better cardiac function at all evaluated timepoints (**Figure 19A, 19B**). LVEF at 40 weeks of age was significantly higher in NDF-fed mice than in all the other groups (including the HFD-fed one) (**Figure 19C, 19D**). A low-fat diet did not have any impact on cardiac function when compared to the control diet (**Figure 19A, 19B**).

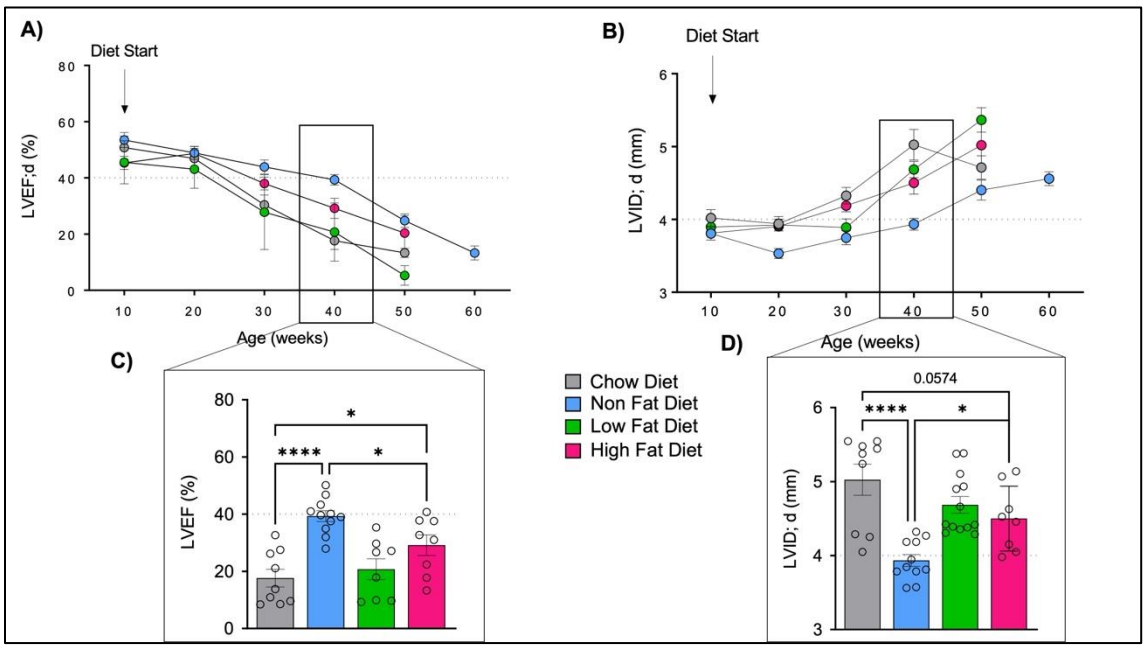

Figure 19. Effects of a control, low, high, and fat-restricted diets on cardiac function of cYKO mice

(A) Echocardiographic evaluation of cardiac function (%LVEF) in cYKO mice under a chow diet (grey), non-fat diet (blue), low fat diet (green) and high fat diet (pink). Y axis represent %LVEF. X axis represent mice age in weeks. Black dotted line to represent % of LVEF of cardiac dysfunction (40%). Data represent means ± SEM (N=9-14)

(B) Echocardiographic evaluation of left ventricular internal diameter (LVID; mm) in cYKO mice under a chow diet (grey), non-fat diet (blue), low fat diet (green) and high fat diet (pink). Y axis represent LVID; mm. X axis represent mice age in weeks. Black dotted line to represent mm of LVID of cardiac dysfunction (4mm). Data represent means ± SEM.

(C) 40-week-old cardiac function (%LVEF) in cYKO mice under a chow diet (grey), non-fat diet (blue), low fat diet (green) and high fat diet (pink). Y axis represent %LVEF. X axis represent mice age in weeks. Black dotted line to represent % of LVEF of cardiac dysfunction (40%). Data represent means ± SEM, *P<0.05, **** P<0.0001 after One-Way ANOVA test with Šidák´s multiple comparisons test.

(D) 40-week-old ventricular enlargement (LVID; mm) in cYKO mice under a chow diet (grey), non-fat diet (blue), low fat diet (green) and high fat diet (pink). Y axis represent %LVEF. X axis represent mice age in weeks. Black dotted line to represent mm of LVID of cardiac dysfunction (4mm). Data represent means ± SEM, *P<0.05, **** P<0.0001 after One-Way ANOVA test with Šidák´s multiple comparisons test.

We have previously shown that cardiomyocyte specific *Yme1l* ablation significantly reduces life expectancy due to advanced HF. Given the effects observed in cardiac function by different diets, we wanted to explore whether this translated into life prolongation. As shown in **Figure 20A, 20B**, cYKO mice receiving NFD from the age of 10 weeks had a significantly longer life expectancy than animals receiving any other type of diet. Of note, the modest effect of HFD on cardiac function did not translate into any survival benefit compared to the control diet (**Figure 20A, 20B**).

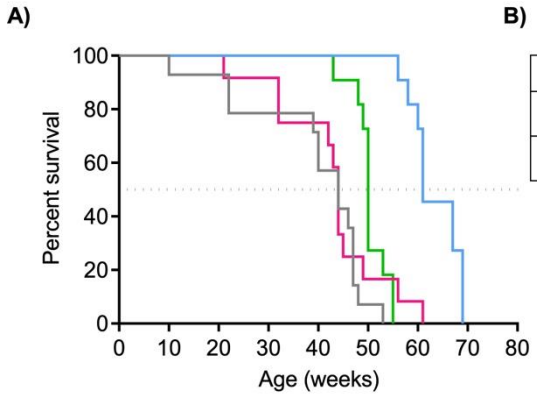

B)

	Chow Diet	Non Fat Diet	Low Fat Diet	High Fat Diet
Median Survival (weeks)	44	61	50	44
Log-rank (Mantel-Cox) test		****	***	n.s.

Figure 20. Lifespan of cYKO mice under a CD, NFD, LFD and HFD.

A) Lifespan of cYKO mice under a chow diet (grey), non-fat diet (blue), low fat diet (green) and high fat diet (pink). Black dotted line represents 50% survival rate.

B) Median survival (weeks) of mice cYKO under a chow diet, non-fat diet, low fat diet and high fat diet. ***P<0.001, **** P<0.0001 after Log-rank (Mantel-Cox) test (N=9-14).

After identifying the best nutritional approach in terms of cardiac function improvement and life expectancy, we wanted to explore the mechanism leading to such a benefit.

Non-fat diet impacts cardiac metabolism

The heart is an omnivore organ which can use different metabolic substrates. However, in homeostatic circumstances (i.e., healthy hearts), the preferred substrate is fatty acids due to the higher energetic efficiency of fatty acid oxidation. It is well described that in HF conditions of different etiologies, a metabolic switch characterized by preferential glucose utilization occurs. We previously reported that cYKO mice with overt DCM phenotype display a significant increase in myocardial glucose uptake (Wai et al., 2015). Here we wanted to explore the effect of NFD on cardiac metabolic substrate utilization by *in vivo* micro-PET/CT imaging using glucose and fatty acid tracers. For in vivo glucose uptake imaging, we used the commercially available 18F-Fluorodeoxyglucose (^{18}F-FDG) tracer. Since no commercial PET tracer for *in vivo* imaging of fatty acids uptake exists, in collaboration with the advanced imaging unit at CNIC, we generated a fluor-based one: 14 (R, S)-[^{18}F] fluoro-6-thia-heptadecanoic acid (^{18}F-FTHA). We chose 35 weeks of age for imaging since it is a time where cYKO mice already display a DCM phenotype (**Figure 21A**).

As shown in **Figure 21B**, cYKO mice fed with a regular chow diet displayed an increase in cardiac glucose uptake, with no modification of this free fatty acid uptake (**Figure 21C**). cYKO mice fed with NFD displayed a normalization of glucose uptake (which returned to levels similar to WT littermates), and a highly significant reduction in this fatty acid use.

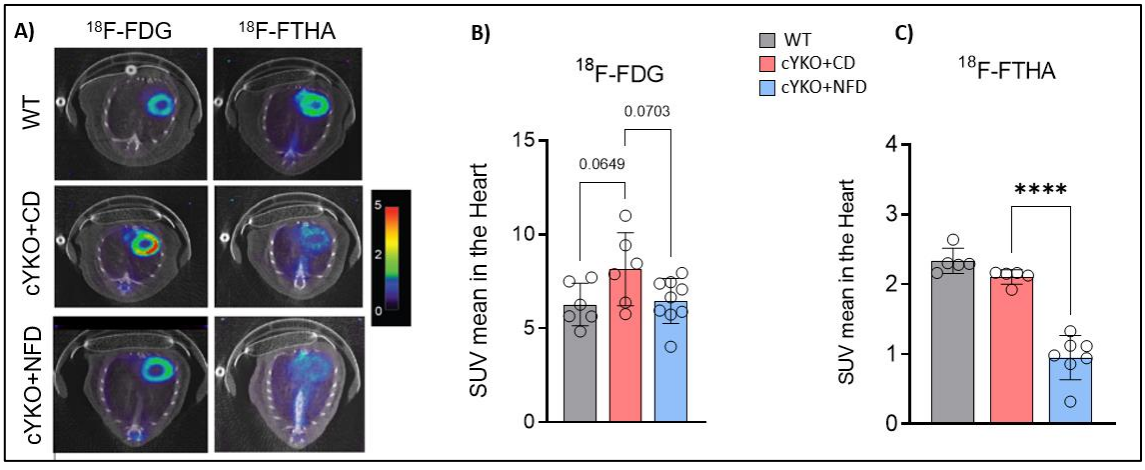

Figure 21. Effect of diets on glucose and fatty acid heart metabolism

(A) Representative micro-PET/CT scans of [^{18}F] FDG and [^{18}F] FTHA injections uptake of 30-week-old WT, cYKO+CD and cYKO+ NFD mice. Color scale define the intensity: warm color>cold color

(B) Average standardized uptake value (SUV) of [^{18}F] FDG in WT, cYKO+CD and cYKO+NFD mice hearts. Data represent means ± SD. One-Way ANOVA test (N=6-9) with Dunnett´s multiple comparisons test.

(C) Average standardized uptake value (SUV) of [^{18}F] FTHA in WT, cYKO+CD and cYKO+NFD mice hearts. Data represent means ± SD. ****P<0.0001 after One-Way ANOVA test (N=6-9) with Dunnett´s multiple comparisons test.

These results show that the heart has an enormous metabolic flexibility for adapting to nutritional restrictions. However, whether the changes in cardiac metabolism entailed by a non-fat diet are responsible for the improvement in cardiac function observed with this diet, remains to be elucidated.

Non-fat diet does not result in a caloric restriction

Although the calories of the diets were chosen to be equal (chow diet: 16,88 MJ/kg vs non-fat diet: 17,2 MJ/kg), we observed a significant difference in body weight between the two groups (**Figure 22A**). To confirm that the beneficial effect of the lack of fat in the animals´ diet was not a problem in food consumption, the animals were subjected to metabolic cages to measure food intake (**Figure 22B**)**.** Despite a lower body weight in the cYKO-treated mice, there was no difference in food consumption (**Figure 22C, 22D**), endorsing the idea that the lack of fat and not a caloric restriction due to no food consumption was responsible for the cardioprotection and life-span extension.

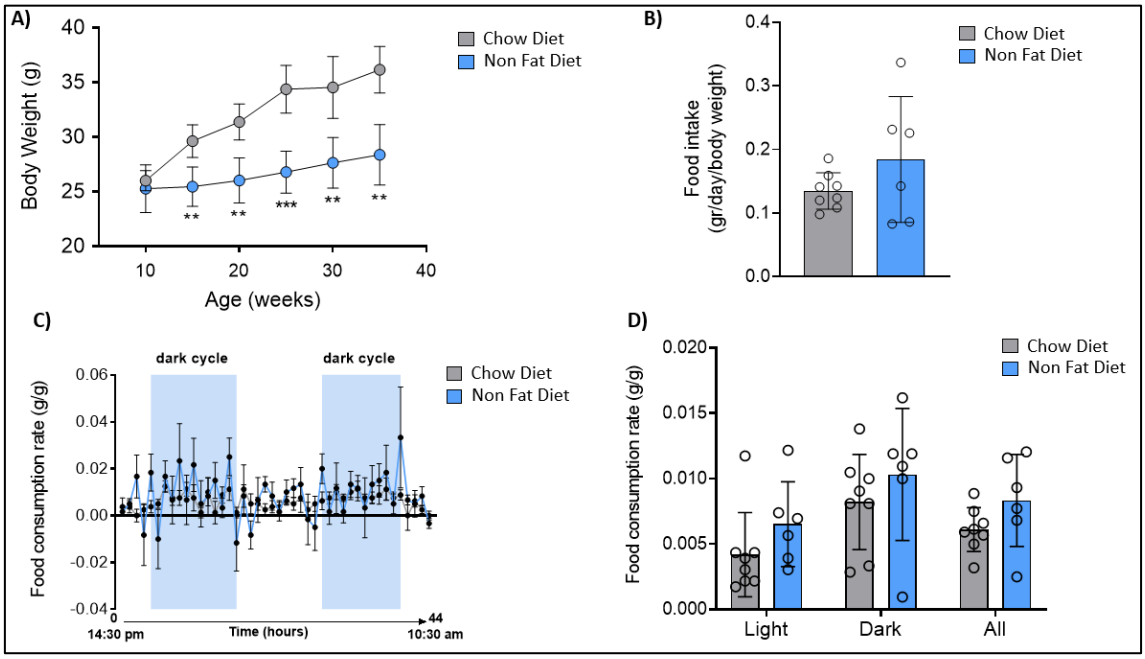

Figure 22. Food consumption analysis of cYKO under a CD and NFD

(A) Body weight (gr) of cYKO mice under a chow diet (grey) or a non-fat diet (blue). X axis represents age of mice (weeks). Data represent means ± SD. **P<0.01, ***P<0.001 **** after One-Way ANOVA test (N=6-8) with Dunnett´s multiple comparisons test.

(B) Food intake represented as grams per day per body weight (gr) of cYKO mice under a chow diet (grey) or a non-fat diet (blue). Data represent means ± SD (N=6-8).

(C) Food consumption rate represented as the weight of food (gr) consumed by unit of animal weight (gr) and calculated for each user defined interval of time (44hours). cYKO mice under a chow diet (grey) and cYKO under a non-fat diet (blue).

(D) Food consumption rate represented in light/dark cycles and altogether of cYKO mice under a chow diet (grey) and cYKO under a non-fat diet (blue). Data represent means ± SD.

Non-fat diet prevents mitochondrial fragmentation

Lack of YME1L results in inability of mitochondrial fusion. As shown before (**Figure 7**), to compensate this cardiomyocyte mitochondria lack YME1L enlarge in early stages of life until the system fails, and the mitochondria become fragmented concurring with overt development of the DCM and HF phenotype. Here we investigated the impact of NFD on mitochondrial structure and function. For mitochondrial ultrastructure, hearts from 35-week-old cYKO mice fed with NFD or regular chow (as well as WT littermates) were studied by TEM (**Figure 23A**). By analyzing the number of mitochondria and in accordance with our previous publication (Wai et al., 2015), cYKO mice under a chow diet displayed an increase in mitochondria number, together with a reduction in their size when compared to WT mice (**Figure 23B, 23C**).

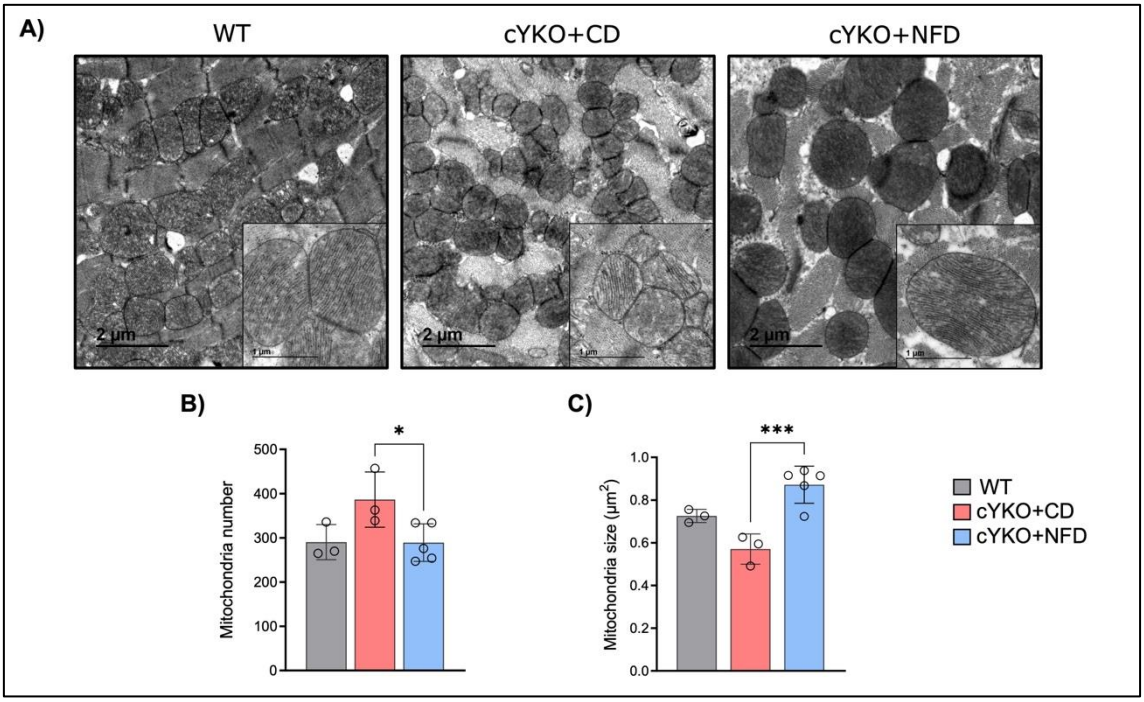

Figure 23. Impact of NFD in mitochondria ultrastructure

(A) Representative transmission electron microscopy (TEM) images of heart tissue from 35-week-old WT, cYKO+CD and cYKO+NFD mice. Scale bar corresponds to 2um. Scale bar corresponds to 1um in amplified figures.

(B) Mitochondrial number. Data represent means ± SD. *P<0.05 after One-Way ANOVA test (N=3-5) with Šidák´s multiple comparisons test.

(C) Mitochondrial size (μm^2). Data represent means ± SD. ***P<0.001, after One-Way ANOVA test (N=3-5) with Šidák´s multiple comparisons test.

The typical mitochondrial fragmentation (smaller and more numerous mitochondria) systematically seen in cYKO middle-aged mice was completely prevented by NFD. Mitochondria from cYKO NFD-fed mice were structurally similar to those of WT mice. (**Figure 23B, 23C**).

To evaluate whether preservation of the mitochondrial structure by NFD feeding was resulting from normalization of OPA1 processing, we studied the density of its different isoforms (**Figure 24A**). As expected, (since the genetic ablation of *Yme1l* was still present), NFD did not rescue OPA1 isoforms (**Figure 24B**).

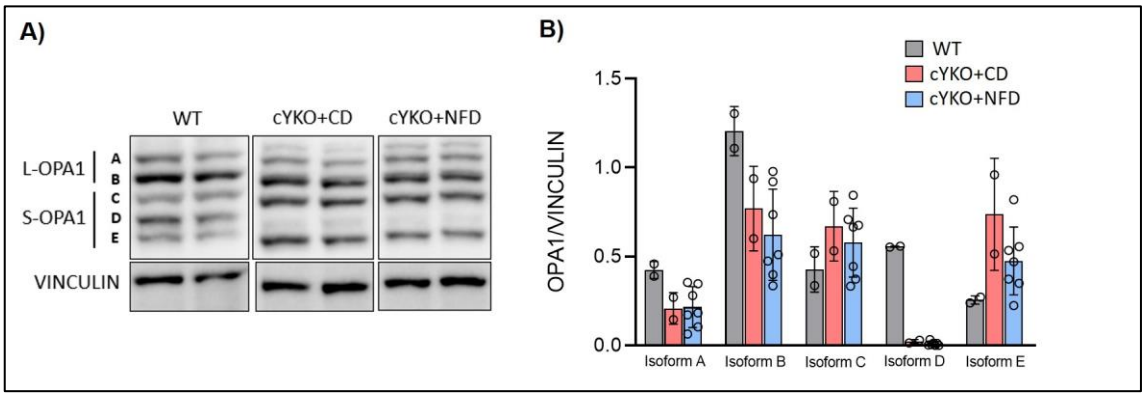

Figure 24. Effect of NFD on OPA1 expression

(A) Immunoblot analysis of expression of OPA1 isoforms in heart tissue from WT, cYKO+CD, cYKO+NFD 35-week-old mice. VINCULIN was used as a loading control

(B) Quantification of expression of OPA1 isoforms OPA1 in heart tissue from WT, cYKO+CD, cYKO+NFD 35-week-old mice. Data represent means ± SD (N=2-7)

Non-fat diet does not increase mitochondrial respiration capacity

After documenting the changes in mitochondrial structure after NFD, we explored the ETS status. Bioenergetics using the HRR-O2k system were quantified in mitochondria isolated from 35-week-old cYKO mice on a chow diet or NFD, as well as in their WT littermates.

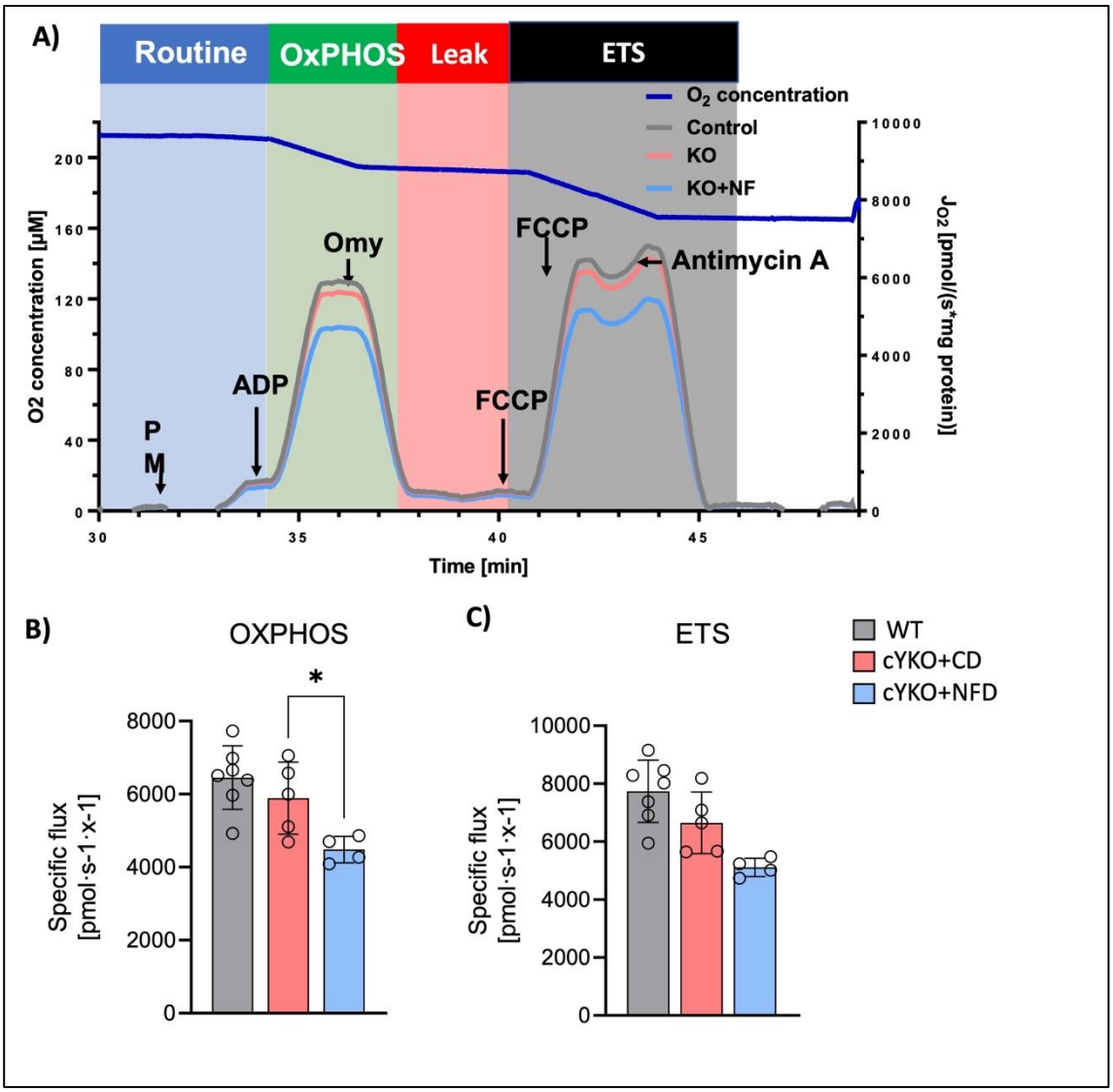

Figure 25. Effect of NFD on mitochondrial respiration

A) Representative trace of High Resolution Respirometry taken from the DatLab software. Left axis refers to O_2 concentration [µM], right axis refers to O2 flux per Volume [pmol/(s*ml)], X axis represents time in hours and minutes [h:m]. Blue line along the trace indicates oxygen concentration, grey, red, and blue lines indicate oxygen consumption or (JO2) by the biological sample, WT, cYKO+CD and cYKO+NFD, respectively.

B) Oxidative phosphorylation (OxPHOS) from isolated heart mitochondria from WT, cYKO+CD, cYKO+NFD 35-week-old mice. Oxygen consumption of mitochondria was measured in the presence of Pyruvate + Malate (PM), adenosine diphosphate (ADP) and oligomycin. Data represent means ± SD. *P<0.05 after parametric unpaired t-test (N=4-7) with Šidák´s multiple comparisons test.

C) Maximal respiration of the electron transport system (ETS) from isolated heart mitochondria from WT, cYKO+CD and cYKO+NFD 35-week-old mice. ETS was measured in the presence of uncoupler FCCP + Antimycin A. Data represent means ± SD (N=4-7) with Šidák´s multiple comparisons test.

As previously shown, the compensatory increased respiration capacity observed in isolated mitochondria from 10-week-old cYKO mice is lost when animals reach the overt DCM phenotype: at 35 weeks of age respiration and ETS capacity in cYKO mice are no different from that of WT littermates (Figure 25B, 25C).

Unexpectedly, OxPHOS capacity was reduced in mitochondria isolated from NFD-fed cYKO mice, along with attenuated ETS capacity.

After documenting that improved mitochondrial function was not the leading mechanism driving the improvement in cardiac function, we explored interactions between mitochondria and ER.

Fat restricted diet maintains the close spatial relationship between mitochondria and ER

As shown in **Figure 15**, the early compensatory mechanism including a close interaction between mitochondria and ER is lost at later stages of life, concurring with the development of the DCM and HF phenotype. Here we explored the impact of NFD on these inter-organelle interactions by TEM (**Figure 26A**). When compared to animals receiving a chow diet, NFD was associated with a significant decrease in mitochondria MAM's coverage (**Figure 26C**), ER length (**Figure 26D**), and ER dilation (**Figure 26E**). However, while in a subclinical stage the distance of ER-mitochondria was reduced (**Figure 15D**), at this point where we have cardiac dysfunction the distance between the two organelles increases in cYKO mice regardless of the diet used (**Figure 26F**).

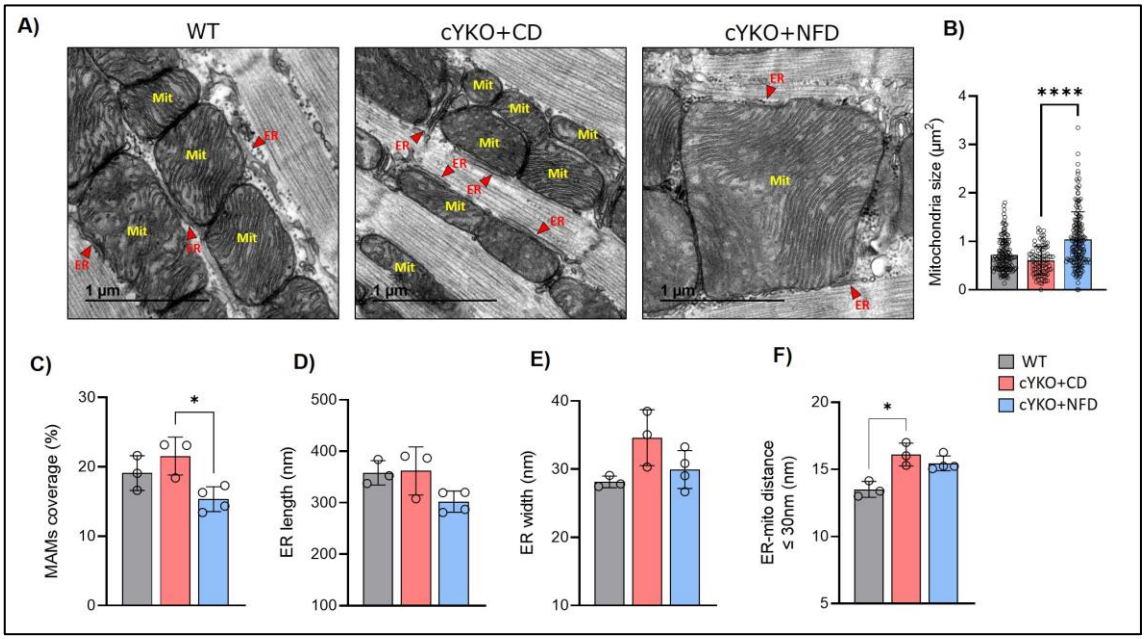

Figure 26. Effect of NFD on MAMs association

(A) Representative transmission electron microscopy (TEM) images of isolated adult cardiomyocytes from 20-week-old WT, cYKO+CD and cYKO+NFD mice. Mit (yellow)=mitochondria, ER (red)=Endoplasmic Reticulum. Scale bar corresponds to 1um

(B) Mitochondrial size (μm^2). Data represent individual mitochondria ± SD. ****P<0.0001, after nonparametric Kruskal Wallis test.

(C) Mitochondrial associated membrane (MAM) coverage (%), represented as the ratio between the ER length in touch with mitochondria and mitochondrial perimeter. Data represent individual animals ± SD. *P<0.05, after nonparametric Kruskal-Wallis's test (N=3-4)

(D) Endoplasmic reticulum (ER) length (nm), represented as the length of ER in touch with mitochondria. Data represent individual animals ± SD (N=3-4)

(E) Endoplasmic reticulum (ER) width, represented as the width of ER in touch with mitochondria. Data represent individual animals ± SD (N=3-4)

(F) Endoplasmic reticulum (ER)-mitochondria distance (nm), represented as the distance between ER and mitochondria. Data represent individual animals ± SD. *P<0.05, after nonparametric Kruskal-Wallis's test (N=3-4)

Higher distances between the two organelles were further supported by a significant decrease in MFN2, known as a MAM-tethering protein, under a chow diet (**Figure 27A, 27B**). Interestingly, this MFN2 inhibition was partially reestablished by the non-fat diet (**Figure 27A, 27B**).

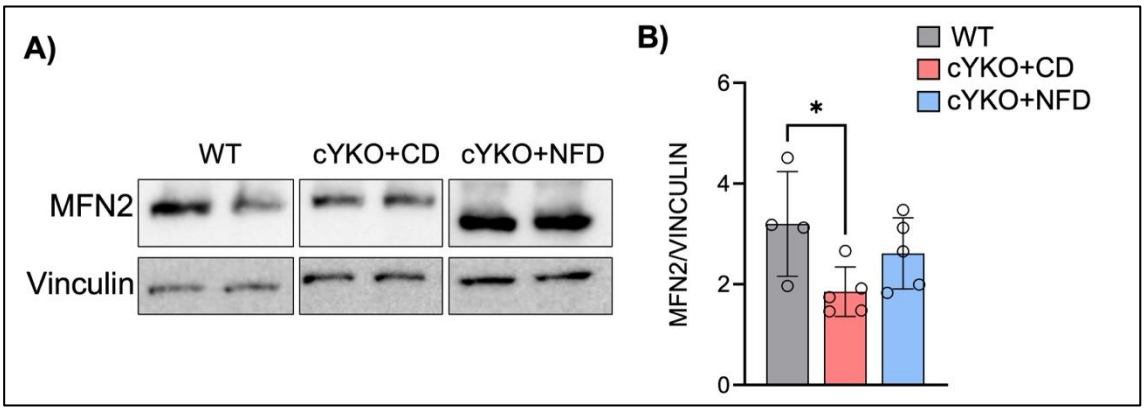

Figure 27. Effect of diets on mitochondrial dynamics

(A) Immunoblot analysis of MFN2 expression in heart tissue from WT, cYKO+CD, cYKO+NFD 35-week-old mice. VINCULIN was used as a loading control.

(B) Quantification of MFN2 expression in hearts from WT, cYKO+CD, cYKO+NFD 35-week-old mice. Data represent means ± SD. *P<0.05, after parametric One-Way ANOVA test (N=4-5) with Šidák´s multiple comparisons test.

Collectively, structural analysis shows that NFD prolongs the compensatory status seen in early ages of cYKO mice without apparent DCM and HF phenotype. This prolongation of the compensatory status is in line with the preserved cardiac function when cYKO mice are subjected to NFD.

One of the principal association roles of MAMs is Ca^{2+} signaling through the IP3R1/Grp75/VDAC1 complex. We hypothesized that the NFD might alter the Ca^{2+} channeling complex in order to reestablish Ca^{2+} flux between ER and mitochondria.

We isolated heart mitochondria from WT, cYKO+CD and cYKO+NFD and measure mitochondrial calcium with Oroboros, confirming disrupted Ca^{2+} handling in cYKO mice and reestablished to basal levels by a non-fat diet (**Figure 28A**). We next explored MCU, the mitochondrial uniporter that acts as a gatekeeper of Ca^{2+} entry into the mitochondrial matrix. Congruently with our hypothesis, cYKO animals under a chow diet have an increased MCU expression which directly correlates with the increase in Ca^{2+}. In accordance, animals under a NFD present restored MCU expression levels (**Figure 28B, 28C**).

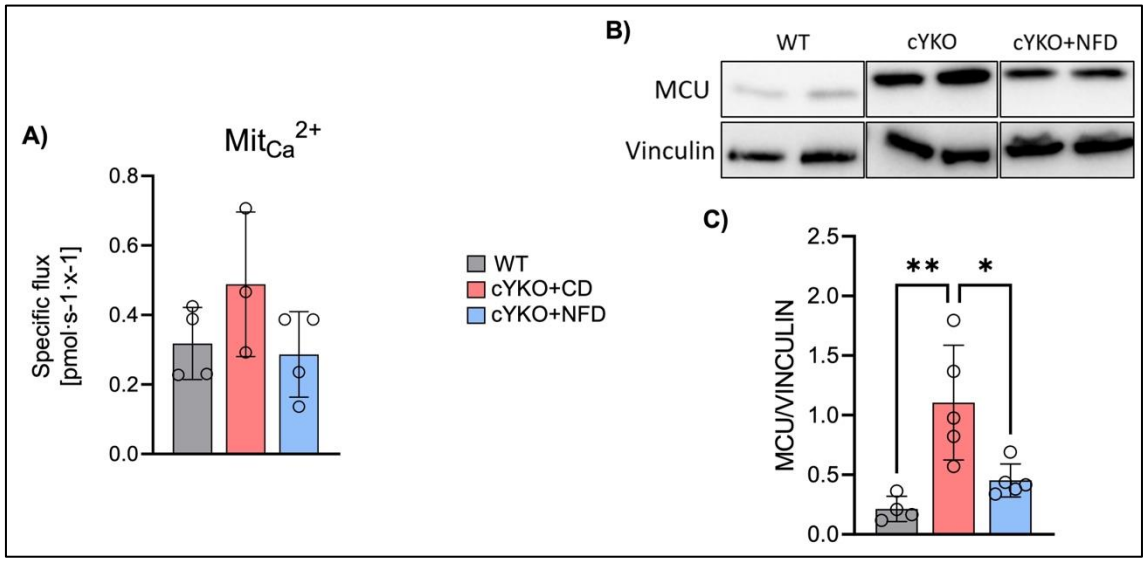

Figure 28. Impact of NFD on Ca^{2+} flux

(A) Mitochondrial Ca^{2+} content in isolated heart mitochondria from WT (grey), cYKO+CD (red), cYKO+NFD (blue) from 35-week-old mice. Data represent means ± SD. (N=3-4).

(B) Immunoblot analysis of MCU expression in heart tissue from WT, cYKO+CD, cYKO+NFD 35-week-old mice. VINCULIN was used as a loading control.

(C) Quantification of MCU expression in hearts from WT, cYKO+CD, cYKO+NFD 35-week-old mice. Data represent means ± SD. *P<0.05, **P<0.01 after parametric One-Way ANOVA test (N=4-5) with Šidák´s multiple comparisons test.

Taking all of this into consideration, analysis of isolated mitochondria revealed that cYKO mice present an overload of mitochondrial Ca^{2+}, restored by the use of a fat restricted diet. This restoration concurs with the cardioprotective status at this timepoint.

Fat restricted diet does not prevent ER stress

As shown before, lack of YME1L in cardiomyocytes is associated with subtle ER stress at early stages (**Figure 17**). This process is "exhausted" at later stages, as evidenced by the significant reduction of ATF4 protein levels (**Figure 29D, 29E**), becoming overt later in life (35 weeks). NFD was not associated with changes in the levels of proteins related to ER stress (**Figure 29D, 29E**).

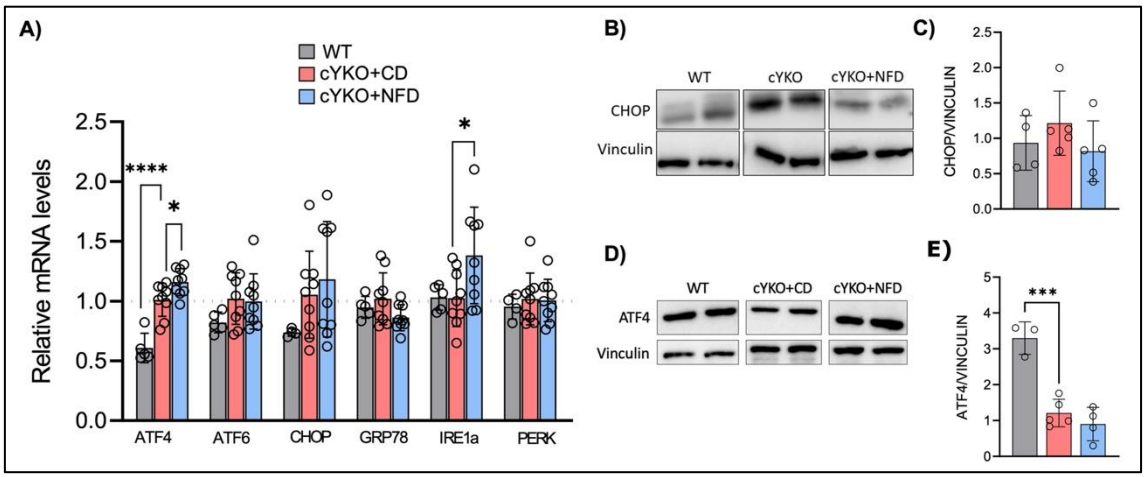

Figure 29. Effect of NFD on ER stress

(A) mRNA expression of *Atf4, Atf6, Chop, Grp78, Ire1a, Perk* in heart tissue from WT, cYKO+CD, cYKO+NFD 35-week-old mice. Data represent means ± SD. *P<0.05, ****P<0.0001 after parametric One-Way ANOVA test (N=5-8) with Šidák´s multiple comparisons test.

(B) Immunoblot analysis of CHOP expression in heart tissue from WT, cYKO+CD, cYKO+NFD 35-week-old mice. VINCULIN was used as a loading control.

(C) Quantification of CHOP expression in heart tissue from WT, cYKO+CD, cYKO+NFD 35-week-old mice. Data represent means ± SD (N=4-5)

(D) Immunoblot analysis of ATF4 expression in heart tissue from WT, cYKO+CD, cYKO+NFD 35-week-old mice. VINCULIN was used as a loading control.

(E) Quantification of ATF4 expression in heart tissue from WT, cYKO+CD, cYKO+NFD 35-week-old mice. Data represent means ± SD (N=3-5). ***P<0.001 after parametric One-Way ANOVA test.

Fat-restricted diet does not alleviate autophagy impairment of late stages

Autophagosome-lysosome fusion is inhibited in cardiomyocytes from cYKO mice. Here we explored whether NFD could alleviate this blockage and restore autophagic flux. We first measured the steady state of LC3 and BECLIN1. Remarkably, in cYKO mice NFD resulted in a prominent accumulation of LC3-II as compared to those under a chow diet (**Figure 30A, 30B**). When autophagosome to lysosome fusion was inhibited by intraperitoneal administration of leupeptin (40 min before sacrifice), LC3-II levels did not increase, showing that the autophagosome to lysosome was not restored in NFD conditions (**Figure 30A, 30B**).

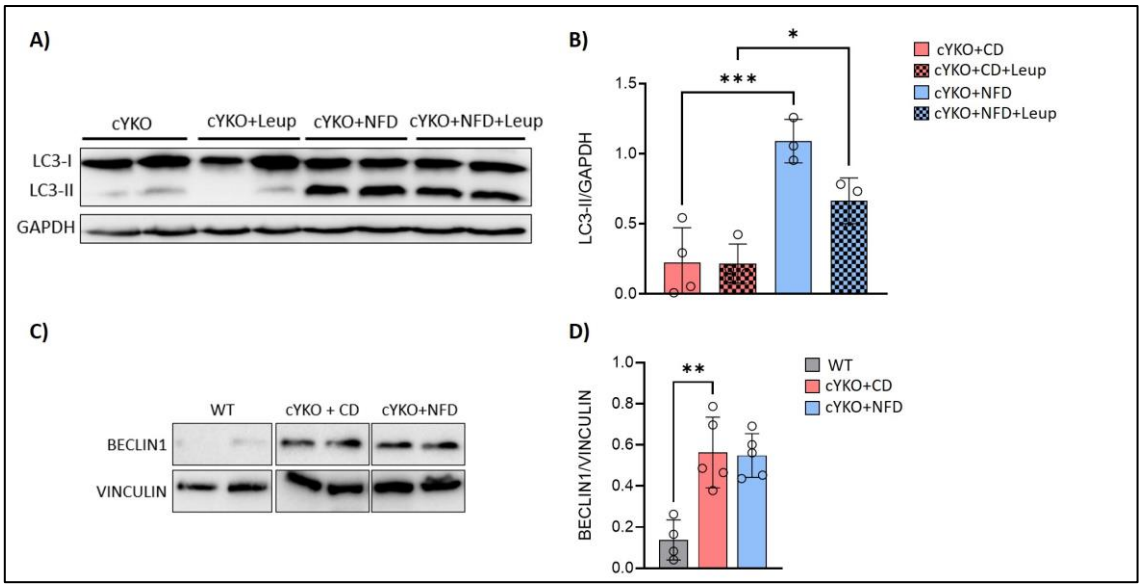

Figure 30. Effect of NFD on autophagic flux

(A) Immunoblot analysis of LC3 expression in heart tissue from WT, cYKO+CD and cYKO+NFD 35-week-old mice under 40mins of 40mg/kg of the lysosomal inhibitor leupeptin. GAPDH was used as a loading control.

(B) Quantification of LC3 expression in heart tissue from WT, cYKO+CD and cYKO+NFD 35-week-old mice under 40mins of 40mg/kg of the lysosomal inhibitor leupeptin. Data represent means ± SD. *P<0.05, ***P<0.001 after parametric One-Way ANOVA test (N=3-4) with Holm-Šidák´s multiple comparisons test.

(C) Immunoblot analysis of BECLIN1 expression in heart tissue from WT, cYKO+CD and cYKO+NFD 35-week-old mice. VINCULIN was used as a loading control

(D) Quantification of BECLIN1 expression in heart tissue from WT, cYKO+CD and cYKO+NFD 35-week-old mice. Data represent means ± SD. **P<0.01 after parametric One-Way ANOVA test (N=4-5)

To analyze the cause of massive LC3-II accumulation, we measured p-AMPK levels since this is a nutrient sensing marker of autophagy induction (**Figure 31A**). As shown in (**Figure 31B**), pAMPK levels were remarkably upregulated in cYKO mice receiving NFD, together with a non-significant increase in PARKIN-mediated autophagy (**Figure. 31D**).

Thus, the increase of p-AMPK and LC3-II in cYKO mice fed with NFD might be responsible for an increase in the initiation step of autophagy. However, NFD does not alleviate the impaired autophagic flux associated with lack of YME1L.

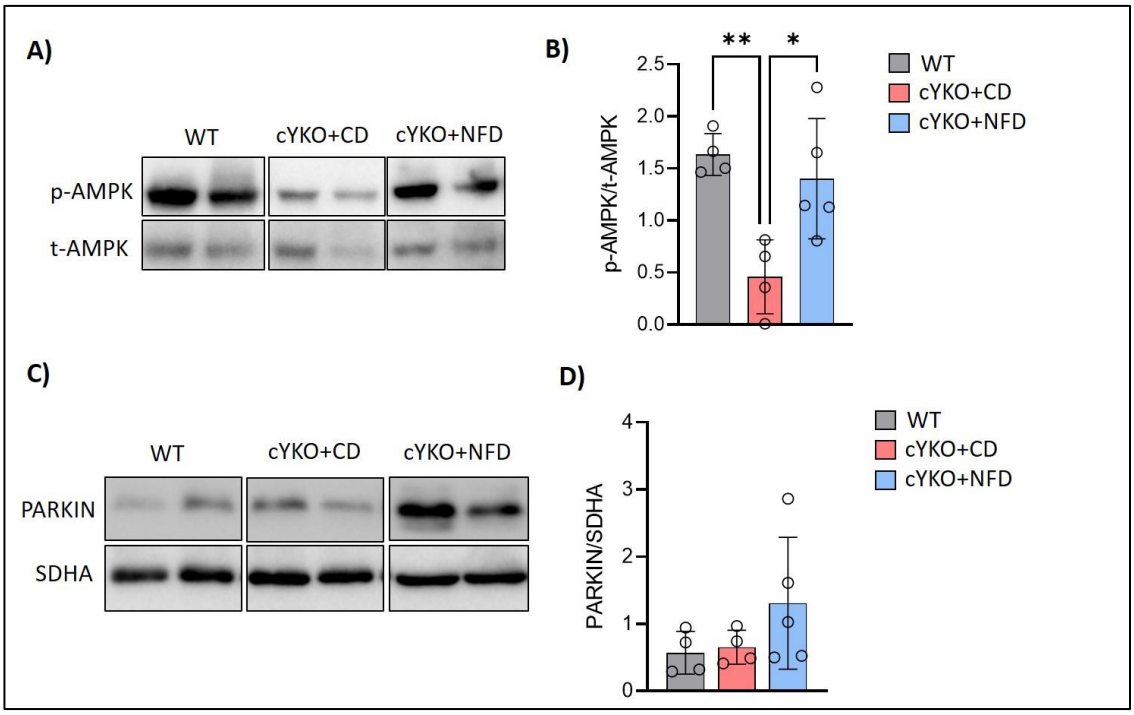

Figure 31. Effect of NFD on autophagy-related pathways

(A) Immunoblot analysis of p-AMPK expression in heart tissue from WT, cYKO+CD and cYKO+NFD 35-week-old mice. t-AMPK was used as a loading control

(B) Quantification of p-AMPK expression in heart tissue from WT, cYKO+CD and cYKO+NFD 35-week-old mice. Data represent means ± SD. *P<0.05, **P<0.01 after parametric One-Way ANOVA test (N=4-5) with Šidák´s multiple comparisons test.

(C) Immunoblot analysis of PARKIN expression in heart tissue from WT, cYKO+CD and cYKO+NFD 35-week-old mice. SDHA was used as a loading control

(D) Quantification of PARKIN expression in heart tissue from WT, cYKO+CD and cYKO+NFD 35-week-old mice. Data represent means ± SD (N=4-5)

Synergistic beneficial effect of intermittent fasting and NFD

After documenting that NFD resulted in a significant induction of autophagy, although the flux is not restored, we wanted to explore whether another intervention known to increase the early steps of the process could have an additional benefit.

Firstly, we tested the effect on lifespan and cardiac function of an isolated caloric restriction. To this aim, 20-week-old cYKO mice were placed on an intermittent fasting regimen consisting of 2 consecutive days fasting followed by 5 days on regular chow (2:5). Cardiac function was measured by echocardiography every 10 weeks (**Figure 32A**).

As expected, compared to the control chow diet, 2:5 intermittent fasting was associated with an improvement in cardiac function (**Figure 32B**) together with a modest prolongation in lifespan (**Figure 32C**).

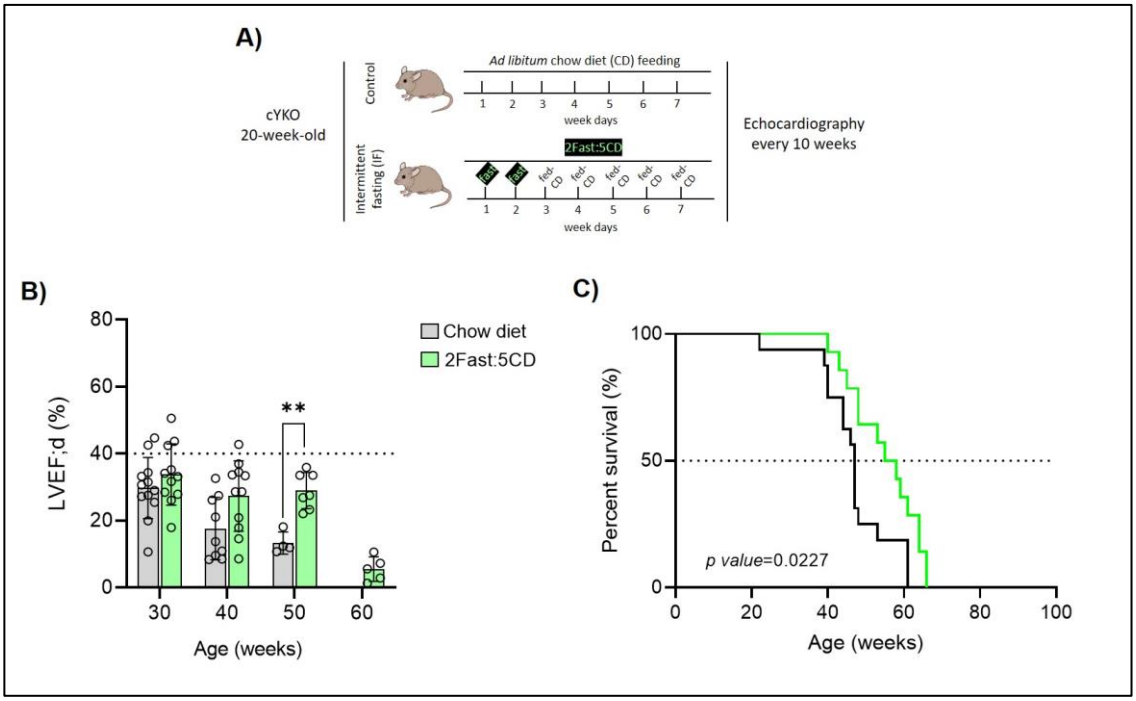

Figure 32. Effect of 2:5CD IF protocol on cardiac function and lifespan of cYKO mice

(A) Experimental design scheme with cYKO mice under *ad libitum* chow diet (n=12) and animals under IF protocol 2 days fasting + 5 days chow diet (n=11). CD: chow diet

(B) Echocardiography evaluation of LVEF in cYKO male mice under *ad libitum* chow diet (grey) or 2Fast:5CD (green) feeding protocol. Data represent means ± SD. **P<0.01, after multiple unpaired t-test. Black dotted line represents the limit established for cardiac dysfunction. LVEF: left ventricular ejection fraction

(C) Lifespan of cYKO mice under *ad libitum* chow diet (black) or 2Fast:5CD (green) feeding protocol. Log-rank (Mantel-Cox) test, *P<0.05.

We tested a more aggressive intermittent fasting protocol, consisting of (2 days fasting → 1 day of regular chow diet → 2 days fasting→ 2 days regular chow diet) (**Figure 33A**). As shown in **Figure 33B**, the benefits in cardiac function compared to regular chow were much more modest than those of the less aggressive intermittent fasting shown before. No impact of intermittent fasting on lifespan was observed (**Figure 33C**).

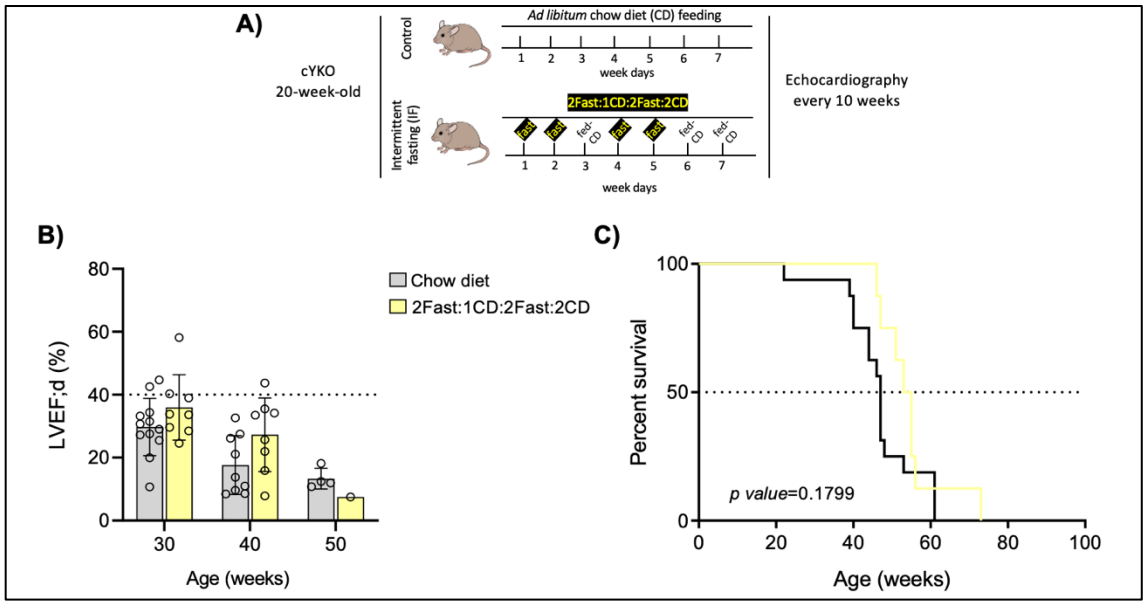

Figure 33. Effect of 2:1:2:2 IF protocol on cardiac function and lifespan of cYKO mice

(A) Experimental design scheme with cYKO mice under *ad libitum* chow diet (n=12) and animals under IF protocol 2 days fasting + 1 chow diet + 2 days fasting + 2 chow diet (n=7). CD: chow diet

(B) Echocardiography evaluation of LVEF in cYKO male mice under *ad libitum* chow diet (grey) or 2Fast:1CD:2Fast:2CD (yellow) feeding protocol. Data represent means ± SD. *p value*=n.s., after multiple unpaired t-test. Black dotted line represents the limit established for cardiac dysfunction. LVEF: left ventricular ejection fraction, n.s.: non-significant

(C) Lifespan of cYKO mice under *ad libitum* chow diet (black) or 2Fast:1CD:2Fast:2CD (yellow) feeding protocol. Log-rank (Mantel-Cox) test. *p value*=n.s.

We then combined both dietary approaches (intermittent fasting and NFD). 20-week-old cYKO mice were placed on the 2:5 intermittent fasting protocol, NFD being the diet used for the 5 days of feeding (**Figure 34A**). A much more pronounced cardioprotective effect was observed, as evidenced by a significantly higher LVEF at all timepoints measured (**Figure 34B**). Of note, lifespan was significantly prolonged by this protocol (**Figure 34C**). These data show a synergistic effect of both dietary interventions.

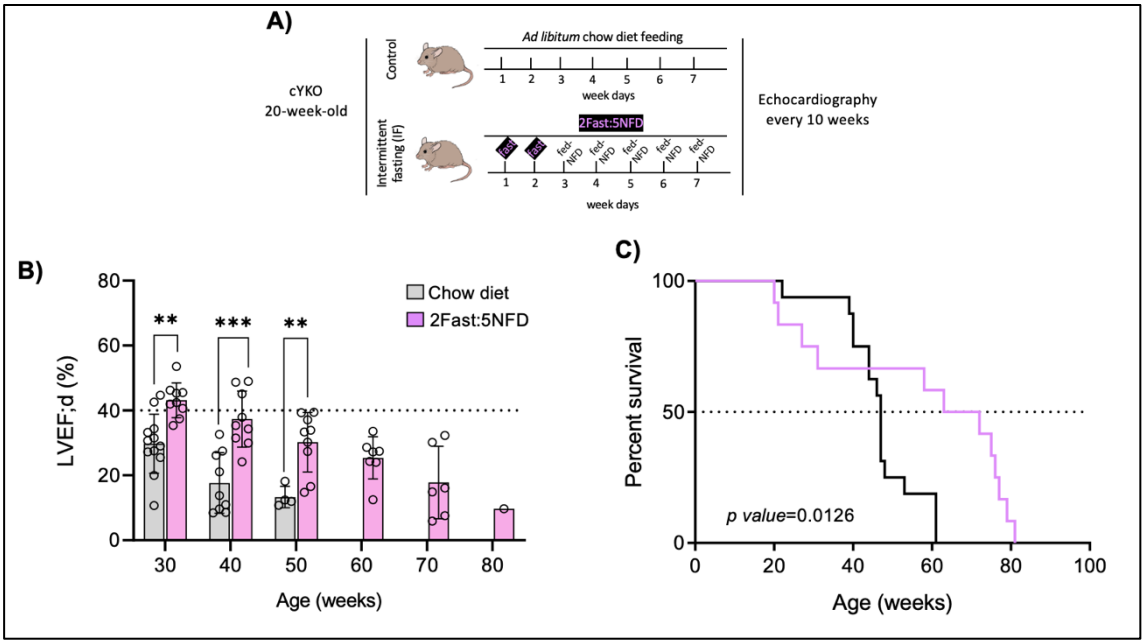

Figure 34. Effect of 2:5NFD IF protocol on cardiac function and lifespan of cYKO mice

(A) Experimental design scheme with cYKO mice under *ad libitum* chow diet (n=12) and animals under IF protocol 2 days fasting + 5 days non-fat diet (n=12). NFD: non-fat diet

(B) Echocardiography evaluation of LVEF in cYKO male mice under *ad libitum* chow diet (grey) or 2Fast:5NFD (purple) feeding protocol. Data represent means ± SD. **P<0.01,***P<0.001 after multiple unpaired t-test. Black dotted line represents the limit established for cardiac dysfunction. LVEF: left ventricular ejection fraction

(C) Lifespan of cYKO mice under *ad libitum* chow diet (black) or 2Fast:5NFD (purple) feeding protocol. Log-rank (Mantel-Cox) test, *P<0.05.

Finally, in order to demonstrate that the sooner the pathological process is compensated the higher cardiovascular benefits, we explored whether an earlier initiation of NFD (i.e., at 10 weeks of age rather than 20) could show stronger cardioprotective effects. To this aim, mice were placed on NFD at 10 weeks of age followed by a later (20 weeks) initiation of the 2:5 intermittent fasting protocol (**Figure 35A**). Strikingly, the effects on cardiac function and lifespan were massively improved as compared to all previous interventions (**Figure 35B, 35C**).

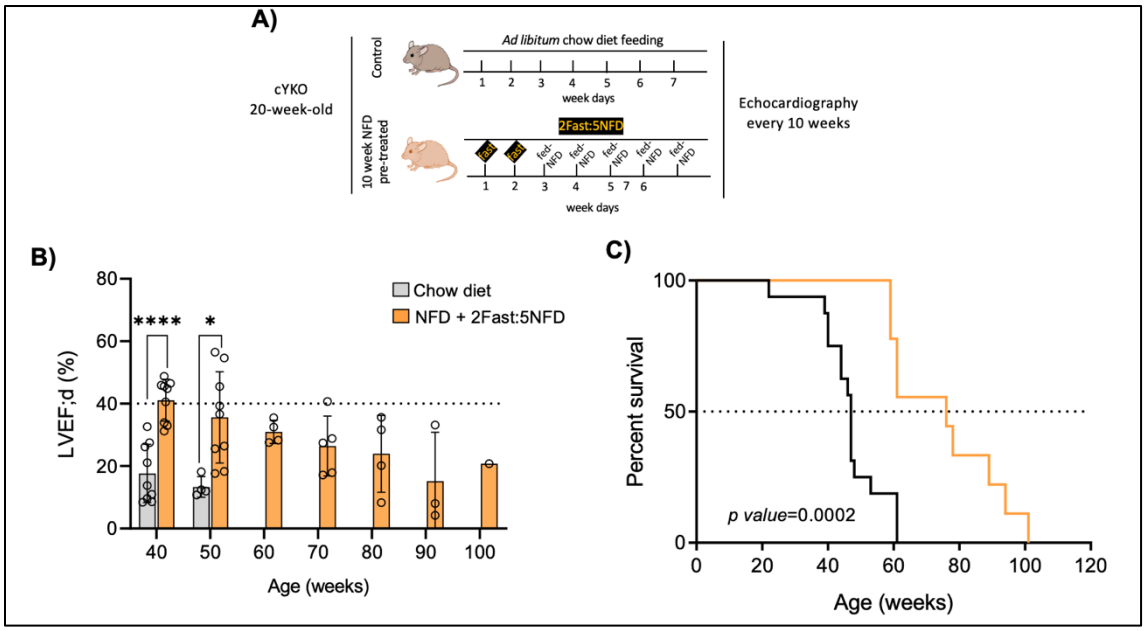

Figure 35. Effect of pretreatment with NFD + 2:5NFD IF protocol on cardiac function and lifespan of cYKO mice

(A) Experimental design scheme with cYKO mice under *ad libitum* chow diet (n=12) and animals under 10 weeks NFD pretreatment + IF protocol 2 days fasting + 5 days NFD (n=10). NFD: non-fat diet

(B) Echocardiography evaluation of LVEF in cYKO male mice under *ad libitum* chow diet (grey) or NFD+2Fast:5NFD (orange) feeding protocol. Data represent means ± SD. *P<0.05, ****P<0.0001 after multiple unpaired t-test. Black dotted line represents the limit established for cardiac dysfunction. LVEF: left ventricular ejection fraction.

(C) Lifespan of cYKO mice under *ad libitum* chow diet (black) or NFD+2Fast:5NFD (orange) feeding protocol. Log-rank (Mantel-Cox) test, ***P<0.001. NFD: non-fat diet

Throughout this dissertation we have demonstrated the beneficial use of a fat-restricted diet in cardiac function and lifespan. In this last chapter, we demonstrate a positive effect on cardiac function solely by the implementation of a mild food-restriction protocol (2:5days) that is strongly accentuated when combined with a NFD. Despite not having the molecular mechanism pathway responsible for this cardioprotection, this synergic effect of both therapies opens the door to further exploring the combination of more nutritional approaches aimed at modulating cardiac dysfunction despite a cardiac-genetic defect.

Discussion

Dilated cardiomyopathy remains the leading cause of heart failure worldwide (Merlo et al., 2018, Schultheiss et al., 2019). However, the lack of specific therapies for this cardiovascular disease remains a huge problem. Current emerging studies highlight mitochondria, the *powerhouse* of the cell, as a common factor in the diagnosis of many cases of HF (Brown et al., 2017, Ramaccini et al., 2020). This doctoral thesis seeks to uncover a new potential relation between mitochondrial dysfunction led by *Yme1l* cardiac deficiency and heart failure. Moreover, we explore the role of nutritional approaches as a tool for preventing the late stage of heart failure.

During the performance of the project, we have stated two phases of the disease: 1) Prior to the onset of DCM, in which all the results will reflect the consequence of *Yme1l* cardiac genetic ablation; and 2) once DCM is already established, where we investigate how to revert the consequences observed by *Yme1l* deletion.

The role of YME1L in the progression of dilated cardiomyopathy

The role of the protease YME1L in OPA1 processing and mitochondrial fragmentation has been widely discussed (Ruan et al., 2013, Anand et al., 2014). Mitochondria contribution in the heart represents a high percentage and its correct function is essential for cardiac wellness (Piquereau et al., 2013).

Considering that cYKO mice developed a marked mitochondrial fragmentation at late stages (Wai et al., 2015), we wanted to establish the first connection: Does this fragmentation occurs prior to the onset of DCM? Paradoxically, we found the opposite: an increase in mitochondria size with a lower number of them in cYKO young animals. The increase in the volume of mitochondria under specific cardiac deficiency of YME1L is contrary to our thoughts that decreased fusion proteins results in mitochondrial fragmentation. However, two independent laboratories unexpectedly demonstrated that cardiac-specific *Mfn2* knockout mouse models evoked mitochondrial enlargement (Papanicolaou et al., 2011, Chen et al., 2012, Dorn et al., 2015). This interesting data in a subclinical stage of the disease confirm that despite the gene defect involved in mitochondrial dynamics, this is not present at early stages but may concur with the onset of DCM.

Moreover, this modest change in mitochondrial volume does not correlate with an increase in mtDNA, but rather a decrease. It is not new that heart failure pathologies accompany defects in mtDNA, helping to predict and evaluate cardiovascular risk (Hong et al., 2020, Wang et al., 2021b). Thus, we next wanted to investigate whether this early marker of mtDNA damage was sufficient to cause a mitochondrial respiratory defect.

Mitochondrial dynamics and metabolic regulation are closely linked (Zorzano et al., 2010). Either L-OPA and S-OPA1 isoforms can preserve cristae structure and respiration when expressed individually in OPA1 deficient cells (Del Dotto et al., 2017, Lee et al., 2017). Thus, OPA1 processing apparently does not regulate the formation of cristae or the maintenance of respiratory chain complexes. However, the downregulation of OPA1 can lead to mitochondrial fragmentation and reduced oxygen consumption (Zorzano et al., 2010). Among the functions of YME1L, it degrades damaged or non-assembled IMM proteins such as respiratory chain subunits (Stiburek et al., 2012, Rainbolt et al., 2013). In the literature, loss of YME1L impairs function of respiratory complex I (Cesnekova et al., 2018). In adult neural stem and progenitor cells (NSPCs), *Yme1l* deletion is not associated with mitochondrial dysfunction and aberrant ultrastructures (Wani et al., 2022). In spinal cord mitochondria, the absence of YME1L in neurons at early stages of axonal degeneration does not have an impact on respiration. Whereas a late onset of respiratory deficiency was observed in these animals together with aberrant cristae structure deterioration (Sprenger et al., 2019). Taking all these into consideration, we were expecting to see either no effect or a decrease in respiratory function in cYKO mice. Contrary to our thoughts, prior to the onset of the disease, isolated heart mitochondria from cYKO mice display a higher oxidation capacity, together with maximum respiration values and an increased ATP production and less ROS production. Despite not measuring super complexes formation, our preliminary data on individual respiratory complexes does not indicate an increased protein expression that could explain the high respiration activity.

Thus, although our model displays a cardiac ablation of *Yme1l* from birth, this is not translated into an early mitochondrial fragmentation, which leads us to speculate that mitochondrial fragmentation is not triggering cardiac dysfunction but concurs with its onset. Intriguingly, mtDNA is decreased, although mitochondria respiration remains higher and with lower ROS production. Altogether, malfunctioning and/or dysmorphology of mitochondria is not present prior to the onset of DCM in cYKO mice, although mtDNA could serve as a damage risk predictor.

Although regenerative medicine is an emerging topic, the poor capacity of cardiomyocyte to regenerate is accepted, which is almost inexistent (Eschenhagen et al., 2017). Thus, having a good elimination system of damaged organelles in the cell (autophagy) is vital for avoiding cell death in the heart. Most of the studies conducted thus far have demonstrated a decline in autophagy once cardiac dysfunction is established or due to genetic alterations (Kaludercic et al., 2020). Autophagy is also crucial for maintaining mitochondrial respiration. In fact, an increase in autophagy/mitophagy could result in more efficient elimination of damaged organelles, leaving *robust* mitochondria with higher respiratory capacities.

Could cardiac *Yme1l* ablation disrupt autophagy? Changes in autophagy due to mitochondrial morphology are not new. Deletion of DRP1, a fission protein, in β-cells has been shown to decrease mitochondrial autophagy and reduce respiration, among others (Twig et al., 2008). In yeast, YME1L was required for selective mitophagy through the processing of the autophagy related protein 32 (Atg32) (Wang et al., 2013). In mouse embryonic fibroblasts (MEFs) it was observed that elongated mitochondria are spared from autophagic degradation. Moreover, in $OPA^{-/-}$ MEFs, the use of wortmannin, which blocks autophagosome formation, prevents mitochondrial elimination, indicating that mitochondria were degraded by autophagy (Gomes et al., 2011). Interestingly, new evidence indicates that most of the mitochondrial protein turnover occurs through non-autophagic processes (Vincow et al., 2019).

For our purpose, we initially investigated selective autophagy mediated by macroautophagy. In our working model, data indicate an elevation of LC3-II in cYKO pre-symptomatic animals. The amount of autophagosomes (LC3-II) in the cytosol can be increased by two different mechanisms: increased autophagosome synthesis by upstream processes or a blockade of lysosomal-autophagosome during a later stage. To discriminate between these two scenarios, we measured BECLIN1 and p62 markers. Both proteins were elevated in cYKO mice hearts. p62 has been proven to be degraded during autophagy. Congruently, when autophagy is inhibited, p62 accumulates in the cell, as in our model. Additionally, cardiac accumulation of p62 was also observed in several heart diseases associated with protein quality control (PQC). In its role in selective autophagy, p62 directly interacts with LC3. In our model, we therefore evidenced an impaired capacity of the cardiomyocyte to eliminate dysfunctional organelles. However, these results only reflect the steady state. To clearly prove its impairment, the use of a lysosomal inhibitor (leupeptin) was used to measure the autophagic flux. As expected, leupeptin had no effects on LC3-II levels.

Hence, autophagy flux was inhibited at late stage. However, whether the autophagy failure arises from an impairment of autophagosome-lysosome fusion or from a problem during degradation phase has yet to be elucidated. Further studies co-localizing LC3 (autophagosome) and LAMP1 (lysosome) will clarify this aspect.

The possible inhibition at the degradation stage of autophagy may involve lysosome as a contributor of the impairment. Red fluorescence by lysotracker staining was increased in cardiomyocytes from cYKO mice, indicating an accumulation of acidic organelles. In addition, cYKO mice display an upregulated expression of LAMP1, TFEB, CTSD, indicating a possible role of lysosomal dysfunction. However, lysosomal function in heart tissue from cYKO of CTSD, CTSB, CTSL remains normal. Although direct activity on isolated lysosomes was not performed, this data may suggest that autophagosome-lysosome fusion performs adequately but the problem in the late stage might reside in the degradation stage.

Thus, we have established a new role of YME1L as a contributor of autophagy inhibition. These experiments provide a new insight into the relationship between mitochondrial dynamics and autophagy.

Thus far we have demonstrated: 1) unexpected mitochondrial dynamic phenotype by the cardiac deletion of *Yme1l*, 2) a decrease in mtDNA with a higher mitochondrial capacity and ATP production, and 3) autophagy inhibition at the late stage of the flux. Considering the possible common pattern for these three features, we introduced a key player that could govern these changes: the endoplasmic reticulum (ER), or sarcoplasmic reticulum (SR) in the heart.

In the literature, ER is involved in autophagosome formation (Yamamoto and Noda, 2020), ER stress boosts respiration (Strzyz, 2019) and ER stress modulates autophagic flux (Yorimitsu et al., 2006, Gonzalez-Rodriguez et al., 2014, Wiersma et al., 2017). Moreover, many studies relate ER dysfunction with the failing heart (Wang et al., 2018).

Here, we have contributed to the understanding of ER stress in the development of DCM. First, we measured mRNA levels of the three ER arms that govern UPR stress. Our data indicate an upregulation of CHOP and a modest upregulation of ATF4 in cYKO mice hearts, both downstream effectors of the PERK branch, suggesting an increased ER stress.

CHOP induction has also been related to other UPR branches. Moreover, the role of CHOP has also been associated with apoptosis, as such its high levels promote cell death (Hu et al., 2018). Whether CHOP induces cell death prior to the onset of DCM is not clear. Unfortunately, we were only able to measure protein levels of CHOP and ATF4, which slightly increase in cYKO animals.

To our concern, the role of YME1L during ER stress has been poorly studied. Lebeau *et al.,* demonstrated that the PERK arm of the UPR response regulates mitochondrial morphology during acute ER stress. To this aim, the authors confirm that *Yme1l* depletion decreases elongated mitochondria during ER stress (Lebeau et al., 2018). Thus, our data concur with this study confirming pre-existing ER stress in cYKO mice. Moreover, to further confirm this result, we used the well-known ER stressor, tunicamycin, to prove the effect of accelerating ER stress on cardiac function. As expected, after three days of tunicamycin injection, cYKO animals dramatically decreased cardiac function. These results suggest for the first time that cardiac genetic ablation of *Yme1l* predisposes to ER stress-mediated cardiac dysfunction.

Both ER/SR and mitochondria membranes are closely apposed forming contact sites through tethering complexes (Gao et al., 2020). In fact, up to 20% of mitochondria are opposed to ER. Dysregulation of this ER-mitochondria contact site is one of the main triggers of ER stress (Wang et al., 2021a). We therefore wanted to explore how the contact sites between ER and mitochondria were affected by the deletion of *Yme1l.*

We isolated adult cardiomyocytes and analyzed MAMs coverage by TEM, ER length and ER to mitochondria distance. We noticed a decrease in the percentage of ER covering mitochondria (MAM's coverage) in cYKO mice accompanied by a non-significant decrease in length. The distance between ER and OMM is highly variable, ranging from 10 to 100nm. In fact, dysfunctional mitochondria-ER connections are responsible for many diseases. Decreased distance has been shown in response to ER stress (Bravo et al., 2011) or starvation (Sood et al., 2014), while an increased distance is shown with high glucose levels (Theurey and Rieusset, 2017).

In our model, we observed a reduced ER to mitochondria distance. Whether this shortening is affecting the communication between the two organelles and therefore affecting ER stress still needs to be elucidated.

As previously described, Ca^{2+} uptake is clearly dependent on ER-mitochondria distance. There are eight protein complexes described tethering the physical distance between ER and mitochondria. Here, we have only considered IP3R1 (or RyRs in the heart)-GRP75-VDAC1-MCU, which participates in the Ca^{2+} transfer from ER to mitochondria. In isolated cardiac mitochondria from cYKO mice, our results indicate an increase in mitochondrial Ca^{2+} uptake. These results are further supported by the increased levels of MCU, the calcium uniporter in the IMM involved in Ca^{2+} transfer from the IMM to the mitochondrial matrix. Significantly, Ca^{2+} uptake not only affects the modulation of cytosolic ions transient but also activates enzymes of the Krebs cycle to modulate ATP production (Dorn and Maack, 2013, Holmstrom et al., 2015, Yu et al., 2018), which also agrees with our results showing higher respiratory capacity and higher ATP production. Whether this increase in MCU levels is a maladaptive response of the cardiomyocyte leading to mitochondrial Ca^{2+} overload and cell death remains elusive. The role of MCU in the pathogenesis of heart failure is widely discussed. In mice with pressure overload-lead to HF, MCU levels were increased (Yu et al., 2018, Zaglia et al., 2017). However, in diabetic cardiomyopathy, MCU levels were decreased (Suarez et al., 2018). In the heart, during acute injuries, MCU may mediate acute mitochondrial Ca^{2+} overload (Kwong et al., 2015). To further characterize the implication of ER stress in Ca^{2+} dysregulation in cardiomyocytes, we are conducting experiments studying the role of Serca2a, the ATPase pump involved in transfering back the calcium ions from cytosol to mitochondria, as a player in this scenario (Liu et al., 2011, Mekahli et al., 2011).

Interestingly, isolated heart mitochondria from cYKO mice display low levels of ROS production. This result does not agree with published literature, in which mitochondrial Ca^{2+} overload is induced by mitochondrial ROS, both involved in a vicious cycle resulting in cardiac dysfunction (Bertero and Maack, 2018a). This correlation was beyond the scope of the study, but future data will clarify this connection.

Nonetheless, our data suggest that cardiac-specific genetic ablation of *Yme1l* induce autophagy dysregulation with altered ER behavior, accompanied by an acceleration of Ca^{2+} influx from ER to mitochondria, predictably increasing metabolic respiratory capacities and ATP production in the cell.

Nutritional approaches for YME1L-HF prevention

Considering our group's previous study (Wai et al., 2015), we decided to conduct a more extensive analysis of diets with different compositions in macronutrients (fat, carbohydrates, and proteins). As published, high-fat diet preserves cardiac function at 30 weeks in cYKO mice (Wai et al., 2015). Unexpectedly for us, a fat-restricted diet was the best dietary approach regarding cardioprotection at later HF-stages and lifespan extension. Although interesting, for the purpose of this thesis the possible difference in cardioprotection among the diets will not be extensively discussed. Nonetheless, although our main interest is the heart, we hypothesize different possibilities to explain these results: lipotoxicity driven by high fat amounts could result in early death despite improved cardiac function; other organs might have an influence; a metabolic problem for fatty acid metabolism; macronutrient ratio as players in the (non) protection and/or late deleterious effect. In any event, the possibility that DCM patients could respond to a metabolic approach despite an underlying genetic defect is thus intriguing.

To date, this is the first preclinical study using a nearly complete fat restricted diet (<0.2%) in the prevention of cardiovascular disease. In our working model, results indicate that implementation of a non-fat diet to cYKO mice not only prevents onset of the disease but also expands lifespan by 30%. Since these mice display a lower body weight than those subjected to a chow diet, we firstly hypothesized that the animals were under a calorie restriction (Redman and Ravussin, 2011). Previous studies in the field have demonstrated that caloric restriction promotes healthy aging (Anton and Leeuwenburgh, 2013). In the context of heart disease, its use is linked to reduced oxidative stress, reduced inflammation and better prognosis of some cardiac dysfunctions (Weiss and Fontana, 2011). To discard this possibility, food intake values demonstrate no differences in food consumption between animals. Thus, we demonstrate that the beneficial cardiovascular effect is strictly associated with fat elimination in the diet rather than to a reduced caloric intake.

These experiments provide a new insight into the relationship between development of the disease and the use of nutritional approaches focusing on macronutrients rather than on calories.

In our previous study, we did show an increase in glucose (FDG) uptake by PET/CT in 40-week-old cYKO mice, a late-stage of HF considering their median survival of 44 weeks (Wai et al., 2015). This result agrees with the literature, in which a shift toward glycolysis is also present (Tran and Wang, 2019, Lopaschuk et al., 2021).

However, as mentioned in the introduction, whether there is a reduction in fatty acid uptake due to the preferential use of glucose remains controversial. For this purpose, we used a fluor based palmitic-acid tracer (^{18}F-FTHA) to follow fatty acid used by the heart by PET/CT with the collaboration of the CNIC advanced imaging unit.

In our work setting, we established 35 weeks old as the age for measuring PET/CT ^{18}F-FDG and ^{18}F-FTHA uptake. We did see a modest increase in FDG uptake in cYKO mice under a chow fat diet, reestablished to almost basal levels after a non-fat diet. The first result could have two explanations: 1) this metabolic switch to glycolytic pathways is mainly due to the onset of disease or 2) underlies *Yme1l* deletion. Recent evidence points to YME1L together with mTOR and LIPIN1 (a lipid signaling phosphatase) as regulators in the interface between metabolism and mitochondrial dynamics during a specific type of cancer (MacVicar et al., 2019). Currently, we are conducting a longitudinal study of cYKO from young ages to later stages with both tracers to confirm the second explanation: that *Yme1l* deletion already alters metabolism.

The evaluation of myocardial fatty acid (FA) metabolism with PET using ^{18}F-FTHA radiotracer has been performed in pathologies such as coronary artery disease and DCM (Schulz et al., 1996, Taylor et al., 2001). Although in most of the studies there is a shift from fatty acids to glucose during HF, in this last study, patients suffering from HF display an increase myocardial fatty acid uptake and a decreased glucose uptake. Nonetheless, in our model, fatty acid was unaltered in the onset of disease. Whether FA uptake could change during later stages of the disease may be a possibility. Moreover, FA uptake levels were dramatically decreased after a fat-restricted diet. Hence, in our model, at the onset of disease there is a metabolic switch towards glucose uptake with no influence in fatty acid uptake. The use of a non-fat diet partially rescues the glycolytic shift and enormously influences FA uptake.

The heart exhibits a high abundance of lipids in the cardiomyocyte and mitochondrial membranes (Pradas et al., 2018), playing an important role in cardiac energy production, plasma membrane composition and pathogenesis of CVD (Sparagna et al., 2007, Sysi-Aho et al., 2011, Le et al., 2014). The use of different fat-based diets has been demonstrated to alter the heart lipidome (McCombie et al., 2012, Pakiet et al., 2020). YME1L processes OPA1, which is in the inner mitochondrial membrane. Whether the imbalanced OPA1 processing alters lipid membrane composition, and a non-fat diet is able to bypass this defect and promotes cardioprotection could be a possibility. A study performed in humans demonstrated that while a low-fat diet stimulates *de novo* lipogenesis (DNL), high-fat contribution to DNL was depreciable (Hudgins et al., 1996), giving importance to the endogenous synthesis of lipids rather than direct dietary intake.

After evaluating cardiac function and providing some understanding of metabolism, we wanted to explore the impact of a fat-restricted diet in mitochondrial remodeling.

Results from TEM indicate a decrease in mitochondrial size and an increased number of mitochondria when cardiac *Yme1l* is ablated in 35-week-old mice under a chow diet. These results are in line with those we published in 2015 (Wai et al., 2015). Interestingly, after a non-fat diet, mitochondrial size was highly augmented, and the number of mitochondria was reduced when compared to animals under a chow diet, a phenotype similar to a pre-symptomatic stage of cYKO mice previously described. Damaged mitochondria may be selectively degraded by mitophagy. PARKIN, the most studied gene known to eliminate dysfunctional mitochondria was only slightly elevated. However, we cannot discard alternative mitophagy pathways involved in this process. Considering the important role of *Parkin* in other HF models, we are currently studying how a double ablation of *Parkin* and *Yme1l* could influence development of the disease.

We then speculated that the reduction in mitochondrial number when compared to animals under a chow diet could be due to a reduction in mitochondrial fission when a fat restricted diet is used. However, OPA1 isoforms remains altered promoting a state of fission. The augmented mitochondria size is the other feature that we observed under TEM. We speculate different mechanisms: 1) considering that there were no changes in OPA1 isoforms, we studied MFN2, since it is involved in mitochondrial fusion of the outer membrane.

We did observe a higher expression of MFN2 with a non-fat diet. This result could explain the increase in size. 2) Another hypothesis is that since under the use of this diet mitochondria morphology remains similar to pre-symptomatic cYKO mice, mitochondria under this scenario never go under the fission process and they become even more “inflated” as a compensatory mechanism. Evidence suggests the association of “giant mitochondria” to nutritional deficiencies, among others. These “giant mitochondria” are formed due to cellular lipid accumulation and increased β-oxidation during the formation and breakdown of triglycerides (Shami et al., 2021). Other studies relate exercise to incremented mitochondrial volume, to cope with the respiratory capacity, being more efficient for ATP production (Sorriento et al., 2021).

With regards to respiratory capacity, our results suggest a non-significant modest decrease in OxPHOS capacity in cYKO mice under chow diet. Interestingly, this deficiency in mitochondrial performance was not observed in pre-symptomatic animals. Surprisingly, animals fed with a non-fat diet dramatically reduce respiratory capacity.

These results are significant in one important respect. Many authors have directly linked deficient mitochondrial respiration to heart failure (Lemieux et al., 2011, Sabbah, 2020). However, here we observe greater respiration in animals with worse cardiac function and the opposite for animals with a reestablished heart function. Thus, we venture that there should be another mechanism supporting cardiovascular wellness in these animals.

Taken together, these lines of evidence demonstrate that despite mitochondria represent 25-30% of the myocardium, their respiration is not always a hallmark of cardiac performance, as demonstrated with the normal cardiac performance under a non-fat diet.

Continuing with possible mechanism of cardioprotection, we wanted to explore the possible effect of a non-fat diet in ER modulation. We isolated cardiomyocytes from 20-week-old mice and explored the three previously commented features of ER: ER stress, Ca^{2+} handling and MAMs.

On the one hand, our current study found higher ER-mitochondria distance in cYKO mice non-dependent on the diet with a decreased MFN2 expression, slightly rescued by a non-fat diet. These two results suggest a dysregulated ER-mitochondria tethering, favoring its separation, as seen in the literature (de Brito and Scorrano, 2008, Dorn and Scorrano, 2010).

On the other hand, we demonstrated higher mitochondrial Ca^{2+} levels, rescued by a non-fat diet in accordance with higher MCU expression, reestablished by a non-fat diet, favoring a closer ER-mitochondria contact.

There are several explanations for these apparently opposed results:

First. To date, an average distance of 15nm for Ca^{2+} transfer between ER and mitochondria is established (Csordas et al., 2006, Csordas et al., 2010). It is not clear how a distance wider than that would impact Ca^{2+} transfer. However, distances wider than 25nm would not withstand the IP3-GRP75-VDAC complex, compromising Ca^{2+} transfer (Filadi and Pozzan, 2015). Although statically different, if we consider ER-mitochondria distance non-pathological and the level of MFN2 as a product of mitochondrial fragmentation due to *Yme1l* ablation, then the increase of Ca^{2+} uptake by mitochondria and the MCU expression will be due to a closer proximity of ER to mitochondria. This closer proximity will be reestablished by a non-fat diet treatment, together with an increase of MFN2 levels and the restoration of Ca^{2+} handling.

Second. Along the same line, if we consider both TEM results and MFN2 levels a real reflection of the two-organelle connection, this will imply that mitochondria are pathologically separated from the ER. This loss of interaction has been shown to promote aging and cardiac disease. In some studies, mutations in *Mfn2* result in disruption of the structure and function of MAMs, by decreasing tethering by 30%. Then, as previously mentioned, either mitochondria will need to be exposed to a very high concentration of cytosolic Ca^{2+} levels or to increase MCU to uptake the cytosolic Ca^{2+} as a compensatory mechanism of its detachment from the ER. If we consider this second scenario, treatment with a fat restricted diet will partially preserve the ER-mitochondria contact and ameliorate Ca^{2+} handling and MCU levels in mitochondria. These data do not match those observed in earlier studies, in which an increase in mitochondrial Ca^{2+} was due to a closer proximity of mitochondria to ER. Remarkably, ER stress ATF4 and IRE1a were upregulated in non-fat diet cYKO mice. However, the protein levels of ATF4 were dramatically decreased under both diets, suggesting a transcriptional regulation of UPR response. Further experiments should be done to confirm this.

Therefore, although YME1L has been previously linked to ER stress, this is the first study associating cardiac *Yme1l* ablation to a dysregulation of MAMs and an alteration of Ca^{2+} handling during the development of heart failure.

Moreover, the use of a fat restricted diet as a potential target for modulating MAMs defects and Ca^{2+} dysregulation is a promising tool to modulate this cardiovascular pathology.

In our model, treatment with NFD increases levels of LC3-II even above the levels of the actual impaired cYKO mice under a chow diet. Interestingly, the use of leupeptin does not further increase LC3-II levels in NFD animals. Thus, NFD was stimulating the first part of the autophagy by promoting the autophagosome formation. Accordingly, the use of a non-fat diet as a modulator of autophagy may not be responsible for its cardioprotective effect. However, a fat restricted diet could represent a very potent therapeutic option in models in which general autophagy is diminished, such as cardiac aging or acute myocardial infarction (AMI) (Wu et al., 2014, Abdellatif et al., 2018). During AMI, autophagy was found to be induced in the acute phase and impaired in the latter phase of AMI.

Treatment with 3MA, a potent pharmacological inhibitor of autophagy, exacerbated cardiac dysfunction. Treatment with rapamycin, an autophagy enhancer, attenuates cardiac remodeling (Wu et al., 2014). In another study, crossing a desmin-related cardiomyopathy mouse model (DRC) in which autophagy is impaired with a transgenic Atg7 mouse restores autophagy flux, ameliorates ventricular dysfunction, decreases cardiac hypertrophy, and prolongs survival (Bhuiyan et al., 2013). To complete our understanding of the autophagy blockage in these animals and the potential use of different nutritional approaches in autophagy deficient cardiomyopathies, we are currently generating animals in which ATG7 – a protein in charge of promoting expansion of the autophagosome– and *Yme1l* are both deleted in the heart. Further analysis with the non-fat diet and other therapies under these double knock-out mice will provide a clue regarding the exact mechanism of autophagy and its possible modulation.

In recent years, many studies indicated modulation of autophagy as a therapy for expanding lifespan and promoting healthy aging. In our working model, we have an impaired autophagic flux in pre-symptomatic mice due to the cardiac genetic ablation of *Yme1l*. Whether this condition aggravates the disease or is the cause remains unclear. In the literature, several approaches have been used to restore autophagic impairment (Abdellatif et al., 2018). Caloric restriction is known as the most potent physiological stimulus of autophagy that ameliorates cardiac dysfunction.

Ketogenic diets seem to improve cardiac phenotype, and although the mechanism remains unclear, the use of ketone bodies proves the most reasonable hypothesis for this improvement (Nasser et al., 2020). In humans, 3 months of a fasting-mimicking diet is sufficient to lower age-related cardiovascular risk factors, such as inflammation, body mass index, fasting glucose (Wei et al., 2017).

Many studies have related the use of HFD with an impaired cardiac autophagy in animals with diet-induced insulin resistance, metabolic syndrome, and type II diabetes (Sciarretta et al., 2015, Yamamoto et al., 2017, Rabinovich-Nikitin et al., 2019). These three conditions have been demonstrated to be associated with cardiovascular abnormalities. Significantly, HFD has also been shown to inhibit autophagy by affecting fusion of autophagosomes with lysosomes, increasing LC3-II and p62 levels. However, there is little evidence regarding the precise macronutrient or diet component (if any) responsible for these changes.

In the previous study by our group, we also observed that supplementation of a HFD prior to the onset the disease was able to maintain normal cardiac function at the studied timepoint (Wai et al., 2015). Nonetheless, the molecular mechanism of this prevention was not completely understood. At the same time, life expectancy of those mice treated with HFD was similar to the control diet, thus dying at a similar time despite cardiac function improvement.

As mentioned, here we propose the non-fat diet as the best nutritional approach to target not only cardiac function but also expand lifespan.

It is not the first time that nutritional approaches have been used to modulate mitochondrial dysfunction. To date, only the use of low-fat diets or a caloric restricted diet in which the whole number of calories from all the macronutrients was reduced has been studied. This is therefore the first time that the use of a fat-restricted diet has been evaluated to treat HF.

Preclinical and clinical studies have shown the benefit of using intermittent fasting (IF) as a prevention for cardiovascular disease (Ahmet et al., 2005, de Cabo and Mattson, 2019, Dong et al., 2020). In this thesis, our first target was autophagy. Thus, we decided to explore the effect of IF, a potent autophagy inducer, in the development of DCM. Here, we used two different IF approaches, one of them, the 2:5 approach, is used in human trials and in many mice studies.

Comparing the two IF therapies, a 2:5 approach prevents the onset of the disease better and extends lifespan in a significant manner, compared to a more aggressive IF 2:1:2:2 approach. However, none of them was comparable to a fat restricted diet. From the literature, we did expect that IF *per se* would have a higher impact on cardiac function. However, if one of the main targets of IF is promoting autophagy and, in our model, autophagy is impaired, it would be plausible to think that it will have either a non-effect or a very mild one. In fact, these results further support our data. Our study indicates that autophagy is blocked in the second step of the autophagic flux; the degradation step.

Therefore, any therapy aimed at increasing the first part of the autophagy pathway when the degradation step is compromised will have none or a very small impact, as occurred here. However, molecular analysis of the autophagic flux should be performed to clarify this hypothesis.

To our surprise, combining a fat restricted diet and IF was able to increase the survival of animals more than IF itself. In fact, pretreatment of cYKO mice with a non-fat diet prior to the start of IF, incredibly preserves cardiac function and overall lifespan. Although data are still being generated and further analysis will be necessary beyond this Thesis, we speculate that combining therapies will be the ideal target for possible human prevention of heart disease.

These results suggest that a better cardiac response is achieved by changing macronutrient fat content of the diet rather than reducing caloric intake. However, many studies pinpoint not a dietary restriction but a macronutrient ratio as responsible for better overall wellness.

Overall, the contribution of this preclinical project will help to better understand the molecular basis and foundations of DCM that could contribute for clinical application in the human disease in the near future, where a nutritional approach might help to alleviate patients with such a devastating cardiac disease.

Study limitations

In a clinical scenario, patients will already present DCM, and it is relevant to demonstrate that the proposed nutritional intervention can not only prevent but also treat the disease once established. Here, we have only demonstrated the beneficial effect of fasting and/or fat restriction to prevent the onset of the disease. For this reason, an additional study will be needed within this aim to test the effect of fasting and/or a non-fat diet once the DCM has already manifested.

To date, there is no available data in humans relating cardiovascular dysfunction with *YME1L* deficiency. However, this has proved to be a good model for understanding cardiovascular and mitochondrial dysfunction related diseases. Therefore, those diseases sharing common features with the ones we observed in this model could also benefit from similar therapeutic approaches in the last instance.

The use of a diet with 0.2% fat content proves difficult to maintain in a balanced human diet. For this purpose, specific molecules able to mimic the beneficial fasting effects are now being developing by several groups. Moreover, we have demonstrated that specific elimination of fat from diet rather than a reduction in caloric intake was able to delay cardiac dysfunction and to extend lifespan up to 25-30%.

As mentioned, our previous study demonstrates the beneficial short-term use of a high fat diet in this cardiovascular setting. We cannot rule out that a specific fatty acid could be responsible for the cardioprotection through another molecular mechanism.

Conclusions

1. Neither mitochondrial fragmentation nor respiratory reduction are present in a subclinical stage of dilated cardiomyopathy in cYKO mice, but they concur with cardiac dysfunction.

2. Cardiac genetic ablation of *Yme1l* is associated with an impairment of the autophagic flux. This inhibition of autophagy underlies disease and impedes correct functioning of the autophagic flux.

3. Impairment of the autophagic flux is associated with an increase in endoplasmic reticulum stress during the development of dilated cardiomyopathy.

4. Endoplasmic reticulum stress promotes a dysregulation of mitochondrial Ca^{2+} handling between the two organelles.

5. A fat restricted diet delays onset of the disease by preserving cardiac function and expanding lifespan.

6. A fat restricted diet preserves the mitochondrial ultrastructure by conserving mitochondrial number and size. However, these changes do not correlate with enhanced mitochondrial respiration performance.

7. A fat restricted diet does not rescue either autophagic flux impairment or ER stress mediated by *Yme1l* cardiac ablation.

8. A fat restricted diet restores mitochondrial Ca^{2+} uptake, suggesting Ca^{2+} handling as a possible target of the cardioprotective effect.

9. The combination of nutritional approaches such as fasting, and a fat restricted diet ameliorates heart failure, inducing a more preserved cardiac function and an overall increase in lifespan.

Conclusiones

1. Ni la fragmentación mitocondrial ni la reducción respiratoria están presentes en una etapa subclínica de miocardiopatía dilatada en ratones cYKO, pero coinciden con la disfunción cardíaca.

2. La ablación genética de *Yme1l* en el corazón está asociada con un bloqueo del flujo autofágico. Esta inhibición en la autofagia subyace a la enfermedad e impide el correcto funcionamiento del flujo autofágico.

3. El bloqueo en el flujo autofágico está asociado con un incremento del estrés del retículo endoplásmico durante el desarrollo de la cardiomiopatía dilatada.

4. El estrés del retículo endoplásmico provoca una desregulación del manejo del Ca^{2+} mitocondrial.

5. Una dieta sin ácidos grasos retrasa la aparición de la enfermedad, preservando la función cardiaca y alargando la supervivencia.

6. Una dieta sin ácidos grasos preserva la estructura mitocondrial, conservando el número y el tamaño de las mismas. Sin embargo, estos cambios no están asociados a una mejora en la respiración de la mitocondria.

7. Una dieta sin ácidos grasos no consigue mejorar ni el bloqueo autofágico ni el estrés del retículo endoplásmico mediado por la ablación cardiaca del gen *Yme1l*.

8. Una dieta sin ácidos grasos restablece la captación normal de Ca^{2+} mitocondrial, sugiriendo el manejo del Ca^{2+} como posible diana de efecto cardioprotector.

9. La combinación de terapias nutricionales como el ayuno intermitente y una dieta sin ácidos grasos mejora la insuficiencia cardiaca, induciendo una función cardiaca más preservada y un aumento en la supervivencia.

References

ABDELLATIF, M., SEDEJ, S., CARMONA-GUTIERREZ, D., MADEO, F. & KROEMER, G. 2018. Autophagy in Cardiovascular Aging. *Circ Res,* 123**,** 803-824.

ABDULLAH, C. S., ALAM, S., AISHWARYA, R., MIRIYALA, S., BHUIYAN, M. A. N., PANCHATCHARAM, M., PATTILLO, C. B., ORR, A. W., SADOSHIMA, J., HILL, J. A. & BHUIYAN, M. S. 2019. Doxorubicin-induced cardiomyopathy associated with inhibition of autophagic degradation process and defects in mitochondrial respiration. *Sci Rep,* 9**,** 2002.

ACIN-PEREZ, R., LECHUGA-VIECO, A. V., DEL MAR MUNOZ, M., NIETO-ARELLANO, R., TORROJA, C., SANCHEZ-CABO, F., JIMENEZ, C., GONZALEZ-GUERRA, A., CARRASCOSO, I., BENINCA, C., QUIROS, P. M., LOPEZ-OTIN, C., CASTELLANO, J. M., RUIZ-CABELLO, J., JIMENEZ-BORREGUERO, L. J. & ENRIQUEZ, J. A. 2018. Ablation of the stress protease OMA1 protects against heart failure in mice. *Sci Transl Med,* 10.

ADLER, H. T., CHINERY, R., WU, D. Y., KUSSICK, S. J., PAYNE, J. M., FORNACE, A. J., JR. & TKACHUK, D. C. 1999. Leukemic HRX fusion proteins inhibit GADD34-induced apoptosis and associate with the GADD34 and hSNF5/INI1 proteins. *Mol Cell Biol,* 19**,** 7050-60.

AHMET, I., TAE, H. J., DE CABO, R., LAKATTA, E. G. & TALAN, M. I. 2011. Effects of calorie restriction on cardioprotection and cardiovascular health. *J Mol Cell Cardiol,* 51**,** 263-71.

AHMET, I., WAN, R., MATTSON, M. P., LAKATTA, E. G. & TALAN, M. 2005. Cardioprotection by intermittent fasting in rats. *Circulation,* 112**,** 3115-21.

ALEKSANDROVA, K., KOELMAN, L. & RODRIGUES, C. E. 2021. Dietary patterns and biomarkers of oxidative stress and inflammation: A systematic review of observational and intervention studies. *Redox Biol,* 42**,** 101869.

ANAND, R., WAI, T., BAKER, M. J., KLADT, N., SCHAUSS, A. C., RUGARLI, E. & LANGER, T. 2014. The i-AAA protease YME1L and OMA1 cleave OPA1 to balance mitochondrial fusion and fission. *J Cell Biol,* 204**,** 919-29.

ANDERSEN, D. C., JENSEN, C. H., BAUN, C., HVIDSTEN, S., ZEBROWSKI, D. C., ENGEL, F. B. & SHEIKH, S. P. 2016. Persistent scarring and dilated cardiomyopathy suggest incomplete regeneration of the apex resected neonatal mouse myocardium--A 180 days follow up study. *J Mol Cell Cardiol,* 90**,** 47-52.

ANTON, S. & LEEUWENBURGH, C. 2013. Fasting or caloric restriction for healthy aging. *Exp Gerontol,* 48**,** 1003-5.

BAGHERNIYA, M., BUTLER, A. E., BARRETO, G. E. & SAHEBKAR, A. 2018. The effect of fasting or calorie restriction on autophagy induction: A review of the literature. *Ageing Res Rev,* 47**,** 183-197.

BAKER, M. J., LAMPE, P. A., STOJANOVSKI, D., KORWITZ, A., ANAND, R., TATSUTA, T. & LANGER, T. 2014. Stress-induced OMA1 activation and autocatalytic turnover regulate OPA1-dependent mitochondrial dynamics. *EMBO J,* 33**,** 578-93.

BALABAN, R. S. 2009. The role of Ca(2+) signaling in the coordination of mitochondrial ATP production with cardiac work. *Biochim Biophys Acta,* 1787**,** 1334-41.

BAZZANO, L. A., HU, T., REYNOLDS, K., YAO, L., BUNOL, C., LIU, Y., CHEN, C. S., KLAG, M. J., WHELTON, P. K. & HE, J. 2014. Effects of low-carbohydrate and low-fat diets: a randomized trial. *Ann Intern Med,* 161**,** 309-18.

BERNHARD, D. & LAUFER, G. 2008. The aging cardiomyocyte: a mini-review. *Gerontology,* 54**,** 24-31.

BERS, D. M., EISNER, D. A. & VALDIVIA, H. H. 2003. Sarcoplasmic reticulum Ca2+ and heart failure: roles of diastolic leak and Ca2+ transport. *Circ Res,* 93**,** 487-90.

BERTERO, E. & MAACK, C. 2018a. Calcium Signaling and Reactive Oxygen Species in Mitochondria. *Circ Res,* 122**,** 1460-1478.

BERTERO, E. & MAACK, C. 2018b. Metabolic remodelling in heart failure. *Nat Rev Cardiol,* 15**,** 457-470.

BHUIYAN, M. S., PATTISON, J. S., OSINSKA, H., JAMES, J., GULICK, J., MCLENDON, P. M., HILL, J. A., SADOSHIMA, J. & ROBBINS, J. 2013. Enhanced autophagy ameliorates cardiac proteinopathy. *J Clin Invest,* 123**,** 5284-97.

BIRKS, E. J., LATIF, N., ENESA, K., FOLKVANG, T., LUONG LE, A., SARATHCHANDRA, P., KHAN, M., OVAA, H., TERRACCIANO, C. M., BARTON, P. J., YACOUB, M. H. & EVANS, P. C. 2008. Elevated p53 expression is associated with dysregulation of the ubiquitin-proteasome system in dilated cardiomyopathy. *Cardiovasc Res,* 79**,** 472-80.

BOLLEN, I. A., VAN DEEL, E. D., KUSTER, D. W. & VAN DER VELDEN, J. 2014. Peripartum cardiomyopathy and dilated cardiomyopathy: different at heart. *Front Physiol,* 5**,** 531.

BRAVO, R., VICENCIO, J. M., PARRA, V., TRONCOSO, R., MUNOZ, J. P., BUI, M., QUIROGA, C., RODRIGUEZ, A. E., VERDEJO, H. E., FERREIRA, J., IGLEWSKI, M., CHIONG, M., SIMMEN, T., ZORZANO, A., HILL, J. A., ROTHERMEL, B. A., SZABADKAI, G. & LAVANDERO, S. 2011. Increased ER-mitochondrial coupling promotes mitochondrial respiration and bioenergetics during early phases of ER stress. *J Cell Sci,* 124**,** 2143-52.

BROWN, D. A., PERRY, J. B., ALLEN, M. E., SABBAH, H. N., STAUFFER, B. L., SHAIKH, S. R., CLELAND, J. G., COLUCCI, W. S., BUTLER, J., VOORS, A. A., ANKER, S. D., PITT, B., PIESKE, B., FILIPPATOS, G., GREENE, S. J. & GHEORGHIADE, M. 2017. Expert consensus document: Mitochondrial function as a therapeutic target in heart failure. *Nat Rev Cardiol,* 14**,** 238-250.

CAO, D. J., JIANG, N., BLAGG, A., JOHNSTONE, J. L., GONDALIA, R., OH, M., LUO, X., YANG, K. C., SHELTON, J. M., ROTHERMEL, B. A., GILLETTE, T. G., DORN, G. W. & HILL, J. A. 2013. Mechanical unloading activates FoxO3 to trigger Bnip3-dependent cardiomyocyte atrophy. *J Am Heart Assoc,* 2**,** e000016.

CARDOSO, L. D., C; GNAIGER, E 2021. Magnesium Green for fluorometric measurement of ATP production does not interfere with mitochondrial respiration. *Bioenergetic Communications*.

CESNEKOVA, J., RODINOVA, M., HANSIKOVA, H., ZEMAN, J. & STIBUREK, L. 2018. Loss of Mitochondrial AAA Proteases AFG3L2 and YME1L Impairs Mitochondrial Structure and Respiratory Chain Biogenesis. *Int J Mol Sci,* 19.

CHEN, Y., CSORDAS, G., JOWDY, C., SCHNEIDER, T. G., CSORDAS, N., WANG, W., LIU, Y., KOHLHAAS, M., MEISER, M., BERGEM, S., NERBONNE, J. M., DORN, G. W., 2ND & MAACK, C. 2012. Mitofusin 2-containing mitochondrial-reticular microdomains direct rapid cardiomyocyte bioenergetic responses via interorganelle Ca(2+) crosstalk. *Circ Res,* 111**,** 863-75.

CHEN, Y., LIU, Y. & DORN, G. W., 2ND 2011. Mitochondrial fusion is essential for organelle function and cardiac homeostasis. *Circ Res,* 109**,** 1327-31.

CHEN, Y., ZHANG, P., LIN, X., ZHANG, H., MIAO, J., ZHOU, Y. & CHEN, G. 2020. Mitophagy impairment is involved in sevoflurane-induced cognitive dysfunction in aged rats. *Aging (Albany NY),* 12**,** 17235-17256.

COHEN, C. C., LI, K. W., ALAZRAKI, A. L., BEYSEN, C., CARRIER, C. A., CLEETON, R. L., DANDAN, M., FIGUEROA, J., KNIGHT-SCOTT, J., KNOTT, C. J., NEWTON, K. P., NYANGAU, E. M., SIRLIN, C. B., UGALDE-NICALO, P. A., WELSH, J. A., HELLERSTEIN, M. K., SCHWIMMER, J. B. & VOS, M. B. 2021. Dietary sugar restriction reduces hepatic de novo lipogenesis in adolescent boys with fatty liver disease. *J Clin Invest,* 131.

COLOMBI, M., MOLLE, K. D., BENJAMIN, D., RATTENBACHER-KISER, K., SCHAEFER, C., BETZ, C., THIEMEYER, A., REGENASS, U., HALL, M. N. & MORONI, C. 2011. Genome-wide shRNA screen reveals increased mitochondrial dependence upon mTORC2 addiction. *Oncogene,* 30**,** 1551-65.

CSORDAS, G., RENKEN, C., VARNAI, P., WALTER, L., WEAVER, D., BUTTLE, K. F., BALLA, T., MANNELLA, C. A. & HAJNOCZKY, G. 2006. Structural and functional features and significance of the physical linkage between ER and mitochondria. *J Cell Biol,* 174**,** 915-21.

CSORDAS, G., VARNAI, P., GOLENAR, T., ROY, S., PURKINS, G., SCHNEIDER, T. G., BALLA, T. & HAJNOCZKY, G. 2010. Imaging interorganelle contacts and local calcium dynamics at the ER-mitochondrial interface. *Mol Cell,* 39**,** 121-32.

CUI, L., ZHAO, L. P., YE, J. Y., YANG, L., HUANG, Y., JIANG, X. P., ZHANG, Q., JIA, J. Z., ZHANG, D. X. & HUANG, Y. 2020. The Lysosomal Membrane Protein Lamp2 Alleviates Lysosomal Cell Death by Promoting Autophagic Flux in Ischemic Cardiomyocytes. *Front Cell Dev Biol,* 8**,** 31.

DAI, W. & JIANG, L. 2019. Dysregulated Mitochondrial Dynamics and Metabolism in Obesity, Diabetes, and Cancer. *Front Endocrinol (Lausanne),* 10**,** 570.

DAI, W., WANG, G., CHWA, J., OH, M. E., ABEYWARDANA, T., YANG, Y., WANG, Q. A. & JIANG, L. 2020. Mitochondrial division inhibitor (mdivi-1) decreases oxidative metabolism in cancer. *Br J Cancer,* 122**,** 1288-1297.

DAS, R. & CHAKRABARTI, O. 2020. Mitochondrial hyperfusion: a friend or a foe. *Biochem Soc Trans,* 48**,** 631-644.

DAVILA-ROMAN, V. G., VEDALA, G., HERRERO, P., DE LAS FUENTES, L., ROGERS, J. G., KELLY, D. P. & GROPLER, R. J. 2002. Altered myocardial fatty acid and glucose metabolism in idiopathic dilated cardiomyopathy. *J Am Coll Cardiol,* 40**,** 271-7.

DAY, S. M. 2013. The ubiquitin proteasome system in human cardiomyopathies and heart failure. *Am J Physiol Heart Circ Physiol,* 304**,** H1283-93.

DE BRITO, O. M. & SCORRANO, L. 2008. Mitofusin 2 tethers endoplasmic reticulum to mitochondria. *Nature,* 456**,** 605-10.

DE CABO, R. & MATTSON, M. P. 2019. Effects of Intermittent Fasting on Health, Aging, and Disease. *N Engl J Med,* 381**,** 2541-2551.

DE LUCIA, C., GAMBINO, G., PETRAGLIA, L., ELIA, A., KOMICI, K., FEMMINELLA, G. D., D'AMICO, M. L., FORMISANO, R., BORGHETTI, G., LICCARDO, D., NOLANO, M., HOUSER, S. R., LEOSCO, D., FERRARA, N., KOCH, W. J. & RENGO, G. 2018. Long-Term Caloric Restriction Improves Cardiac Function, Remodeling, Adrenergic Responsiveness, and Sympathetic Innervation in a Model of Postischemic Heart Failure. *Circ Heart Fail,* 11**,** e004153.

DEGRADO, T. R. 1991. Synthesis of 14 (R,S)-[18F]fluoro-6-thia-heptadecanoic acid (FTHA). *Journal of labelled compounds and radiopharmaceuticals,* XXIX.

DEL DOTTO, V., FOGAZZA, M., CARELLI, V., RUGOLO, M. & ZANNA, C. 2018. Eight human OPA1 isoforms, long and short: What are they for? *Biochim Biophys Acta Bioenerg,* 1859**,** 263-269.

DEL DOTTO, V., MISHRA, P., VIDONI, S., FOGAZZA, M., MARESCA, A., CAPORALI, L., MCCAFFERY, J. M., CAPPELLETTI, M., BARUFFINI, E., LENAERS, G., CHAN, D., RUGOLO, M., CARELLI, V. & ZANNA, C. 2017. OPA1 Isoforms in the Hierarchical Organization of Mitochondrial Functions. *Cell Rep,* 19**,** 2557-2571.

DELMAR, M. & MCKENNA, W. J. 2010. The cardiac desmosome and arrhythmogenic cardiomyopathies: from gene to disease. *Circ Res,* 107**,** 700-14.

DEPRE, C., WANG, Q., YAN, L., HEDHLI, N., PETER, P., CHEN, L., HONG, C., HITTINGER, L., GHALEH, B., SADOSHIMA, J., VATNER, D. E., VATNER, S. F. & MADURA, K. 2006. Activation of the cardiac proteasome during pressure overload promotes ventricular hypertrophy. *Circulation,* 114**,** 1821-8.

DI MALTA, C., CINQUE, L. & SETTEMBRE, C. 2019. Transcriptional Regulation of Autophagy: Mechanisms and Diseases. *Front Cell Dev Biol,* 7**,** 114.

DISTELHORST, C. W. & MCCORMICK, T. S. 1996. Bcl-2 acts subsequent to and independent of Ca2+ fluxes to inhibit apoptosis in thapsigargin- and glucocorticoid-treated mouse lymphoma cells. *Cell Calcium,* 19**,** 473-83.

DOLINSKY, V. W. & DYCK, J. R. 2011. Calorie restriction and resveratrol in cardiovascular health and disease. *Biochim Biophys Acta,* 1812**,** 1477-89.

DONG, T. A., SANDESARA, P. B., DHINDSA, D. S., MEHTA, A., ARNESON, L. C., DOLLAR, A. L., TAUB, P. R. & SPERLING, L. S. 2020. Intermittent Fasting: A Heart Healthy Dietary Pattern? *Am J Med,* 133**,** 901-907.

DORN, G. W., 2ND & MAACK, C. 2013. SR and mitochondria: calcium cross-talk between kissing cousins. *J Mol Cell Cardiol,* 55**,** 42-9.

DORN, G. W., 2ND & SCORRANO, L. 2010. Two close, too close: sarcoplasmic reticulum-mitochondrial crosstalk and cardiomyocyte fate. *Circ Res,* 107**,** 689-99.

DORN, G. W., 2ND, SONG, M. & WALSH, K. 2015. Functional implications of mitofusin 2-mediated mitochondrial-SR tethering. *J Mol Cell Cardiol,* 78**,** 123-8.

DRAZNER, M. H. 2011. The progression of hypertensive heart disease. *Circulation,* 123**,** 327-34.

DUAN, Q., CHEN, C., YANG, L., LI, N., GONG, W., LI, S. & WANG, D. W. 2015. MicroRNA regulation of unfolded protein response transcription factor XBP1 in the progression of cardiac hypertrophy and heart failure in vivo. *J Transl Med,* 13**,** 363.

EISNER, D. 2014. Calcium in the heart: from physiology to disease. *Exp Physiol,* 99**,** 1273-82.

EISNER, V., CSORDAS, G. & HAJNOCZKY, G. 2013. Interactions between sarco-endoplasmic reticulum and mitochondria in cardiac and skeletal muscle - pivotal roles in Ca(2)(+) and reactive oxygen species signaling. *J Cell Sci,* 126**,** 2965-78.

EISNER, V., CUPO, R. R., GAO, E., CSORDAS, G., SLOVINSKY, W. S., PAILLARD, M., CHENG, L., IBETTI, J., CHEN, S. R., CHUPRUN, J. K., HOEK, J. B., KOCH, W. J. & HAJNOCZKY, G. 2017. Mitochondrial fusion dynamics is robust in the heart and depends on calcium oscillations and contractile activity. *Proc Natl Acad Sci U S A,* 114**,** E859-E868.

ESCHENHAGEN, T., BOLLI, R., BRAUN, T., FIELD, L. J., FLEISCHMANN, B. K., FRISEN, J., GIACCA, M., HARE, J. M., HOUSER, S., LEE, R. T., MARBAN, E., MARTIN, J. F., MOLKENTIN, J. D., MURRY, C. E., RILEY, P. R., RUIZ-LOZANO, P., SADEK, H. A., SUSSMAN, M. A. & HILL, J. A. 2017. Cardiomyocyte Regeneration: A Consensus Statement. *Circulation,* 136**,** 680-686.

ESCOBAR-HENRIQUES, M. & JOAQUIM, M. 2019. Mitofusins: Disease Gatekeepers and Hubs in Mitochondrial Quality Control by E3 Ligases. *Front Physiol,* 10**,** 517.

ESCOBAR, K. A., COLE, N. H., MERMIER, C. M. & VANDUSSELDORP, T. A. 2019. Autophagy and aging: Maintaining the proteome through exercise and caloric restriction. *Aging Cell,* 18**,** e12876.

ESTRUCH, R., ROS, E., SALAS-SALVADO, J., COVAS, M. I., CORELLA, D., AROS, F., GOMEZ-GRACIA, E., RUIZ-GUTIERREZ, V., FIOL, M., LAPETRA, J., LAMUELA-RAVENTOS, R. M., SERRA-MAJEM, L., PINTO, X., BASORA, J., MUNOZ, M. A., SORLI, J. V., MARTINEZ, J. A., FITO, M., GEA, A., HERNAN, M. A., MARTINEZ-GONZALEZ, M. A. & INVESTIGATORS, P. S. 2018. Primary Prevention of Cardiovascular Disease with a Mediterranean Diet Supplemented with Extra-Virgin Olive Oil or Nuts. *N Engl J Med,* 378**,** e34.

FARAMOUSHI, M., AMIR SASAN, R., SARI SARRAF, V. & KARIMI, P. 2016. Cardiac fibrosis and down regulation of GLUT4 in experimental diabetic cardiomyopathy are ameliorated by chronic exposures to intermittent altitude. *J Cardiovasc Thorac Res,* 8**,** 26-33.

FENG, Y., HE, D., YAO, Z. & KLIONSKY, D. J. 2014. The machinery of macroautophagy. *Cell Res,* 24**,** 24-41.

FERNANDEZ-VIZARRA, E., ENRIQUEZ, J. A., PEREZ-MARTOS, A., MONTOYA, J. & FERNANDEZ-SILVA, P. 2011. Tissue-specific differences in mitochondrial activity and biogenesis. *Mitochondrion,* 11**,** 207-13.

FILADI, R. & POZZAN, T. 2015. Generation and functions of second messengers microdomains. *Cell Calcium,* 58**,** 405-14.

FONSECA, T. B., SANCHEZ-GUERRERO, A., MILOSEVIC, I. & RAIMUNDO, N. 2019. Mitochondrial fission requires DRP1 but not dynamins. *Nature,* 570**,** E34-E42.

FRANK, S., GAUME, B., BERGMANN-LEITNER, E. S., LEITNER, W. W., ROBERT, E. G., CATEZ, F., SMITH, C. L. & YOULE, R. J. 2001. The role of dynamin-related protein 1, a mediator of mitochondrial fission, in apoptosis. *Dev Cell,* 1**,** 515-25.

FRAYSSE, B., NAGI, S. M., BOHER, B., RAGOT, H., LAINE, J., SALMON, A., FISZMAN, M. Y., TOUSSAINT, M. & FROMES, Y. 2010. Ca2+ overload and mitochondrial permeability transition pore activation in living delta-sarcoglycan-deficient cardiomyocytes. *Am J Physiol Cell Physiol,* 299**,** C706-13.

FRIEDMAN, J. R., LACKNER, L. L., WEST, M., DIBENEDETTO, J. R., NUNNARI, J. & VOELTZ, G. K. 2011. ER tubules mark sites of mitochondrial division. *Science,* 334**,** 358-62.

FRIEDMAN, J. R. & NUNNARI, J. 2014. Mitochondrial form and function. *Nature,* 505**,** 335-43.

FU, H. Y., OKADA, K., LIAO, Y., TSUKAMOTO, O., ISOMURA, T., ASAI, M., SAWADA, T., OKUDA, K., ASANO, Y., SANADA, S., ASANUMA, H., ASAKURA, M., TAKASHIMA, S., KOMURO, I., KITAKAZE, M. & MINAMINO, T. 2010. Ablation of C/EBP homologous protein attenuates endoplasmic reticulum-mediated apoptosis and cardiac dysfunction induced by pressure overload. *Circulation,* 122**,** 361-9.

GALLUZZI, L., BRAVO-SAN PEDRO, J. M., LEVINE, B., GREEN, D. R. & KROEMER, G. 2017. Pharmacological modulation of autophagy: therapeutic potential and persisting obstacles. *Nat Rev Drug Discov,* 16**,** 487-511.

GAO, P., YAN, Z. & ZHU, Z. 2020. Mitochondria-Associated Endoplasmic Reticulum Membranes in Cardiovascular Diseases. *Front Cell Dev Biol,* 8**,** 604240.

GARCIA-PRIETO, J., GARCIA-RUIZ, J. M., SANZ-ROSA, D., PUN, A., GARCIA-ALVAREZ, A., DAVIDSON, S. M., FERNANDEZ-FRIERA, L., NUNO-AYALA, M., FERNANDEZ-JIMENEZ, R., BERNAL, J. A., IZQUIERDO-GARCIA, J. L., JIMENEZ-BORREGUERO, J., PIZARRO, G., RUIZ-CABELLO, J., MACAYA, C., FUSTER, V., YELLON, D. M. & IBANEZ, B. 2014. beta3 adrenergic receptor selective stimulation during ischemia/reperfusion improves cardiac function in translational models through inhibition of mPTP opening in cardiomyocytes. *Basic Res Cardiol,* 109**,** 422.

GHOSH, S., BASU BALL, W., MADARIS, T. R., SRIKANTAN, S., MADESH, M., MOOTHA, V. K. & GOHIL, V. M. 2020. An essential role for cardiolipin in the stability and function of the mitochondrial calcium uniporter. *Proc Natl Acad Sci U S A,* 117**,** 16383-16390.

GOMES, L. C., DI BENEDETTO, G. & SCORRANO, L. 2011. During autophagy mitochondria elongate, are spared from degradation and sustain cell viability. *Nat Cell Biol,* 13**,** 589-98.

GOMEZ-SUAGA, P., PAILLUSSON, S., STOICA, R., NOBLE, W., HANGER, D. P. & MILLER, C. C. J. 2017. The ER-Mitochondria Tethering Complex VAPB-PTPIP51 Regulates Autophagy. *Curr Biol,* 27**,** 371-385.

GONZALEZ-RODRIGUEZ, A., MAYORAL, R., AGRA, N., VALDECANTOS, M. P., PARDO, V., MIQUILENA-COLINA, M. E., VARGAS-CASTRILLON, J., LO IACONO, O., CORAZZARI, M., FIMIA, G. M., PIACENTINI, M., MUNTANE, J., BOSCA, L., GARCIA-MONZON, C., MARTIN-SANZ, P. & VALVERDE, A. M. 2014. Impaired autophagic flux is associated with increased endoplasmic reticulum stress during the development of NAFLD. *Cell Death Dis,* 5**,** e1179.

GRAJOWER, M. M. & HORNE, B. D. 2019. Clinical Management of Intermittent Fasting in Patients with Diabetes Mellitus. *Nutrients,* 11.

GUO, R., LI, N., YANG, R., LIAO, X. Y., ZHANG, Y., ZHU, B. F., ZHAO, Q., CHEN, L., ZHANG, Y. G. & LEI, Y. 2021. Effects of the Modified DASH Diet on Adults With Elevated Blood Pressure or Hypertension: A Systematic Review and Meta-Analysis. *Front Nutr,* 8**,** 725020.

HAMASAKI, M., FURUTA, N., MATSUDA, A., NEZU, A., YAMAMOTO, A., FUJITA, N., OOMORI, H., NODA, T., HARAGUCHI, T., HIRAOKA, Y., AMANO, A. & YOSHIMORI, T. 2013. Autophagosomes form at ER-mitochondria contact sites. *Nature,* 495**,** 389-93.

HAN, X. & REN, J. 2010. Caloric restriction and heart function: is there a sensible link? *Acta Pharmacol Sin,* 31**,** 1111-7.

HANDOOM, B., MEGDAD, E., AL-QASABI, D., AL MESNED, M., HAWARY, R., AL-NUFIEE, S., AL-HASSNAN, Z., ALSAYED, M. D. & ELDALI, A. 2018. The effects of low protein products availability on growth parameters and metabolic control in selected amino acid metabolism disorders patients. *Int J Pediatr Adolesc Med,* 5**,** 60-68.

HARIHARAN, N., IKEDA, Y., HONG, C., ALCENDOR, R. R., USUI, S., GAO, S., MAEJIMA, Y. & SADOSHIMA, J. 2013. Autophagy plays an essential role in mediating regression of hypertrophy during unloading of the heart. *PLoS One,* 8**,** e51632.

HEIN, S., ARNON, E., KOSTIN, S., SCHONBURG, M., ELSASSER, A., POLYAKOVA, V., BAUER, E. P., KLOVEKORN, W. P. & SCHAPER, J. 2003. Progression from compensated hypertrophy to failure in the pressure-overloaded human heart: structural deterioration and compensatory mechanisms. *Circulation,* 107**,** 984-91.

HERSHBERGER, R. E. & JORDAN, E. 1993. LMNA-Related Dilated Cardiomyopathy. *In:* ADAM, M. P., ARDINGER, H. H., PAGON, R. A., WALLACE, S. E., BEAN, L. J. H., GRIPP, K. W., MIRZAA, G. M. & AMEMIYA, A. (eds.) *GeneReviews((R)).* Seattle (WA).

HERSHBERGER, R. E. & SIEGFRIED, J. D. 2011. Update 2011: clinical and genetic issues in familial dilated cardiomyopathy. *J Am Coll Cardiol,* 57**,** 1641-9.

HOLMSTROM, K. M., PAN, X., LIU, J. C., MENAZZA, S., LIU, J., NGUYEN, T. T., PAN, H., PARKS, R. J., ANDERSON, S., NOGUCHI, A., SPRINGER, D., MURPHY, E. & FINKEL, T. 2015. Assessment of cardiac function in mice lacking the mitochondrial calcium uniporter. *J Mol Cell Cardiol,* 85**,** 178-82.

HONG, Y. S., LONGCHAMPS, R. J., ZHAO, D., CASTELLANI, C. A., LOEHR, L. R., CHANG, P. P., MATSUSHITA, K., GROVE, M. L., BOERWINKLE, E., ARKING, D. E. & GUALLAR, E. 2020. Mitochondrial DNA Copy Number and Incident Heart Failure: The Atherosclerosis Risk in Communities (ARIC) Study. *Circulation,* 141**,** 1823-1825.

HORTON, J. L., DAVIDSON, M. T., KURISHIMA, C., VEGA, R. B., POWERS, J. C., MATSUURA, T. R., PETUCCI, C., LEWANDOWSKI, E. D., CRAWFORD, P. A., MUOIO, D. M., RECCHIA, F. A. & KELLY, D. P. 2019. The failing heart utilizes 3-hydroxybutyrate as a metabolic stress defense. *JCI Insight,* 4.

HOSHINO, A., MITA, Y., OKAWA, Y., ARIYOSHI, M., IWAI-KANAI, E., UEYAMA, T., IKEDA, K., OGATA, T. & MATOBA, S. 2013. Cytosolic p53 inhibits Parkin-mediated mitophagy and promotes mitochondrial dysfunction in the mouse heart. *Nat Commun,* 4**,** 2308.

HU, H., TIAN, M., DING, C. & YU, S. 2018. The C/EBP Homologous Protein (CHOP) Transcription Factor Functions in Endoplasmic Reticulum Stress-Induced Apoptosis and Microbial Infection. *Front Immunol,* 9**,** 3083.

HU, T., MILLS, K. T., YAO, L., DEMANELIS, K., ELOUSTAZ, M., YANCY, W. S., JR., KELLY, T. N., HE, J. & BAZZANO, L. A. 2012. Effects of low-carbohydrate diets versus low-fat diets on metabolic risk factors: a meta-analysis of randomized controlled clinical trials. *Am J Epidemiol,* 176 Suppl 7**,** S44-54.

HUDGINS, L. C., HELLERSTEIN, M., SEIDMAN, C., NEESE, R., DIAKUN, J. & HIRSCH, J. 1996. Human fatty acid synthesis is stimulated by a eucaloric low fat, high carbohydrate diet. *J Clin Invest,* 97**,** 2081-91.

HYDE, P. N., SAPPER, T. N., CRABTREE, C. D., LAFOUNTAIN, R. A., BOWLING, M. L., BUGA, A., FELL, B., MCSWINEY, F. T., DICKERSON, R. M., MILLER, V. J., SCANDLING, D., SIMONETTI, O. P., PHINNEY, S. D., KRAEMER, W. J., KING, S. A., KRAUSS, R. M. & VOLEK, J. S. 2019. Dietary carbohydrate restriction improves metabolic syndrome independent of weight loss. *JCI Insight,* 4.

IKEDA, Y., SHIRAKABE, A., MAEJIMA, Y., ZHAI, P., SCIARRETTA, S., TOLI, J., NOMURA, M., MIHARA, K., EGASHIRA, K., OHISHI, M., ABDELLATIF, M. & SADOSHIMA, J. 2015. Endogenous Drp1 mediates mitochondrial autophagy and protects the heart against energy stress. *Circ Res,* 116**,** 264-78.

JANKET, S. J., MANSON, J. E., SESSO, H., BURING, J. E. & LIU, S. 2003. A prospective study of sugar intake and risk of type 2 diabetes in women. *Diabetes Care,* 26**,** 1008-15.

JIN, L., GAO, H., WANG, J., YANG, S., WANG, J., LIU, J., YANG, Y., YAN, T., CHEN, T., ZHAO, Y. & HE, Y. 2017. Role and regulation of autophagy and apoptosis by nitric oxide in hepatic stellate cells during acute liver failure. *Liver Int,* 37**,** 1651-1659.

JOINER, M. L., KOVAL, O. M., LI, J., HE, B. J., ALLAMARGOT, C., GAO, Z., LUCZAK, E. D., HALL, D. D., FINK, B. D., CHEN, B., YANG, J., MOORE, S. A., SCHOLZ, T. D., STRACK, S., MOHLER, P. J., SIVITZ, W. I., SONG, L. S. & ANDERSON, M. E. 2012. CaMKII determines mitochondrial stress responses in heart. *Nature,* 491**,** 269-73.

KALUDERCIC, N., MAIURI, M. C., KAUSHIK, S., FERNANDEZ, A. F., DE BRUIJN, J., CASTOLDI, F., CHEN, Y., ITO, J., MUKAI, R., MURAKAWA, T., NAH, J., PIETROCOLA, F., SAITO, T., SEBTI, S., SEMENZATO, M., TSANSIZI, L., SCIARRETTA, S. & MADRIGAL-MATUTE, J. 2020. Comprehensive autophagy evaluation in cardiac disease models. *Cardiovasc Res,* 116**,** 483-504.

KANG, R., ZEH, H. J., LOTZE, M. T. & TANG, D. 2011. The Beclin 1 network regulates autophagy and apoptosis. *Cell Death Differ,* 18**,** 571-80.

KARWI, Q. G., UDDIN, G. M., HO, K. L. & LOPASCHUK, G. D. 2018. Loss of Metabolic Flexibility in the Failing Heart. *Front Cardiovasc Med,* 5**,** 68.

KESHERWANI, V., CHAVALI, V., HACKFORT, B. T., TYAGI, S. C. & MISHRA, P. K. 2015. Exercise ameliorates high fat diet induced cardiac dysfunction by increasing interleukin 10. *Front Physiol,* 6**,** 124.

KOCATURK, N. M. & GOZUACIK, D. 2018. Crosstalk Between Mammalian Autophagy and the Ubiquitin-Proteasome System. *Front Cell Dev Biol,* 6**,** 128.

KWONG, J. Q., LU, X., CORRELL, R. N., SCHWANEKAMP, J. A., VAGNOZZI, R. J., SARGENT, M. A., YORK, A. J., ZHANG, J., BERS, D. M. & MOLKENTIN, J. D. 2015. The Mitochondrial Calcium Uniporter Selectively Matches Metabolic Output to Acute Contractile Stress in the Heart. *Cell Rep,* 12**,** 15-22.

KYRIAKOUDI, S., DROUSIOTOU, A. & PETROU, P. P. 2021. When the Balance Tips: Dysregulation of Mitochondrial Dynamics as a Culprit in Disease. *Int J Mol Sci,* 22.

LE, C. H., MULLIGAN, C. M., ROUTH, M. A., BOUMA, G. J., FRYE, M. A., JECKEL, K. M., SPARAGNA, G. C., LYNCH, J. M., MOORE, R. L., MCCUNE, S. A., BRISTOW, M., ZARINI, S., MURPHY, R. C. & CHICCO, A. J. 2014. Delta-6-desaturase links polyunsaturated fatty acid metabolism with phospholipid remodeling and disease progression in heart failure. *Circ Heart Fail,* 7**,** 172-83.

LEBEAU, J., SAUNDERS, J. M., MORAES, V. W. R., MADHAVAN, A., MADRAZO, N., ANTHONY, M. C. & WISEMAN, R. L. 2018. The PERK Arm of the Unfolded Protein Response Regulates Mitochondrial Morphology during Acute Endoplasmic Reticulum Stress. *Cell Rep,* 22**,** 2827-2836.

LEBEAUPIN, C., VALLEE, D., HAZARI, Y., HETZ, C., CHEVET, E. & BAILLY-MAITRE, B. 2018. Endoplasmic reticulum stress signalling and the pathogenesis of non-alcoholic fatty liver disease. *J Hepatol,* 69**,** 927-947.

LEE, H., SMITH, S. B. & YOON, Y. 2017. The short variant of the mitochondrial dynamin OPA1 maintains mitochondrial energetics and cristae structure. *J Biol Chem,* 292**,** 7115-7130.

LEMIEUX, H., SEMSROTH, S., ANTRETTER, H., HOFER, D. & GNAIGER, E. 2011. Mitochondrial respiratory control and early defects of oxidative phosphorylation in the failing human heart. *Int J Biochem Cell Biol,* 43**,** 1729-38.

LEWIS, S. C., UCHIYAMA, L. F. & NUNNARI, J. 2016. ER-mitochondria contacts couple mtDNA synthesis with mitochondrial division in human cells. *Science,* 353**,** aaf5549.

LI, D. L., WANG, Z. V., DING, G., TAN, W., LUO, X., CRIOLLO, A., XIE, M., JIANG, N., MAY, H., KYRYCHENKO, V., SCHNEIDER, J. W., GILLETTE, T. G. & HILL, J. A. 2016a. Doxorubicin Blocks Cardiomyocyte Autophagic Flux by Inhibiting Lysosome Acidification. *Circulation,* 133**,** 1668-87.

LI, S., LIU, C., GU, L., WANG, L., SHANG, Y., LIU, Q., WAN, J., SHI, J., WANG, F., XU, Z., JI, G. & LI, W. 2016b. Autophagy protects cardiomyocytes from the myocardial ischaemia-reperfusion injury through the clearance of CLP36. *Open Biol,* 6.

LI, X., LIU, J., HU, H., LU, S., LU, Q., QUAN, N., ROUSSELLE, T., PATEL, M. S. & LI, J. 2019. Dichloroacetate Ameliorates Cardiac Dysfunction Caused by Ischemic Insults Through AMPK Signal Pathway-Not Only Shifts Metabolism. *Toxicol Sci,* 167**,** 604-617.

LIAO, R., JAIN, M., CUI, L., D'AGOSTINO, J., AIELLO, F., LUPTAK, I., NGOY, S., MORTENSEN, R. M. & TIAN, R. 2002. Cardiac-specific overexpression of GLUT1 prevents the development of heart failure attributable to pressure overload in mice. *Circulation,* 106**,** 2125-31.

LIU, W. J., YE, L., HUANG, W. F., GUO, L. J., XU, Z. G., WU, H. L., YANG, C. & LIU, H. F. 2016. p62 links the autophagy pathway and the ubiqutin-proteasome system upon ubiquitinated protein degradation. *Cell Mol Biol Lett,* 21**,** 29.

LIU, X., KWAK, D., LU, Z., XU, X., FASSETT, J., WANG, H., WEI, Y., CAVENER, D. R., HU, X., HALL, J., BACHE, R. J. & CHEN, Y. 2014a. Endoplasmic reticulum stress sensor protein kinase R-like endoplasmic reticulum kinase (PERK) protects against pressure overload-induced heart failure and lung remodeling. *Hypertension,* 64**,** 738-44.

LIU, X. H., ZHANG, Z. Y., ANDERSSON, K. B., HUSBERG, C., ENGER, U. H., RAEDER, M. G., CHRISTENSEN, G. & LOUCH, W. E. 2011. Cardiomyocyte-specific disruption of Serca2 in adult mice causes sarco(endo)plasmic reticulum stress and apoptosis. *Cell Calcium,* 49**,** 201-7.

LIU, Y. S., WU, Q. J., XIA, Y., ZHANG, J. Y., JIANG, Y. T., CHANG, Q. & ZHAO, Y. H. 2019. Carbohydrate intake and risk of metabolic syndrome: A dose-response meta-analysis of observational studies. *Nutr Metab Cardiovasc Dis,* 29**,** 1288-1298.

LIU, Z., CAI, H., ZHU, H., TOQUE, H., ZHAO, N., QIU, C., GUAN, G., DANG, Y. & WANG, J. 2014b. Protein kinase RNA-like endoplasmic reticulum kinase (PERK)/calcineurin signaling is a novel pathway regulating intracellular calcium accumulation which might be involved in ventricular arrhythmias in diabetic cardiomyopathy. *Cell Signal,* 26**,** 2591-600.

LOOS, B., DU TOIT, A. & HOFMEYR, J. H. 2014. Defining and measuring autophagosome flux-concept and reality. *Autophagy,* 10**,** 2087-96.

LOPASCHUK, G. D., KARWI, Q. G., TIAN, R., WENDE, A. R. & ABEL, E. D. 2021. Cardiac Energy Metabolism in Heart Failure. *Circ Res,* 128**,** 1487-1513.

LOPEZ-CRISOSTO, C., PENNANEN, C., VASQUEZ-TRINCADO, C., MORALES, P. E., BRAVO-SAGUA, R., QUEST, A. F. G., CHIONG, M. & LAVANDERO, S. 2017. Sarcoplasmic

reticulum-mitochondria communication in cardiovascular pathophysiology. *Nat Rev Cardiol,* 14**,** 342-360.

LU, L., WU, W., YAN, J., LI, X., YU, H. & YU, X. 2009. Adriamycin-induced autophagic cardiomyocyte death plays a pathogenic role in a rat model of heart failure. *Int J Cardiol,* 134**,** 82-90.

LUO, M. & ANDERSON, M. E. 2013. Mechanisms of altered Ca(2)(+) handling in heart failure. *Circ Res,* 113**,** 690-708.

MACVICAR, T., OHBA, Y., NOLTE, H., MAYER, F. C., TATSUTA, T., SPRENGER, H. G., LINDNER, B., ZHAO, Y., LI, J., BRUNS, C., KRUGER, M., HABICH, M., RIEMER, J., SCHWARZER, R., PASPARAKIS, M., HENSCHKE, S., BRUNING, J. C., ZAMBONI, N. & LANGER, T. 2019. Lipid signalling drives proteolytic rewiring of mitochondria by YME1L. *Nature,* 575**,** 361-365.

MAKRECKA-KUKA, M., KORZH, S., VIDEJA, M., VILSKERSTS, R., SEVOSTJANOVS, E., ZHARKOVA-MALKOVA, O., ARSENYAN, P., KUKA, J., DAMBROVA, M. & LIEPINSH, E. 2020. Inhibition of CPT2 exacerbates cardiac dysfunction and inflammation in experimental endotoxaemia. *J Cell Mol Med,* 24**,** 11903-11911.

MATSUI, Y., TAKAGI, H., QU, X., ABDELLATIF, M., SAKODA, H., ASANO, T., LEVINE, B. & SADOSHIMA, J. 2007. Distinct roles of autophagy in the heart during ischemia and reperfusion: roles of AMP-activated protein kinase and Beclin 1 in mediating autophagy. *Circ Res,* 100**,** 914-22.

MCCOMBIE, G., MEDINA-GOMEZ, G., LELLIOTT, C. J., VIDAL-PUIG, A. & GRIFFIN, J. L. 2012. Metabolomic and Lipidomic Analysis of the Heart of Peroxisome Proliferator-Activated Receptor-gamma Coactivator 1-beta Knock Out Mice on a High Fat Diet. *Metabolites,* 2**,** 366-81.

MCGARRY, J. D. & BROWN, N. F. 1997. The mitochondrial carnitine palmitoyltransferase system. From concept to molecular analysis. *Eur J Biochem,* 244**,** 1-14.

MCLENDON, P. M. & ROBBINS, J. 2011. Desmin-related cardiomyopathy: an unfolding story. *Am J Physiol Heart Circ Physiol,* 301**,** H1220-8.

MCNALLY, E., ALLIKIAN, M., WHEELER, M. T., MISLOW, J. M. & HEYDEMANN, A. 2003. Cytoskeletal defects in cardiomyopathy. *J Mol Cell Cardiol,* 35**,** 231-41.

MCNALLY, E. M. & MESTRONI, L. 2017. Dilated Cardiomyopathy: Genetic Determinants and Mechanisms. *Circ Res,* 121**,** 731-748.

MEKAHLI, D., BULTYNCK, G., PARYS, J. B., DE SMEDT, H. & MISSIAEN, L. 2011. Endoplasmic-reticulum calcium depletion and disease. *Cold Spring Harb Perspect Biol,* 3.

MERLO, M., CANNATA, A., GOBBO, M., STOLFO, D., ELLIOTT, P. M. & SINAGRA, G. 2018. Evolving concepts in dilated cardiomyopathy. *Eur J Heart Fail,* 20**,** 228-239.

MIZUSHIMA, N., YOSHIMORI, T. & OHSUMI, Y. 2011. The role of Atg proteins in autophagosome formation. *Annu Rev Cell Dev Biol,* 27**,** 107-32.

MOATT, J. P., SAVOLA, E., REGAN, J. C., NUSSEY, D. H. & WALLING, C. A. 2020. Lifespan Extension Via Dietary Restriction: Time to Reconsider the Evolutionary Mechanisms? *Bioessays,* 42**,** e1900241.

NAKAGAWA, T., ZHU, H., MORISHIMA, N., LI, E., XU, J., YANKNER, B. A. & YUAN, J. 2000. Caspase-12 mediates endoplasmic-reticulum-specific apoptosis and cytotoxicity by amyloid-beta. *Nature,* 403**,** 98-103.

NASSER, S., VIALICHKA, V., BIESIEKIERSKA, M., BALCERCZYK, A. & PIROLA, L. 2020. Effects of ketogenic diet and ketone bodies on the cardiovascular system: Concentration matters. *World J Diabetes,* 11**,** 584-595.

NASZAI, A., TERHES, E., KASZAKI, J., BOROS, M. & JUHASZ, L. 2019. Ca((2+))N It Be Measured? Detection of Extramitochondrial Calcium Movement With High-Resolution FluoRespirometry. *Sci Rep,* 9**,** 19229.

NISHIDA, K., KYOI, S., YAMAGUCHI, O., SADOSHIMA, J. & OTSU, K. 2009. The role of autophagy in the heart. *Cell Death Differ,* 16**,** 31-8.

NISHIDA, K. & OTSU, K. 2017. Inflammation and metabolic cardiomyopathy. *Cardiovasc Res,* 113**,** 389-398.

NISHINO, I., FU, J., TANJI, K., YAMADA, T., SHIMOJO, S., KOORI, T., MORA, M., RIGGS, J. E., OH, S. J., KOGA, Y., SUE, C. M., YAMAMOTO, A., MURAKAMI, N., SHANSKE, S., BYRNE, E., BONILLA, E., NONAKA, I., DIMAURO, S. & HIRANO, M. 2000. Primary LAMP-2 deficiency causes X-linked vacuolar cardiomyopathy and myopathy (Danon disease). *Nature,* 406**,** 906-10.

OKADA, K., MINAMINO, T., TSUKAMOTO, Y., LIAO, Y., TSUKAMOTO, O., TAKASHIMA, S., HIRATA, A., FUJITA, M., NAGAMACHI, Y., NAKATANI, T., YUTANI, C., OZAWA, K., OGAWA, S., TOMOIKE, H., HORI, M. & KITAKAZE, M. 2004. Prolonged endoplasmic reticulum stress in hypertrophic and failing heart after aortic constriction: possible contribution of endoplasmic reticulum stress to cardiac myocyte apoptosis. *Circulation,* 110**,** 705-12.

OKERE, I. C., YOUNG, M. E., MCELFRESH, T. A., CHESS, D. J., SHAROV, V. G., SABBAH, H. N., HOIT, B. D., ERNSBERGER, P., CHANDLER, M. P. & STANLEY, W. C. 2006. Low carbohydrate/high-fat diet attenuates cardiac hypertrophy, remodeling, and altered gene expression in hypertension. *Hypertension,* 48**,** 1116-23.

OKOSHI, K., CEZAR, M. D. M., POLIN, M. A. M., PALADINO, J. R., JR., MARTINEZ, P. F., OLIVEIRA, S. A., JR., LIMA, A. R. R., DAMATTO, R. L., PAIVA, S. A. R., ZORNOFF, L. A. M. & OKOSHI, M. P. 2019. Influence of intermittent fasting on myocardial infarction-induced cardiac remodeling. *BMC Cardiovasc Disord,* 19**,** 126.

ONG, S. B., SUBRAYAN, S., LIM, S. Y., YELLON, D. M., DAVIDSON, S. M. & HAUSENLOY, D. J. 2010. Inhibiting mitochondrial fission protects the heart against ischemia/reperfusion injury. *Circulation,* 121**,** 2012-22.

OSMAN, C., VOELKER, D. R. & LANGER, T. 2011. Making heads or tails of phospholipids in mitochondria. *J Cell Biol,* 192**,** 7-16.

PAKIET, A., JAKUBIAK, A., MIERZEJEWSKA, P., ZWARA, A., LIAKH, I., SLEDZINSKI, T. & MIKA, A. 2020. The Effect of a High-Fat Diet on the Fatty Acid Composition in the Hearts of Mice. *Nutrients,* 12.

PAPANICOLAOU, K. N., KHAIRALLAH, R. J., NGOH, G. A., CHIKANDO, A., LUPTAK, I., O'SHEA, K. M., RILEY, D. D., LUGUS, J. J., COLUCCI, W. S., LEDERER, W. J., STANLEY, W. C. & WALSH, K. 2011. Mitofusin-2 maintains mitochondrial structure and contributes to stress-induced permeability transition in cardiac myocytes. *Mol Cell Biol,* 31**,** 1309-28.

PAPANICOLAOU, K. N., KIKUCHI, R., NGOH, G. A., COUGHLAN, K. A., DOMINGUEZ, I., STANLEY, W. C. & WALSH, K. 2012. Mitofusins 1 and 2 are essential for postnatal metabolic remodeling in heart. *Circ Res,* 111**,** 1012-26.

PEREYRA, A. S., HASEK, L. Y., HARRIS, K. L., BERMAN, A. G., DAMEN, F. W., GOERGEN, C. J. & ELLIS, J. M. 2017. Loss of cardiac carnitine palmitoyltransferase 2 results in

rapamycin-resistant, acetylation-independent hypertrophy. *J Biol Chem,* 292**,** 18443-18456.

PIQUEREAU, J., CAFFIN, F., NOVOTOVA, M., LEMAIRE, C., VEKSLER, V., GARNIER, A., VENTURA-CLAPIER, R. & JOUBERT, F. 2013. Mitochondrial dynamics in the adult cardiomyocytes: which roles for a highly specialized cell? *Front Physiol,* 4**,** 102.

PITTS, K. R., YOON, Y., KRUEGER, E. W. & MCNIVEN, M. A. 1999. The dynamin-like protein DLP1 is essential for normal distribution and morphology of the endoplasmic reticulum and mitochondria in mammalian cells. *Mol Biol Cell,* 10**,** 4403-17.

PRADAS, I., HUYNH, K., CABRE, R., AYALA, V., MEIKLE, P. J., JOVE, M. & PAMPLONA, R. 2018. Lipidomics Reveals a Tissue-Specific Fingerprint. *Front Physiol,* 9**,** 1165.

QIN, J., GUO, Y., XUE, B., SHI, P., CHEN, Y., SU, Q. P., HAO, H., ZHAO, S., WU, C., YU, L., LI, D. & SUN, Y. 2020. ER-mitochondria contacts promote mtDNA nucleoids active transportation via mitochondrial dynamic tubulation. *Nat Commun,* 11**,** 4471.

RABINOVICH-NIKITIN, I., DHINGRA, R. & KIRSHENBAUM, L. A. 2019. Activation of Mitophagy in High-Fat Diet-Induced Diabetic Cardiomyopathy. *Circ Res,* 124**,** 1288-1290.

RAINBOLT, T. K., ATANASSOVA, N., GENEREUX, J. C. & WISEMAN, R. L. 2013. Stress-regulated translational attenuation adapts mitochondrial protein import through Tim17A degradation. *Cell Metab,* 18**,** 908-19.

RAMACCINI, D., MONTOYA-URIBE, V., AAN, F. J., MODESTI, L., POTES, Y., WIECKOWSKI, M. R., KRGA, I., GLIBETIC, M., PINTON, P., GIORGI, C. & MATTER, M. L. 2020. Mitochondrial Function and Dysfunction in Dilated Cardiomyopathy. *Front Cell Dev Biol,* 8**,** 624216.

REDMAN, L. M. & RAVUSSIN, E. 2011. Caloric restriction in humans: impact on physiological, psychological, and behavioral outcomes. *Antioxid Redox Signal,* 14**,** 275-87.

REICHART, D., MAGNUSSEN, C., ZELLER, T. & BLANKENBERG, S. 2019. Dilated cardiomyopathy: from epidemiologic to genetic phenotypes: A translational review of current literature. *J Intern Med,* 286**,** 362-372.

RIZZUTO, R., MARCHI, S., BONORA, M., AGUIARI, P., BONONI, A., DE STEFANI, D., GIORGI, C., LEO, S., RIMESSI, A., SIVIERO, R., ZECCHINI, E. & PINTON, P. 2009. Ca(2+) transfer from the ER to mitochondria: when, how and why. *Biochim Biophys Acta,* 1787**,** 1342-51.

ROSENBAUM, A. N., AGRE, K. E. & PEREIRA, N. L. 2020. Genetics of dilated cardiomyopathy: practical implications for heart failure management. *Nat Rev Cardiol,* 17**,** 286-297.

RUAN, Y., LI, H., ZHANG, K., JIAN, F., TANG, J. & SONG, Z. 2013. Loss of Yme1L perturbates mitochondrial dynamics. *Cell Death Dis,* 4**,** e896.

RUIZ-MEANA, M., BOU-TEEN, D., FERDINANDY, P., GYONGYOSI, M., PESCE, M., PERRINO, C., SCHULZ, R., SLUIJTER, J. P. G., TOCCHETTI, C. G., THUM, T. & MADONNA, R. 2020. Cardiomyocyte ageing and cardioprotection: consensus document from the ESC working groups cell biology of the heart and myocardial function. *Cardiovasc Res,* 116**,** 1835-1849.

RUSINOL, A. E., CUI, Z., CHEN, M. H. & VANCE, J. E. 1994. A unique mitochondria-associated membrane fraction from rat liver has a high capacity for lipid synthesis and contains pre-Golgi secretory proteins including nascent lipoproteins. *J Biol Chem,* 269**,** 27494-502.

RUSSELL, R. C., TIAN, Y., YUAN, H., PARK, H. W., CHANG, Y. Y., KIM, J., KIM, H., NEUFELD, T. P., DILLIN, A. & GUAN, K. L. 2013. ULK1 induces autophagy by phosphorylating Beclin-1 and activating VPS34 lipid kinase. *Nat Cell Biol,* 15**,** 741-50.

SABBAH, H. N. 2000. Apoptotic cell death in heart failure. *Cardiovasc Res,* 45**,** 704-12.

SABBAH, H. N. 2020. Targeting the Mitochondria in Heart Failure: A Translational Perspective. *JACC Basic Transl Sci,* 5**,** 88-106.

SALA-VILA, A., NAVARRO-LERIDA, I., SANCHEZ-ALVAREZ, M., BOSCH, M., CALVO, C., LOPEZ, J. A., CALVO, E., FERGUSON, C., GIACOMELLO, M., SERAFINI, A., SCORRANO, L., ENRIQUEZ, J. A., BALSINDE, J., PARTON, R. G., VAZQUEZ, J., POL, A. & DEL POZO, M. A. 2016. Interplay between hepatic mitochondria-associated membranes, lipid metabolism and caveolin-1 in mice. *Sci Rep,* 6**,** 27351.

SALEH, M., MATHISON, J. C., WOLINSKI, M. K., BENSINGER, S. J., FITZGERALD, P., DROIN, N., ULEVITCH, R. J., GREEN, D. R. & NICHOLSON, D. W. 2006. Enhanced bacterial clearance and sepsis resistance in caspase-12-deficient mice. *Nature,* 440**,** 1064-8.

SALVATORE, T., PAFUNDI, P. C., GALIERO, R., ALBANESE, G., DI MARTINO, A., CATURANO, A., VETRANO, E., RINALDI, L. & SASSO, F. C. 2021. The Diabetic Cardiomyopathy: The Contributing Pathophysiological Mechanisms. *Front Med (Lausanne),* 8**,** 695792.

SANDESARA, P. B. & SPERLING, L. S. 2018. Caloric Restriction as a Therapeutic Approach to Heart Failure: Can Less Be More in (Mice) and Men? *Circ Heart Fail,* 11**,** e004930.

SANTESSO, N., AKL, E. A., BIANCHI, M., MENTE, A., MUSTAFA, R., HEELS-ANSDELL, D. & SCHUNEMANN, H. J. 2012. Effects of higher- versus lower-protein diets on health outcomes: a systematic review and meta-analysis. *Eur J Clin Nutr,* 66**,** 780-8.

SCHAPER, J., MEISER, E. & STAMMLER, G. 1985. Ultrastructural morphometric analysis of myocardium from dogs, rats, hamsters, mice, and from human hearts. *Circ Res,* 56**,** 377-91.

SCHMITT, J. P., DEBOLD, E. P., AHMAD, F., ARMSTRONG, A., FREDERICO, A., CONNER, D. A., MENDE, U., LOHSE, M. J., WARSHAW, D., SEIDMAN, C. E. & SEIDMAN, J. G. 2006. Cardiac myosin missense mutations cause dilated cardiomyopathy in mouse models and depress molecular motor function. *Proc Natl Acad Sci U S A,* 103**,** 14525-30.

SCHULTHEISS, H. P., FAIRWEATHER, D., CAFORIO, A. L. P., ESCHER, F., HERSHBERGER, R. E., LIPSHULTZ, S. E., LIU, P. P., MATSUMORI, A., MAZZANTI, A., MCMURRAY, J. & PRIORI, S. G. 2019. Dilated cardiomyopathy. *Nat Rev Dis Primers,* 5**,** 32.

SCHULZ, G., VON DAHL, J., KAISER, H. J., KOCH, K. C., SABRI, O., BANNEITZ, L., CREMERIUS, U. & BUELL, U. 1996. Imaging of beta-oxidation by static PET with 14(R,S)-[18F]-fluoro-6-thiaheptadecanoic acid (FTHA) in patients with advanced coronary heart disease: a comparison with 18FDG-PET and 99Tcm-MIBI SPET. *Nucl Med Commun,* 17**,** 1057-64.

SCIARRETTA, S., BOPPANA, V. S., UMAPATHI, M., FRATI, G. & SADOSHIMA, J. 2015. Boosting autophagy in the diabetic heart: a translational perspective. *Cardiovasc Diagn Ther,* 5**,** 394-402.

SCIARRETTA, S., FORTE, M., FRATI, G. & SADOSHIMA, J. 2018. New Insights Into the Role of mTOR Signaling in the Cardiovascular System. *Circ Res,* 122**,** 489-505.

SELVARAJ, S., KELLY, D. P. & MARGULIES, K. B. 2020. Implications of Altered Ketone Metabolism and Therapeutic Ketosis in Heart Failure. *Circulation,* 141**,** 1800-1812.

SHAMI, G. J., CHENG, D., VERHAEGH, P., KOEK, G., WISSE, E. & BRAET, F. 2021. Three-dimensional ultrastructure of giant mitochondria in human non-alcoholic fatty liver disease. *Sci Rep,* 11**,** 3319.

SHANG, L., CHEN, S., DU, F., LI, S., ZHAO, L. & WANG, X. 2011. Nutrient starvation elicits an acute autophagic response mediated by Ulk1 dephosphorylation and its subsequent dissociation from AMPK. *Proc Natl Acad Sci U S A,* 108**,** 4788-93.

SHENG, R. & QIN, Z. H. 2015. The divergent roles of autophagy in ischemia and preconditioning. *Acta Pharmacol Sin,* 36**,** 411-20.

SHIRAKABE, A., ZHAI, P., IKEDA, Y., SAITO, T., MAEJIMA, Y., HSU, C. P., NOMURA, M., EGASHIRA, K., LEVINE, B. & SADOSHIMA, J. 2016. Drp1-Dependent Mitochondrial Autophagy Plays a Protective Role Against Pressure Overload-Induced Mitochondrial Dysfunction and Heart Failure. *Circulation,* 133**,** 1249-63.

SOOD, A., JEYARAJU, D. V., PRUDENT, J., CARON, A., LEMIEUX, P., MCBRIDE, H. M., LAPLANTE, M., TOTH, K. & PELLEGRINI, L. 2014. A Mitofusin-2-dependent inactivating cleavage of Opa1 links changes in mitochondria cristae and ER contacts in the postprandial liver. *Proc Natl Acad Sci U S A,* 111**,** 16017-22.

SORRIENTO, D., DI VAIA, E. & IACCARINO, G. 2021. Physical Exercise: A Novel Tool to Protect Mitochondrial Health. *Front Physiol,* 12**,** 660068.

SPARAGNA, G. C., CHICCO, A. J., MURPHY, R. C., BRISTOW, M. R., JOHNSON, C. A., REES, M. L., MAXEY, M. L., MCCUNE, S. A. & MOORE, R. L. 2007. Loss of cardiac tetralinoleoyl cardiolipin in human and experimental heart failure. *J Lipid Res,* 48**,** 1559-70.

SPRENGER, H. G., WANI, G., HESSELING, A., KONIG, T., PATRON, M., MACVICAR, T., AHOLA, S., WAI, T., BARTH, E., RUGARLI, E. I., BERGAMI, M. & LANGER, T. 2019. Loss of the mitochondrial i-AAA protease YME1L leads to ocular dysfunction and spinal axonopathy. *EMBO Mol Med,* 11.

STEGEMANN, C., PECHLANER, R., WILLEIT, P., LANGLEY, S. R., MANGINO, M., MAYR, U., MENNI, C., MOAYYERI, A., SANTER, P., RUNGGER, G., SPECTOR, T. D., WILLEIT, J., KIECHL, S. & MAYR, M. 2014. Lipidomics profiling and risk of cardiovascular disease in the prospective population-based Bruneck study. *Circulation,* 129**,** 1821-31.

STIBUREK, L., CESNEKOVA, J., KOSTKOVA, O., FORNUSKOVA, D., VINSOVA, K., WENCHICH, L., HOUSTEK, J. & ZEMAN, J. 2012. YME1L controls the accumulation of respiratory chain subunits and is required for apoptotic resistance, cristae morphogenesis, and cell proliferation. *Mol Biol Cell,* 23**,** 1010-23.

STRZYZ, P. 2019. ER stress boosts respiration. *Nat Rev Mol Cell Biol,* 20**,** 453.

SU, H. & WANG, X. 2011. Autophagy and p62 in cardiac protein quality control. *Autophagy,* 7**,** 1382-3.

SUAREZ, J., CIVIDINI, F., SCOTT, B. T., LEHMANN, K., DIAZ-JUAREZ, J., DIEMER, T., DAI, A., SUAREZ, J. A., JAIN, M. & DILLMANN, W. H. 2018. Restoring mitochondrial calcium uniporter expression in diabetic mouse heart improves mitochondrial calcium handling and cardiac function. *J Biol Chem,* 293**,** 8182-8195.

SUN, D., LI, C., LIU, J., WANG, Z., LIU, Y., LUO, C., CHEN, Y. & WEN, S. 2019. Expression Profile of microRNAs in Hypertrophic Cardiomyopathy and Effects of microRNA-

20 in Inducing Cardiomyocyte Hypertrophy Through Regulating Gene MFN2. *DNA Cell Biol,* 38**,** 796-807.

SUN, F., XU, X., WANG, X. & ZHANG, B. 2016. Regulation of autophagy by Ca(2). *Tumour Biol*.

SUN, Y., YAO, X., ZHANG, Q. J., ZHU, M., LIU, Z. P., CI, B., XIE, Y., CARLSON, D., ROTHERMEL, B. A., SUN, Y., LEVINE, B., HILL, J. A., WOLF, S. E., MINEI, J. P. & ZANG, Q. S. 2018. Beclin-1-Dependent Autophagy Protects the Heart During Sepsis. *Circulation,* 138**,** 2247-2262.

SYSI-AHO, M., KOIKKALAINEN, J., SEPPANEN-LAAKSO, T., KAARTINEN, M., KUUSISTO, J., PEUHKURINEN, K., KARKKAINEN, S., ANTILA, M., LAUERMA, K., REISSELL, E., JURKKO, R., LOTJONEN, J., HELIO, T. & ORESIC, M. 2011. Serum lipidomics meets cardiac magnetic resonance imaging: profiling of subjects at risk of dilated cardiomyopathy. *PLoS One,* 6**,** e15744.

SZEGEZDI, E., FITZGERALD, U. & SAMALI, A. 2003. Caspase-12 and ER-stress-mediated apoptosis: the story so far. *Ann N Y Acad Sci,* 1010**,** 186-94.

TANAKA, Y., GUHDE, G., SUTER, A., ESKELINEN, E. L., HARTMANN, D., LULLMANN-RAUCH, R., JANSSEN, P. M., BLANZ, J., VON FIGURA, K. & SAFTIG, P. 2000. Accumulation of autophagic vacuoles and cardiomyopathy in LAMP-2-deficient mice. *Nature,* 406**,** 902-6.

TANEIKE, M., YAMAGUCHI, O., NAKAI, A., HIKOSO, S., TAKEDA, T., MIZOTE, I., OKA, T., TAMAI, T., OYABU, J., MURAKAWA, T., NISHIDA, K., SHIMIZU, T., HORI, M., KOMURO, I., TAKUJI SHIRASAWA, T. S., MIZUSHIMA, N. & OTSU, K. 2010. Inhibition of autophagy in the heart induces age-related cardiomyopathy. *Autophagy,* 6**,** 600-6.

TANG, H., TAO, A., SONG, J., LIU, Q., WANG, H. & RUI, T. 2017. Doxorubicin-induced cardiomyocyte apoptosis: Role of mitofusin 2. *Int J Biochem Cell Biol,* 88**,** 55-59.

TAYAL, U., GREGSON, J., BUCHAN, R., WHIFFIN, N., HALLIDAY, B. P., LOTA, A., ROBERTS, A. M., BAKSI, A. J., VOGES, I., JARMAN, J. W. E., BARUAH, R., FRENNEAUX, M., CLELAND, J. G. F., BARTON, P., PENNELL, D. J., WARE, J. S., COOK, S. A. & PRASAD, S. K. 2022. Moderate excess alcohol consumption and adverse cardiac remodelling in dilated cardiomyopathy. *Heart,* 108**,** 619-625.

TAYLOR, M., WALLHAUS, T. R., DEGRADO, T. R., RUSSELL, D. C., STANKO, P., NICKLES, R. J. & STONE, C. K. 2001. An evaluation of myocardial fatty acid and glucose uptake using PET with [18F]fluoro-6-thia-heptadecanoic acid and [18F]FDG in Patients with Congestive Heart Failure. *J Nucl Med,* 42**,** 55-62.

TERNACLE, J., WAN, F., SAWAKI, D., SURENAUD, M., PINI, M., MERCEDES, R., ERNANDE, L., AUDUREAU, E., DUBOIS-RANDE, J. L., ADNOT, S., HUE, S., CZIBIK, G. & DERUMEAUX, G. 2017. Short-term high-fat diet compromises myocardial function: a radial strain rate imaging study. *Eur Heart J Cardiovasc Imaging,* 18**,** 1283-1291.

THARP, C. A., HAYWOOD, M. E., SBAIZERO, O., TAYLOR, M. R. G. & MESTRONI, L. 2019. The Giant Protein Titin's Role in Cardiomyopathy: Genetic, Transcriptional, and Post-translational Modifications of TTN and Their Contribution to Cardiac Disease. *Front Physiol,* 10**,** 1436.

THEUREY, P. & RIEUSSET, J. 2017. Mitochondria-Associated Membranes Response to Nutrient Availability and Role in Metabolic Diseases. *Trends Endocrinol Metab,* 28**,** 32-45.

TONDERA, D., GRANDEMANGE, S., JOURDAIN, A., KARBOWSKI, M., MATTENBERGER, Y., HERZIG, S., DA CRUZ, S., CLERC, P., RASCHKE, I., MERKWIRTH, C., EHSES, S., KRAUSE, F., CHAN, D. C., ALEXANDER, C., BAUER, C., YOULE, R., LANGER, T. & MARTINOU, J. C. 2009. SLP-2 is required for stress-induced mitochondrial hyperfusion. *EMBO J,* 28**,** 1589-600.

TONG, M., SAITO, T., ZHAI, P., OKA, S. I., MIZUSHIMA, W., NAKAMURA, M., IKEDA, S., SHIRAKABE, A. & SADOSHIMA, J. 2019. Mitophagy Is Essential for Maintaining Cardiac Function During High Fat Diet-Induced Diabetic Cardiomyopathy. *Circ Res,* 124**,** 1360-1371.

TRAN, D. H. & WANG, Z. V. 2019. Glucose Metabolism in Cardiac Hypertrophy and Heart Failure. *J Am Heart Assoc,* 8**,** e012673.

TWIG, G., ELORZA, A., MOLINA, A. J., MOHAMED, H., WIKSTROM, J. D., WALZER, G., STILES, L., HAIGH, S. E., KATZ, S., LAS, G., ALROY, J., WU, M., PY, B. F., YUAN, J., DEENEY, J. T., CORKEY, B. E. & SHIRIHAI, O. S. 2008. Fission and selective fusion govern mitochondrial segregation and elimination by autophagy. *EMBO J,* 27**,** 433-46.

UJFALUSI, Z., VERA, C. D., MIJAILOVICH, S. M., SVICEVIC, M., YU, E. C., KAWANA, M., RUPPEL, K. M., SPUDICH, J. A., GEEVES, M. A. & LEINWAND, L. A. 2018. Dilated cardiomyopathy myosin mutants have reduced force-generating capacity. *J Biol Chem,* 293**,** 9017-9029.

VAN MEER, G., VOELKER, D. R. & FEIGENSON, G. W. 2008. Membrane lipids: where they are and how they behave. *Nat Rev Mol Cell Biol,* 9**,** 112-24.

VANG, S., CORYDON, T. J., BORGLUM, A. D., SCOTT, M. D., FRYDMAN, J., MOGENSEN, J., GREGERSEN, N. & BROSS, P. 2005. Actin mutations in hypertrophic and dilated cardiomyopathy cause inefficient protein folding and perturbed filament formation. *FEBS J,* 272**,** 2037-49.

VIDONI, S., ZANNA, C., RUGOLO, M., SARZI, E. & LENAERS, G. 2013. Why mitochondria must fuse to maintain their genome integrity. *Antioxid Redox Signal,* 19**,** 379-88.

VINCOW, E. S., THOMAS, R. E., MERRIHEW, G. E., SHULMAN, N. J., BAMMLER, T. K., MACDONALD, J. W., MACCOSS, M. J. & PALLANCK, L. J. 2019. Autophagy accounts for approximately one-third of mitochondrial protein turnover and is protein selective. *Autophagy,* 15**,** 1592-1605.

WAI, T., GARCIA-PRIETO, J., BAKER, M. J., MERKWIRTH, C., BENIT, P., RUSTIN, P., RUPEREZ, F. J., BARBAS, C., IBANEZ, B. & LANGER, T. 2015. Imbalanced OPA1 processing and mitochondrial fragmentation cause heart failure in mice. *Science,* 350**,** aad0116.

WAI, T. & LANGER, T. 2016. Mitochondrial Dynamics and Metabolic Regulation. *Trends Endocrinol Metab,* 27**,** 105-117.

WANG, D., HE, X., ZHENG, C., WANG, C., PENG, P., GAO, C., XU, X., MA, Y., LIU, M., YANG, L. & LUO, Z. 2021a. Endoplasmic Reticulum Stress: An Emerging Therapeutic Target for Intervertebral Disc Degeneration. *Front Cell Dev Biol,* 9**,** 819139.

WANG, K., JIN, M., LIU, X. & KLIONSKY, D. J. 2013. Proteolytic processing of Atg32 by the mitochondrial i-AAA protease Yme1 regulates mitophagy. *Autophagy,* 9**,** 1828-36.

WANG, L., ZHANG, Q., YUAN, K. & YUAN, J. 2021b. mtDNA in the Pathogenesis of Cardiovascular Diseases. *Dis Markers,* 2021**,** 7157109.

WANG, S., BINDER, P., FANG, Q., WANG, Z., XIAO, W., LIU, W. & WANG, X. 2018. Endoplasmic reticulum stress in the heart: insights into mechanisms and drug targets. *Br J Pharmacol,* 175**,** 1293-1304.

WANI, G. A., SPRENGER, H. G., NDOCI, K., CHANDRAGIRI, S., ACTON, R. J., SCHATTON, D., KOCHAN, S. M. V., SAKTHIVELU, V., JEVTIC, M., SEEGER, J. M., MULLER, S., GIAVALISCO, P., RUGARLI, E. I., MOTORI, E., LANGER, T. & BERGAMI, M. 2022. Metabolic control of adult neural stem cell self-renewal by the mitochondrial protease YME1L. *Cell Rep,* 38**,** 110370.

WATANABE, S. 2017. Low-protein diet for the prevention of renal failure. *Proc Jpn Acad Ser B Phys Biol Sci,* 93**,** 1-9.

WEI, M., BRANDHORST, S., SHELEHCHI, M., MIRZAEI, H., CHENG, C. W., BUDNIAK, J., GROSHEN, S., MACK, W. J., GUEN, E., DI BIASE, S., COHEN, P., MORGAN, T. E., DORFF, T., HONG, K., MICHALSEN, A., LAVIANO, A. & LONGO, V. D. 2017. Fasting-mimicking diet and markers/risk factors for aging, diabetes, cancer, and cardiovascular disease. *Sci Transl Med,* 9.

WEI, M. C., ZONG, W. X., CHENG, E. H., LINDSTEN, T., PANOUTSAKOPOULOU, V., ROSS, A. J., ROTH, K. A., MACGREGOR, G. R., THOMPSON, C. B. & KORSMEYER, S. J. 2001. Proapoptotic BAX and BAK: a requisite gateway to mitochondrial dysfunction and death. *Science,* 292**,** 727-30.

WEISS, E. P. & FONTANA, L. 2011. Caloric restriction: powerful protection for the aging heart and vasculature. *Am J Physiol Heart Circ Physiol,* 301**,** H1205-19.

WESTERMANN, B. 2008. Molecular machinery of mitochondrial fusion and fission. *J Biol Chem,* 283**,** 13501-5.

WIERSMA, M., MEIJERING, R. A. M., QI, X. Y., ZHANG, D., LIU, T., HOOGSTRA-BERENDS, F., SIBON, O. C. M., HENNING, R. H., NATTEL, S. & BRUNDEL, B. 2017. Endoplasmic Reticulum Stress Is Associated With Autophagy and Cardiomyocyte Remodeling in Experimental and Human Atrial Fibrillation. *J Am Heart Assoc,* 6.

WILLIAMS, A., HAYASHI, T., WOLOZNY, D., YIN, B., SU, T. C., BETENBAUGH, M. J. & SU, T. P. 2016. The non-apoptotic action of Bcl-xL: regulating Ca(2+) signaling and bioenergetics at the ER-mitochondrion interface. *J Bioenerg Biomembr,* 48**,** 211-25.

WU, X., HE, L., CHEN, F., HE, X., CAI, Y., ZHANG, G., YI, Q., HE, M. & LUO, J. 2014. Impaired autophagy contributes to adverse cardiac remodeling in acute myocardial infarction. *PLoS One,* 9**,** e112891.

XU, H. X., CUI, S. M., ZHANG, Y. M. & REN, J. 2020. Mitochondrial Ca(2+) regulation in the etiology of heart failure: physiological and pathophysiological implications. *Acta Pharmacol Sin,* 41**,** 1301-1309.

YAMAMOTO, T., TAKABATAKE, Y., TAKAHASHI, A., KIMURA, T., NAMBA, T., MATSUDA, J., MINAMI, S., KAIMORI, J. Y., MATSUI, I., MATSUSAKA, T., NIIMURA, F., YANAGITA, M. & ISAKA, Y. 2017. High-Fat Diet-Induced Lysosomal Dysfunction and Impaired Autophagic Flux Contribute to Lipotoxicity in the Kidney. *J Am Soc Nephrol,* 28**,** 1534-1551.

YAMAMOTO, Y. H. & NODA, T. 2020. Autophagosome formation in relation to the endoplasmic reticulum. *J Biomed Sci,* 27**,** 97.

YARAS, N., UGUR, M., OZDEMIR, S., GURDAL, H., PURALI, N., LACAMPAGNE, A., VASSORT, G. & TURAN, B. 2005. Effects of diabetes on ryanodine receptor Ca release channel (RyR2) and Ca2+ homeostasis in rat heart. *Diabetes,* 54**,** 3082-8.

YORIMITSU, T., NAIR, U., YANG, Z. & KLIONSKY, D. J. 2006. Endoplasmic reticulum stress triggers autophagy. *J Biol Chem,* 281**,** 30299-304.

YOSHII, S. R. & MIZUSHIMA, N. 2017. Monitoring and Measuring Autophagy. *Int J Mol Sci,* 18.

YU, Z., CHEN, R., LI, M., YU, Y., LIANG, Y., HAN, F., QIN, S., CHEN, X., SU, Y. & GE, J. 2018. Mitochondrial calcium uniporter inhibition provides cardioprotection in pressure overload-induced heart failure through autophagy enhancement. *Int J Cardiol,* 271**,** 161-168.

ZAGLIA, T., CERIOTTI, P., CAMPO, A., BORILE, G., ARMANI, A., CARULLO, P., PRANDO, V., COPPINI, R., VIDA, V., STOLEN, T. O., ULRIK, W., CERBAI, E., STELLIN, G., FAGGIAN, G., DE STEFANI, D., SANDRI, M., RIZZUTO, R., DI LISA, F., POZZAN, T., CATALUCCI, D. & MONGILLO, M. 2017. Content of mitochondrial calcium uniporter (MCU) in cardiomyocytes is regulated by microRNA-1 in physiologic and pathologic hypertrophy. *Proc Natl Acad Sci U S A,* 114**,** E9006-E9015.

ZHU, H., TANNOUS, P., JOHNSTONE, J. L., KONG, Y., SHELTON, J. M., RICHARDSON, J. A., LE, V., LEVINE, B., ROTHERMEL, B. A. & HILL, J. A. 2007. Cardiac autophagy is a maladaptive response to hemodynamic stress. *J Clin Invest,* 117**,** 1782-93.

ZORZANO, A., LIESA, M., SEBASTIAN, D., SEGALES, J. & PALACIN, M. 2010. Mitochondrial fusion proteins: dual regulators of morphology and metabolism. *Semin Cell Dev Biol,* 21**,** 566-74.

Related publications

1. IBANEZ, B. & **VILLENA-GUTIERREZ, R**. 2021. Cardiac Mitochondrial Transplantation: The Force Awakens. J Am Coll Cardiol, 77, 1089-1092.

2. GALAN-ARRIOLA, C., VILCHEZ-TSCHISCHKE, J. P., LOBO, M., LOPEZ, G. J., DE MOLINA-IRACHETA, A., PEREZ-MARTINEZ, C., **VILLENA-GUTIERREZ, R.**, MACIAS, A., DIAZ-RENGIFO, I. A., OLIVER, E., FUSTER, V., SANCHEZ-GONZALEZ, J. & IBANEZ, B. 2022. Coronary microcirculation damage in anthracycline cardiotoxicity. Cardiovasc Res, 118, 531-541.

3. CLEMENTE-MORAGON, A., GOMEZ, M., **VILLENA-GUTIERREZ, R**., LALAMA, D. V., GARCIA-PRIETO, J., MARTINEZ, F., SANCHEZ-CABO, F., FUSTER, V., OLIVER, E. & IBANEZ, B. 2020. Metoprolol exerts a non-class effect against ischaemia-reperfusion injury by abrogating exacerbated inflammation. Eur Heart J, 41, 4425-4440.

4. GALAN-ARRIOLA, C., **VILLENA-GUTIERREZ, R**., HIGUERO-VERDEJO, M. I., DIAZ-RENGIFO, I. A., PIZARRO, G., LOPEZ, G. J., MOLINA-IRACHETA, A., PEREZ-MARTINEZ, C., GARCIA, R. D., GONZALEZ-CALLE, D., LOBO, M., SANCHEZ, P. L., OLIVER, E., CORDOBA, R., FUSTER, V., SANCHEZ-GONZALEZ, J. & IBANEZ, B. 2021. Remote ischaemic preconditioning ameliorates anthracycline-induced cardiotoxicity and preserves mitochondrial integrity. Cardiovasc Res, 117, 1132-1143.

5. MARTINEZ-MILLA, J., GALAN-ARRIOLA, C., CARNERO, M., COBIELLA, J., PEREZ-CAMARGO, D., BAUTISTA-HERNANDEZ, V., RIGOL, M., SOLANES, N., **VILLENA-GUTIERREZ, R.,** LOBO, M., MATEO, J., VILCHEZ-TSCHISCHKE, J. P., SALINAS, B., CUSSO, L., LOPEZ, G. J., FUSTER, V., DESCO, M., SANCHEZ-GONZALEZ, J. & IBANEZ, B. 2020. Translational large animal model of hibernating myocardium: characterization by serial multimodal imaging. Basic Res Cardiol, 115, 33.

6. GALAN-ARRIOLA, C., LOBO, M., VILCHEZ-TSCHISCHKE, J. P., LOPEZ, G. J., DE MOLINA-IRACHETA, A., PEREZ-MARTINEZ, C., AGUERO, J., FERNANDEZ-JIMENEZ, R., MARTIN-GARCIA, A., OLIVER, E., **VILLENA-GUTIERREZ, R.**, PIZARRO, G., SANCHEZ, P. L., FUSTER, V., SANCHEZ-GONZALEZ, J. & IBANEZ, B. 2019. Serial Magnetic Resonance Imaging to Identify Early Stages of Anthracycline-Induced Cardiotoxicity. J Am Coll Cardiol, 73, 779-791.

7. GARCIA-PRIETO, J., **VILLENA-GUTIERREZ, R**., GOMEZ, M., BERNARDO, E., PUN-GARCIA, A., GARCIA-LUNAR, I., CRAINICIUC, G., FERNANDEZ-JIMENEZ, R., SREERAMKUMAR, V., BOURIO-MARTINEZ, R., GARCIA-RUIZ, J. M., DEL VALLE, A. S., SANZ-ROSA, D., PIZARRO, G., FERNANDEZ-ORTIZ, A., HIDALGO, A., FUSTER, V. & IBANEZ, B. 2017. Neutrophil stunning by metoprolol reduces infarct size. Nat Commun, 8, 14780.